



HEINRICH HEINE
UNIVERSITÄT DÜSSELDORF

**Characterization of the spontaneous SOS response in
Corynebacterium glutamicum and its effect on the
lysogenic prophage CGP3**

Inaugural dissertation

for the attainment of the title of doctor
in the Faculty of Mathematics and Natural Sciences
at the Heinrich-Heine-University Düsseldorf

presented by
Arun Nanda
born in Düsseldorf

Düsseldorf, December 2015

The thesis in hand has been performed at the Institute of Bio- and Geosciences
IBG-1: Biotechnology, Forschungszentrum Jülich, from February 2011 until April
2014 under the supervision of Juniorprof. Dr. Julia Frunzke.

Published with permission of the Faculty of Mathematics and Natural Sciences at
Heinrich-Heine-University Düsseldorf

Supervisor: Juniorprof. Dr. Julia Frunzke
Institute of Bio- and Geosciences
IBG-1: Biotechnology
Forschungszentrum Jülich GmbH

Co-supervisor: Prof. Dr. Joachim Ernst
Institute of Molecular Mycology
Heinrich-Heine-University Düsseldorf

Date of oral examination: April 26th, 2016

Results described in this dissertation have been published in the following original publications:

Nanda, A. M., Heyer, A., Krämer, C., Grünberger, A., Kohlheyer, D., & Frunzke, J. (2014). Analysis of SOS-Induced Spontaneous Prophage Induction in *Corynebacterium glutamicum* at the Single-Cell Level. *Journal of Bacteriology*, **196**(1): 180–8. doi:10.1128/JB.01018-13

Nanda, A. M., Thormann, K., Frunzke, J. (2014) Impact of spontaneous prophage induction on the fitness of bacterial populations and host-microbe interactions. *J Bacteriol* **197**(3): 410-9. doi: 10.1128/JB.02230-14

Arun M. Nanda and Julia Frunzke (2015). The Role of the SOS Response in CGP3 Induction of *Corynebacterium glutamicum*. **Awaiting submission**

Results of further projects not discussed in this thesis have been published in:

Grünberger, A., Probst, C., Helfrich, S., **Nanda, A. M.**, Stute, B., Wiechert, W., von Lieres, E., Nöh, K., Frunzke, J., Kohlheyer, D. (2015). Spatiotemporal microbial single-cell analysis using a high-throughput microfluidics cultivation platform. *Cytometry A*, 2015 Sep 8. Doi: 10.1002/cyto.a.22779. [Epub ahead of print]

Table of Contents

1	Summary	1
1.1	Summary English	1
1.2	Summary German.....	2
2	Introduction	3
2.1	Bacteriophages.....	3
2.2	Genetics of the prophage life cycle	5
2.2.1	Alleviation of the lysogenic state	5
2.3	<i>Corynebacterium glutamicum</i>	7
2.3.1	The SOS response of <i>C. glutamicum</i>	8
2.3.2	Prophages of <i>C. glutamicum</i>	8
2.4	Single-cell analysis.....	9
2.5	Aims of this work.....	11
3	Results	13
3.1	Analysis of SOS-induced Spontaneous Prophage Induction in <i>Corynebacterium glutamicum</i> at the Single-Cell Level	15
3.2	Impact of Spontaneous Prophage Induction on the Fitness of Bacterial Populations and Host-Microbe Interactions.....	25
3.3	Assessing the Role of the SOS Response in the Induction of Prophage CGP3 of <i>Corynebacterium glutamicum</i>	35
3.4	Spatiotemporal Microbial Single-Cell Analysis Using a High-Throughput Microfluidics Cultivation Platform	49

4	Discussion	65
4.1	Mechanisms underlying the spontaneous induction of the <i>C. glutamicum</i> prophage CGP3	65
4.2	Spontaneous SOS response	66
4.3	Spontaneous induction of CGP3.....	68
4.4	The fate of cells with a SI of the SOS response and CGP3	71
4.5	Global response to a deletion of <i>recA</i>	73
5	References	76
6	Appendix	82
6.1	Analysis of SOS-Induced Spontaneous Prophage Induction in <i>Corynebacterium glutamicum</i> at the Single-Cell Level	82
6.2	Assessing the Role of the SOS Response in the induction of prophage CGP3 of <i>Corynebacterium glutamicum</i>	83
6.3	Spatiotemporal Microbial Single-Cell Analysis Using a High-Throughput Microfluidics Cultivation Platform	89

LIST OF ABBREVIATIONS

ABC	ATP-binding cassette
Ala	alanine
Amp ^r	Ampicilline resistance
ATCC	American Type Culture Collection
ATPase	adenosine triphosphatase
BLAST	Basic Local Alignment Search Tool
et al.	<i>et alii</i>
eYFP	enhanced yellow fluorescent protein
FACS	Fluorescence-activated cell sorting
Gly	glycine
HGT	Horizontal Gene Transfer
Kan ^r	Kanamycine resistance
MmC	Mitomycin C
OD ₆₀₀	Optical density at 600 nm
PBP	Penicillin-binding protein
SI	Spontaneous induction
SOEing	Splicing by Overlap Extension
STEC	Shiga Toxigenic Escherichia Coli
w/v	weight per volume
v/v	volume per volume

Further abbreviations not included in this section are according to international standards, e.g. as listed in the author guidelines of *FEBS Journal*.

Author contributions

Analysis of SOS-Induced Spontaneous Prophage Induction in *Corynebacterium glutamicum* at the Single-Cell Level

JF and AMN designed the study which was supervised by JF. The experimental work was performed by AMN (construction of promoter fusions, application in Biolector and FACS, creation of deletion mutants) and AG (time-lapse microscopy in microfluidic chamber). AG and AMN analyzed the data. AMN wrote the manuscript.

Impact of spontaneous prophage induction on the fitness of bacterial populations and host-microbe interactions

JF conceived the review. AMN and JF wrote the manuscript, assisted by KT (prophages in biofilms).

The Role of the SOS Response in CGP3 Induction of *Corynebacterium glutamicum*

JF and AMN designed the study which was supervised by JF. Experimental work was performed by AMN. AMN wrote the manuscript.

Spatiotemporal microbial single-cell analysis using a high-throughput microfluidics cultivation platform

DK, AG and CP designed the study, which was supervised by DK. Experimental work was performed by AG and CP (microfluidics) and AMN (FACS). The experimental data was analyzed by AG, CP and AMN. The manuscript was written by AG and CP.

AG: Alexander Grünberger, AMN: Arun Michael Nanda, CP: Christoph Probst, DK: Dietrich Kohlheyer, JF: Julia Frunzke, KT: Kai Thormann, SH: Stefan Helfrich

1 Summary

1.1 Summary English

Bacteria encounter a multitude of stresses in the environment and have evolved to react to these appropriately. The bacterial SOS response, whose key players are the transcriptional repressor LexA and the single-strand binding protein RecA, is a global response to DNA damage which is present in close to all bacterial phyla and leads to the arrest of the cell cycle and induction of DNA repair mechanisms and mutagenesis.

Advances in bioprocess engineering have led to the advent of microfluidic cultivation of bacterial strains. Microcolonies of bacteria are cultivated and monitored in μm -chambers. To assess the stress bacteria might encounter during microfluidic cultivation, a reporter for *recA* transcriptional activity was constructed and tested.

Application of the sensor in the Gram-positive soil bacterium *Corynebacterium glutamicum* revealed that a small subset of cells have a high transcriptional activity of *recA* under standard cultivation conditions. The main focus of this work lay in analyzing the spontaneous SOS response in *C. glutamicum* and its link to the spontaneous induction of the lysogenic prophage CGP3.

Viability assays revealed a reduced capacity to survive when the SOS response is induced spontaneously. Time-lapse microscopy of microcolonies revealed cell-to-cell variabilities in the output of the SOS response. We could show a correlation between spontaneous SOS response and spontaneous prophage induction by utilizing reporters for SOS and CGP3 gene activity. Key players of the SOS response were deleted and the effects on CGP3 induction were assessed. Whereas constitutive SOS induction led to a high induction of CGP3 genes, a reduction of SOS response led to a decrease in CGP3 gene activity. Furthermore, a gain-of-function mutation of the transcriptional repressor LexA surprisingly led to a high increase in CGP3 gene activity.

Taken together the results emphasize the interplay between the bacterial SOS response and CGP3 induction in *C. glutamicum*.

1.2 Summary German

Bakterien sind in ihrer Umgebung einer Vielzahl von Stressfaktoren ausgesetzt und haben Mechanismen entwickelt, um mit diesen umzugehen. Die bakterielle SOS Antwort, deren Hauptkomponenten der transkriptionelle Repressor LexA und das einzelstrangbindende Protein RecA sind, ist eine universelle Antwort auf DNA Schäden, welche in fast allen bakteriellen Phyla vorkommt. Sie führt zum Zellzyklusarrest und zur Induktion von DNA Reparaturmechanismen und Mutagenese.

Fortschritte in der Bioprozessverfahrenstechnik haben zur Entwicklung von mikrofluidischen Kultivationsmöglichkeiten für bakterielle Stämme geführt. Bakterielle Mikrokolonien werden in Kammern von wenigen μM Größe kultiviert und observiert. Ein Reporter für die transkriptionelle Aktivität von *recA* wurde konstruiert und in den Kammern getestet, um Aufschluss darüber zu erhalten, inwiefern die Bakterien in der Mikrokolonienkultur gestresst werden.

Die Anwendung des Sensors im Gram-positiven Bodenbakterium *Corynebacterium glutamicum* zeigte, dass ein Anteil an Zellen unter normalen Kultivierungsbedingungen eine hohe transkriptionelle *recA* Aktivität aufweist. Der Hauptfokus dieser Arbeit lag darin, die spontane SOS Antwort in *C. glutamicum* zu analysieren und die Verbindung zur spontanen Induktion des lysogenen Prophagen CGP3 zu erforschen.

Experimente zur Überlebensfähigkeit von SOS-gestressten Zellen ergaben, dass diese eine verringerte Überlebensfähigkeit haben. Mikroskopische Zeitrafferaufnahmen von Mikrokolonien zeigten Unterschiede einzelner Zellen in der Intensität ihrer SOS Antwort. Wir konnten eine Korrelation zwischen spontaner SOS Antwort und spontaner Prophageninduktion zeigen, indem wir Reporter für SOS und CGP3 Genaktivität verwendet haben. Zentrale Gene der SOS Antwort wurden deletiert und die Auswirkung auf die Induktion von CGP3 analysiert. Während eine konstitutive SOS Antwort zu einer hohen Induktion von CGP3 Genen führte, führte eine verringerte SOS Antwort zu einer verringerten Aktivität von CGP3 Genen. Weiterhin zeigte eine hypermorphe Mutation des Repressors LexA überraschenderweise eine hohe Aktivität der CGP3 Gene.

Zusammenfassend betonen die Ergebnisse das Zusammenspiel zwischen der bakteriellen SOS Antwort und der Induktion des Prophagen CGP3 in *C. glutamicum*.

2 Introduction

2.1 Bacteriophages

Bacteriophages, viruses that infect bacteria, are assumed to be the most abundant biological agents on the planet with an estimated total of 1×10^{31} (Rohwer and Edwards, 2002) in comparison to $2-6 \times 10^{30}$ bacteria (Whitman *et al.*, 1998), outnumbering them by a factor of about 1:10. This large amount of phages constitutes a highly diverse gene pool, which can significantly influence the bacterial host. They are thought to be involved in nutrient cycling through the lysis of bacterial cells (Wilhelm and Suttle, 1999), and play an active role in the transfer of genetic material between bacteria, thus contributing to bacterial evolution (Hatfull and Hendrix, 2011).

Genome sequencing has revealed that bacterial genomes are heavily laced with DNA of viral origin (Casjens, 2003), which can amount to a staggering 20% of the bacterial genome (Casjens *et al.*, 2000a). While some of this DNA is made up of fully functional prophages, which are able to undergo a fully replicative life cycle, the better part of it is made up of prophage-like entities (Casjens *et al.*, 2000a), phage remnants left after incomplete excision events, cryptic prophages or genetic material acquired by horizontal gene transfer (HGT) such as genomic islands (Dobrindt *et al.*, 2004).

The history of phage research in bacteria, from their discovery up to the renewed interest in using phages as therapeutical agents, is a long one (Sulakvelidze *et al.*, 2001). Noteworthy was the work conducted by Frederick Twort who discovered the essential properties of bacteriophages (Twort, 1914), and Felix D'Herelle who coined the term

bacteriophage and imagined them as replicating organisms obligately feeding off of bacteria (D'Herelle, 1917; D'Herelle, 2007). It was D'Herelle who recognized that not only the relationship between human and bacteria deserve attention, but that phages play an integral part in this relationship as well. He truly was a pioneer in phage therapy (d'Herelle, 1931). Nowadays, phage therapy has come into focus again as humanity faces an evolving challenge in the form of antibiotic resistance (Brüssow, 2012). It is by understanding the nature of the phage's contribution to bacterial traits that phage therapy will become a reality in modern medicine.

Horizontally acquired genetic material can influence the bacterial host in a number of ways. They can change the existing genetic network by introducing regulatory genes or by disrupting existing genes via genomic integration, a process which can even lead to the generation of novel proteins (Canchaya *et al.*, 2004a). Introduction of novel genes, which are recognized by the host replication machinery, is an important aspect when considering the virulence of lysogenized bacteria (Brown *et al.*, 2006). Their virulence relies on specific prophage-encoded toxins or on the interplay of diverse prophages, as seen in Shiga toxin-producing *Escherichia coli* (Livny and Friedman, 2004), *Vibrio cholerae* (Waldor and Mekalanos, 1996), and *Corynebacterium diphtheriae* (Freeman, 1951). As shown for STEC, the presence of multiple *stx* gene-carrying prophages modulates the virulence properties of the strains (Serra-Moreno *et al.*, 2008). This is also the case for *Staphylococcus aureus*, *Streptococcus pyogenes*, and *Salmonella enterica* serovar Typhimurium. Here a multitude of prophages incrementally contribute to the bacteria's virulence (Brüssow *et al.*, 2004). By imparting their host with virulent properties, the bacterial cell receives a competitive advantage in comparison to non-lysogens (Bossi *et al.*, 2003). Further fitness advantages

can come in the form of overall metabolic down-regulation to minimize energy expenditure in harsh environments (Paul, 2008), enhancing biofilm formation (Carrolo *et al.*, 2010), or by increasing the host's resistance to osmotic stress and antibiotic treatment (Xiaoxue Wang *et al.*, 2010).

2.2 Genetics of the prophage life cycle

Prophages can generally be categorized into two distinct classes (Fig. 2.2.1): i) Lytic phages form infectious progeny upon infection. Among the proteins expressed during this process are holins and endolysins. Endolysins have muralytic activities against peptide, glycoside or amide bonds of the peptidoglycan (Wang *et al.*, 2003). Holins are small proteins which oligomerize at the host membrane and permeabilize it at late stages of infection when virion assembly nears completion, enabling the endolysins to cross the membrane and reach the peptidoglycan matrix (Wang *et al.*, 2000). In some cases infection leads to an abortive infection in which the bacterium along with the invading phage are killed (Horvath and Barrangou, 2010). ii) Lysogenic prophages on the other hand remain dormant within the bacterial host, either by integration into the bacterial genome or by maintenance as plasmids or linear DNA. Specific triggers can relieve this dormancy and induce the prophages, leading to cell lysis and subsequent rounds of infection and re-integration. The most extensively studied model for prophage-host interactions, as well as lytic and lysogenic life cycles, is the *Escherichia coli* λ phage model.

2.2.1 Alleviation of the lysogenic state

The lysogenic state of phage λ is controlled by CI, the central repressor of phage genes

(Oppenheim *et al.*, 2005a). When levels of CI are altered, e.g. by addition of DNA-damaging antibiotics such as mitomycin C (MmC) (Tomasz, 1995) or fluoroquinolons (Piddock and Wise, 1987), by heat treatment (Rokney *et al.*, 2008), or by UV radiation, the lysogenic state can be reversed. It achieves this by hijacking the cell's DNA repair mechanism.

When the genome's integrity is compromised (indicated by lesions to the DNA), the conserved DNA repair mechanism (SOS response) is triggered (Little and Mount, 1982). The single-strand binding protein RecA polymerizes along single-stranded DNA (ssDNA). Double-strand breaks are first resolved by action of the RecBCD complex by unwinding the double-stranded DNA and creating stretches of single-stranded DNA, which are then bound by RecA. The nucleoprotein filament of ssDNA and activated RecA* acts as a co-protease and facilitates the autocatalytic cleavage of the repressor LexA between a conserved alanine and glycine residue. LexA is released from its DNA targets, the so-called SOS boxes, and the transcription of more than 40 SOS genes is induced (SOS response) (Friedberg *et al.*, 2005).

The life cycle of lambdoid phages (such as phages P22 and 434) is linked to this regulatory pathway (Slilaty *et al.*, 1986). The central repressor CI possesses the same Ala-Gly bond as the protease-sensitive center of LexA as well as similarities in its carboxy-terminal domain, and it is cleaved as well upon the induction of the SOS response (Sauer *et al.*, 1982). Its binding to repressor sites within the prophage is reversed, leading to an expression of genes responsible for the excision of phage DNA, virion assembly, and release of the infectious phage particles into the extracellular space (Oppenheim *et al.*, 2005a).

As early as the 1950's a spontaneous induction of lysogenic phage λ was observed in liquid cultures of *E. coli* (Lwoff, 1953). Remarkably, a decrease in spontaneously induced prophages was shown in recombination-deficient *E. coli* strains (Brooks and Clark, 1967; Hertman and Luria, 1967), implying a role of the SOS response in spontaneous prophage induction.

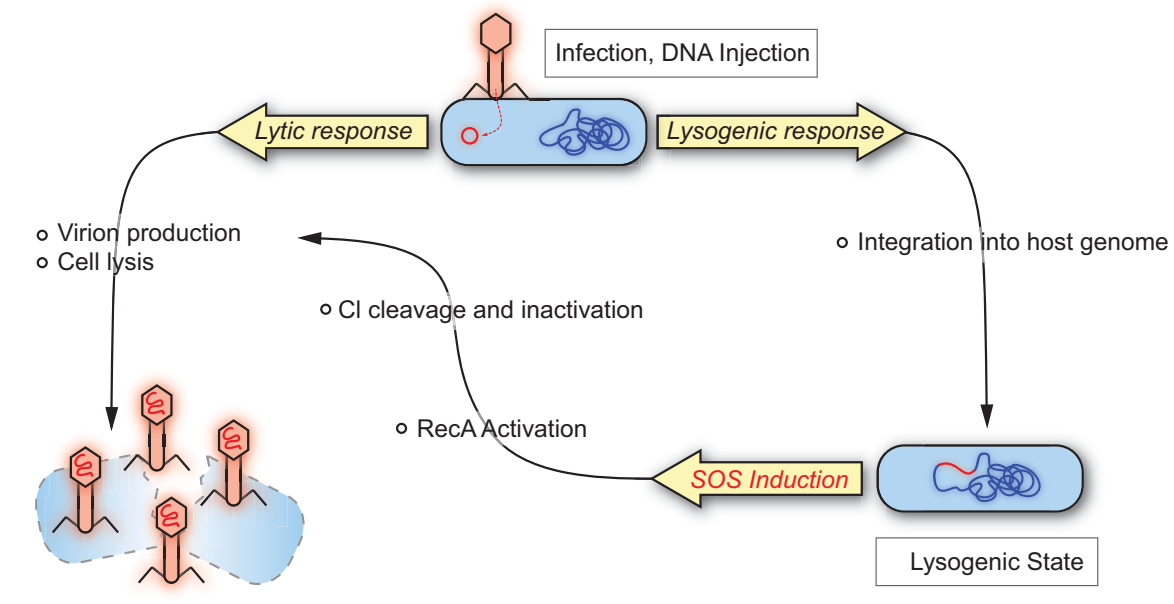


FIGURE 2.2.1 Infection of a bacterial cell by a bacteriophage. Upon infection, host intrinsic factors influence the phage's path of entering the replicative life cycle (lytic response) or integrating into the host genome to co-exist as temperate prophage (lysogenic response). The transfer from lysogenic to lytic response is induced by specific triggers and also occurs spontaneously in a small number of cells.

2.3 *Corynebacterium glutamicum*

The biotechnological platform organism *Corynebacterium glutamicum* is a Gram-positive, biotin-auxotroph soil bacterium that is utilized in the industrial production of more than four million tons of L-glutamate and L-lysine per year (Ajinomoto Co., 2011; Ajinomoto Co., 2012) as well as organic acids (Wieschalka *et al.*, 2013). This is achieved by means of metabolic engineering, i.e. the genetic manipulation of specific regulatory processes.

Furthermore, *C. glutamicum* is used as a model organism for the two phylogenetically close relatives *Corynebacterium diphtheriae* and *Mycobacterium tuberculosis*, which represent two relevant human pathogens.

2.3.1 The SOS response of *C. glutamicum*

The SOS response is conserved across most bacterial phyla (Erill *et al.*, 2007). When DNA is damaged naturally, e.g. by UV irradiation or the occurrence of stalled replication forks, or by action of antibiotics such as mitomycin C or fluoroquinolones, the protein RecA polymerizes along the single-stranded DNA in an ATP-dependent manner and the SOS response is triggered. The LexA regulon was elucidated by transcriptome analysis in *C. glutamicum* (Jochmann *et al.*, 2009). Upon MmC-induced DNA damage, more than 40 genes are induced, among them the key genes *lexA* and *recA*, as well as the cell division inhibitor *divS* (Ogino and Teramoto, 2008; Jochmann *et al.*, 2009). DivS is divergently located to *lexA*, a situation it shares with the genes *rv2719c* of *M. tuberculosis* H37Rv and *yneA* of *Bacillus subtilis*, two proteins responsible for SOS-induced growth inhibition. There is no significant homology between DivS, Rv2719c and YneA, however it was shown that DivS interferes with functional FtsZ ring assembly or is involved in its stability, leading to an inhibited septum formation (Ogino, 2008).

2.3.2 Prophages of *C. glutamicum*

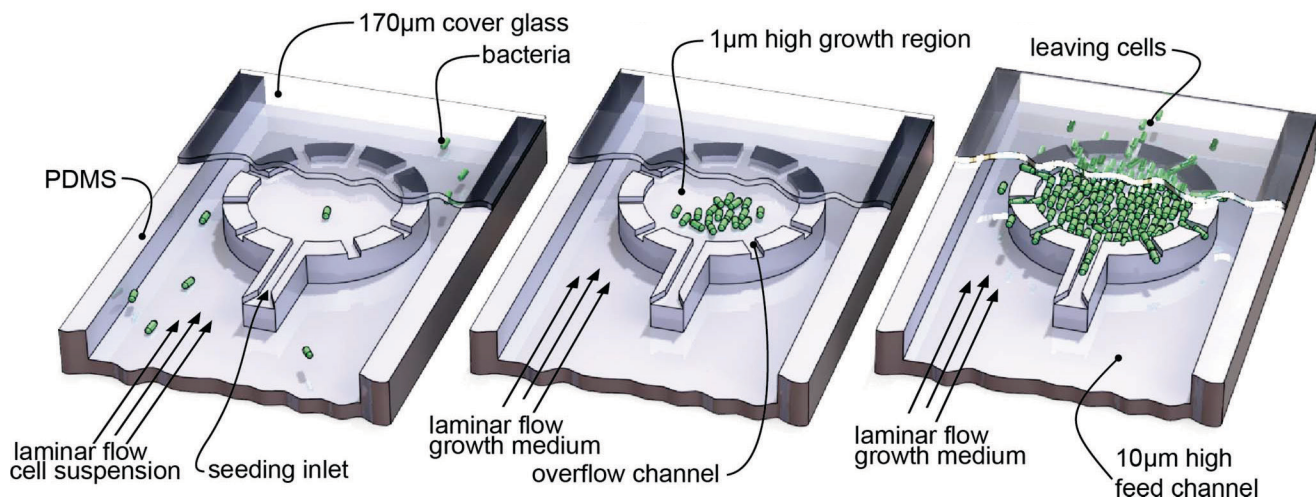
Full genome sequencing of *C. glutamicum* ATCC 13032 revealed three lysogenic prophages, named CGP1-3 (Kalinowski, 2005). CGP1 and CGP2 are highly degenerated, CGP3 however retains the ability to excise from the genome and harbors genes for a

phage integrase (cg2071) and a phage lysin (cg1974) (Frunzke *et al.*, 2008; Nanda *et al.*, 2014). It was shown that a subpopulation of cells (1-3%) spontaneously induces the prophage under normal cultivation conditions (Frunzke *et al.*, 2008) and that treatment with MmC leads to an upregulation of CGP3 genes (Jochmann *et al.*, 2009; Donovan, 2015). So far no fully replicative life cycle has been observed for CGP3. However, upon excision CGP3 is replicated and multiple copies can be observed in a single cell (Frunzke *et al.*, 2008). *C. glutamicum* was cured of all three prophages and submitted to stress and viability assays. Whereas some conditions such as osmotic stress, excess iron or phosphate starvation have no marked impact on the cured strain, the deletion of CGP3 leads to an increase in plasmid copy number and heterologous protein production, an increased transformation efficiency and an increased growth rate when treated with MmC (Baumgart *et al.*, 2013). Therefore, it is safe to assume that lysogenic prophages in *C. glutamicum* have an impact on host physiology despite their inability to complete a fully replicative life cycle.

2.4 Single-cell analysis

Key to studying cellular dynamics underlying the spontaneous induction of prophages at the level of single cells is an advanced platform to analyze single cells. To this end, the growth of microcolonies grown out of single cells, as well as the activity of single promoters and proteins need to be tracked in a time-resolved manner (Locke and Elowitz, 2009). When you factor in the low frequency at which hair trigger events occur, it is obvious that a) the cultivation conditions should have as little impact on the induction

event itself, because small changes could affect experimental outcomes significantly and b) a high number of cells has to be analyzed and processed with a high throughput to obtain an evaluable number of the elusive events. To address the first challenge, the PDMS-based picolitre bioreactor is a suitable environment for observing events such as the spontaneous induction of the SOS response (Grünberger *et al.*, 2014; Grünberger *et al.*, 2015) (Figure 2.4). Up to 500 cultivation chambers are contained on chips the size of a thumbnail. The cultivation medium of choice is introduced through an inlet at a steady force, evenly creating a laminar flow throughout all cultivation chambers. The picolitre volume ensures homogenous conditions throughout all chambers. Furthermore, custom designs can be carved into the PDMS according to the experiment's needs, making it a



flexible system.

Stepping away from the quantitative results that analysis of microcolonies in the microfluidic setup allow, a temporally less resolved, yet more high-throughput analysis is enabled by flow cytometry (Nebe-von-Caron *et al.*, 2000; Wang *et al.*, 2010). The combination of promoter fusions to fluorescent reporter genes with the high number of

analyzed cells per second makes flow cytometry and fluorescence-activated cell sorting (FACS) a powerful tool to monitor huge bacterial populations for spontaneous gene regulatory events and morphological traits simultaneously.

2.5 Aims of this work

Previous studies showed that the prophage CGP3 is able to excise from the host genome spontaneously. The main aim of this work is to characterize this spontaneous induction in further detail and characterize its trigger. To this end, the SOS response will be considered as a putative trigger. Its spontaneous induction will be studied and correlated to the spontaneous induction of CGP3.

To observe the spontaneous induction of specific *C. glutamicum* CGP3 and SOS genes, select promoters will be chosen and cloned in front of genes encoding for fluorescent reporter proteins. The activity of these, as observed by their fluorescent output, will be monitored in a flow cytometric and microfluidic cultivation setup. By incorporating promoter fusions of SOS and CGP3 genes in the same strain, activities of the according genes can be correlated by measuring the fluorescent output of a large number of cells in flow cytometry. Once a correlation has been established between the host SOS response and prophage activity, a higher temporal resolution at the single-cell level will be achieved by cultivating microcolonies, which are derived from single cells, in a custom microfluidic cultivation device (picolitre bioreactor – PLBR).

In an attempt to better understand the SOS response in *C. glutamicum*, key SOS genes will be deleted. The effect that these changes to the SOS pathway have on key CGP3

genes will be analyzed by flow cytometry and cultivation in the Biolector system.

Taken together, this work will further our understanding of the SOS response in the biotechnological platform organism *C. glutamicum* and provide us with a better understanding of the relationship between bacterial hosts and their lysogenic prophages, as well as processes underlying their spontaneous induction.

3 Results

The main focus of this PhD thesis was to elucidate the trigger of spontaneous CGP3 induction, as well as to characterize the spontaneous SOS response and the involved proteins in *C. glutamicum*. One study based on literature research focused on the *status quo* of spontaneous prophage induction in bacteria. The results of the research conducted in this PhD thesis have been summarized in three peer-reviewed publications and a manuscript, which is to be submitted.

In “Spatiotemporal microbial single-cell analysis using a high-throughput microfluidics cultivation platform” the application of the picolitre bio reactor (PLBR) for time-lapse microscopy and quantitative analysis of signals obtained by the SOS reporter (*recA* promoter activity) are reported. In this work the suitability of the PLBR for capturing rare events of population heterogeneity is presented.

The publication “Analysis of SOS-induced spontaneous prophage induction in *Corynebacterium glutamicum* at the single-cell level” reports the findings that a spontaneous SOS response is responsible for the spontaneous induction of lysogenic prophage CGP3. Promoter fusions of key SOS and CGP3 genes to the fluorescent reporter protein Venus and E2-Crimson, respectively, were constructed and transformed into *C. glutamicum* (*C. glutamicum::P_{recA}-venus/pJC1-P_{CGP3}-e2-crimson*). These cells were subjected to flow cytometry to reveal spontaneous SOS and CGP3 induction events. The fluorescent outputs of both promoter fusions were subjected to correlation analysis. Additionally, the temporal course of both SOS and CGP3 promoter activation was observed and compared, and the single-cell dynamics of spontaneous SOS induction were

characterized.

The review “Impact of spontaneous prophage induction on the fitness of bacterial populations and host-microbe interactions” assesses the current state of research on spontaneous prophage induction. Key examples of bacteria containing either lytic or lysogenic prophages, as well as bacteria containing cryptic prophages or pathogenicity islands are shown. The intrinsic and extrinsic factors that are able to induce the activity of this foreign DNA are discussed in detail, as well as the role that stochasticity and genetic noise play in this induction are discussed. The impact that prophages have on an individual cell and on a population-wide scale are discussed by addressing the fitness of lysogenized bacteria and the formation of biofilms in bacterial communities. The last part of the review focuses on the significance of spontaneous prophage induction in regards to host virulence of pathogenic bacteria.

The manuscript “The Role of the SOS Response in CGP3 Induction of *Corynebacterium glutamicum*” focuses on the relationship between the SOS response and CGP3 induction in further detail. Key promoter fusions were transformed into an array of mutant *C. glutamicum* strains missing key SOS and CGP3 genes, as well as a prophage-cured strain. General activity of the genes was assessed under standard cultivation conditions and after addition of MmC. Additionally, the spontaneous activity of the SOS response was compared in the different SOS mutant strains. mRNA of wild type and $\Delta recA$ strains was harvested at defined time points, with and without the addition of MmC, and compared in microarray analyses.



Analysis of SOS-Induced Spontaneous Prophage Induction in *Corynebacterium glutamicum* at the Single-Cell Level

Arun M. Nanda, Antonia Heyer, Christina Krämer, Alexander Grünberger, Dietrich Kohlheyer, Julia Frunzke

Institut für Bio- und Geowissenschaften, IBG-1: Biotechnologie, Forschungszentrum Jülich, Jülich, Germany

The genome of the Gram-positive soil bacterium *Corynebacterium glutamicum* ATCC 13032 contains three integrated prophage elements (CGP1 to -3). Recently, it was shown that the large lysogenic prophage CGP3 (~187 kbp) is excised spontaneously in a small number of cells. In this study, we provide evidence that a spontaneously induced SOS response is partly responsible for the observed spontaneous CGP3 induction. Whereas previous studies focused mainly on the induction of prophages at the population level, we analyzed the spontaneous CGP3 induction at the single-cell level using promoters of phage genes (P_{int2} and P_{lysin}) fused to reporter genes encoding fluorescent proteins. Flow-cytometric analysis revealed a spontaneous CGP3 activity in about 0.01 to 0.08% of the cells grown in standard minimal medium, which displayed a significantly reduced viability. A P_{recA} -*eyfp* promoter fusion revealed that a small fraction of *C. glutamicum* cells (~0.2%) exhibited a spontaneous induction of the SOS response. Correlation of P_{recA} to the activity of downstream SOS genes (P_{divS} and P_{recN}) confirmed a bona fide induction of this stress response rather than stochastic gene expression. Interestingly, the reporter output of P_{recA} and CGP3 promoter fusions displayed a positive correlation at the single-cell level ($\rho = 0.44$ to 0.77). Furthermore, analysis of the P_{recA} -*eyfp*/ P_{int2} -*e2-crimson* strain during growth revealed the highest percentage of spontaneous P_{recA} and P_{int2} activity in the early exponential phase, when fast replication occurs. Based on these studies, we postulate that spontaneously occurring DNA damage induces the SOS response, which in turn triggers the induction of lysogenic prophages.

Genome sequencing projects have revealed a large amount of prophage DNA in bacterial genomes. Although not all prophage DNA accounts for functional prophages, because it includes degenerated phage remnants, this DNA can have a marked impact on bacterial physiology (1). The biotechnological platform organism *Corynebacterium glutamicum* is a Gram-positive, biotin-auxotroph soil bacterium that is used for the industrial production of more than four million tons of L-glutamate and L-lysine per year (2, 3). As revealed by whole-genome sequencing, *C. glutamicum* ATCC 13032 possesses three prophages that are integrated into its genome (CGP1 to -3), of which CGP1 and CGP2 are probably degenerated phage remnants (4–6). Previous studies showed that the large prophage CGP3 (187 kb) retains the ability to be excised from the genome and exist as a circular DNA molecule. Interestingly, a small number of wild-type cells showed a much higher copy number of circular phage DNA per cell than the average of the population (5).

Recent studies in *Shewanella oneidensis* (7) and *Streptococcus pneumoniae* (8) have provided evidence that sacrificing a small number of cells by spontaneous prophage-induced lysis is beneficial to the remainder of the population. For these species, genomic DNA released into the extracellular space following cell lysis supports biofilm formation and maintenance (9, 10). Although these results shed new light on the spontaneous induction of prophages, the mechanisms governing this general microbiological phenomenon are poorly understood to date.

The best-studied model for prophage-host interactions is the *Escherichia coli* λ phage model. As far back as the 1950s, spontaneous induction of lysogenic phage λ was observed in *E. coli* cultures (11). Remarkably, a decrease in spontaneously induced prophages was shown in recombination-deficient *E. coli* strains (12). It remains unknown, however, whether these events are (i) random events caused by promoter noise or by the stochastic distribution of key regulatory components or (ii) the result of specific

induction by intrinsic and/or extrinsic factors. The lysogenic state of phage λ is controlled by cI , the central repressor of phage genes (13). When the integrity of the genome is compromised (as indicated by lesions in the DNA), the protein RecA polymerizes along single-stranded DNA (ssDNA). This nucleoprotein filament of ssDNA and activated RecA* protein catalyzes the autocatalytic cleavage of the repressor LexA, which leads to the derepression of more than 40 SOS genes (SOS response) (14). The life cycle of lambdoid phages is linked to this regulatory pathway. The central repressor cI mimics the autocatalytic center of LexA and thus becomes cleaved upon the induction of the SOS response. Its binding to repressor sites within the prophage is alleviated, leading to an expression of genes responsible for the excision of phage DNA, virion assembly, and release of the infectious phage particles into the extracellular space (13).

In this study, we address the question of whether the spontaneous induction of the lysogenic prophage CGP3 in single *C. glutamicum* cells is linked to the spontaneous activation of the SOS response. The promoters of genes of the SOS pathway and those encoded by CGP3 were fused to the fluorescent reporter genes *eyfp* and *e2-crimson* to analyze the activity of the respective promoters under standard cultivation conditions. Single-cell analysis was performed using flow cytometry and an in-house developed polydimethylsiloxane (PDMS) microfluidic chip setup (15, 16) suit-

Received 27 August 2013 Accepted 21 October 2013

Published ahead of print 25 October 2013

Address correspondence to Julia Frunzke, j.frunzke@fz-juelich.de.

Supplemental material for this article may be found at <http://dx.doi.org/10.1128/JB.01018-13>.

Copyright © 2014, American Society for Microbiology. All Rights Reserved.
doi:10.1128/JB.01018-13

TABLE 1 Bacterial strains and plasmids used in this study

Strain or plasmid	Characteristics	Source or reference
Strains		
<i>E. coli</i> DH5 α	<i>supE44</i> Δ <i>lacU169</i> (ϕ 80 <i>lacZ</i> DM15) <i>hsdR17</i> <i>recA1</i> <i>endA1</i> <i>gyrA96</i> <i>thi-1</i> <i>relA1</i>	Invitrogen
<i>C. glutamicum</i>		
ATCC 13032	Biotin-auxotrophic wild type	36
ATCC 13032 Δ <i>lexA</i>	In-frame deletion of the gene <i>lexA</i> (cg2114)	22
ATCC 13032::P _{<i>recA</i>} - <i>eyfp</i>	Integration of P _{<i>recA</i>} - <i>eyfp</i> into the intergenic region between cg1121 and cg1122	This study
Plasmids		
pJC1	Kan ^r , Amp ^r ; <i>C. glutamicum</i> shuttle vector	38
pEKEx2-P _{<i>tac</i>} - <i>eyfp</i>	Kan ^r ; pEKEx2 containing <i>eyfp</i> with pET16 RBS, under the control of P _{<i>tac</i>}	23
pAN6- <i>e2-crimson</i>	Kan ^r ; pAN6 derivative for expression of E2-Crimson under the control of the P _{<i>tac</i>} promoter	6
pK19 <i>mobsacB</i>	Kan ^r , oriV _{<i>E. coli</i>} <i>sacB lacZ</i> α	37
pK18 <i>mobsacB</i> -cg1121/1122	Kan ^r , oriV _{<i>E. coli</i>} <i>sacB</i>	6
pK18 <i>mobsacB</i> -cg1121/1122-P _{<i>recA</i>} - <i>eyfp</i>	pJC1 derivative containing the promoter of <i>recA</i> (260 bp) fused to <i>eyfp</i> ; the insert includes the promoter of <i>recA</i> and an additional ribosome binding site (pET16) in front of <i>eyfp</i>	This study
pJC1-P _{<i>divS</i>} - <i>e2-crimson</i>	pJC1 derivative containing the promoter of <i>divS</i> (411 bp) fused to <i>e2-crimson</i> ; the insert includes the promoter of <i>divS</i> , 30 bp of the coding sequence, a stop codon, and an additional ribosome binding site (pET16) in front of <i>e2-crimson</i>	This study
pJC1-P _{<i>recN</i>} - <i>e2-crimson</i>	pJC1 derivative containing the promoter of <i>recN</i> (207 bp) fused to <i>e2-crimson</i> ; the insert includes the promoter of <i>recN</i> , 30 bp of the coding sequence, a stop codon, and an additional ribosome binding site (pET16) in front of <i>e2-crimson</i>	This study
pJC1-P _{<i>int2</i>} - <i>e2-crimson</i>	pJC1 derivative containing the promoter of <i>int2</i> (250 bp) fused to <i>e2-crimson</i> ; the insert includes the promoter of <i>int2</i> , 30 bp of the coding sequence, a stop codon, and an additional ribosome binding site (pET16) in front of <i>e2-crimson</i>	This study
pJC1-P _{<i>lysin</i>} - <i>e2-crimson</i>	pJC1 derivative containing the promoter of <i>lysin</i> (250 bp) fused to <i>e2-crimson</i> ; the insert includes the promoter of <i>lysin</i> , 30 bp of the coding sequence, a stop codon, and an additional ribosome binding site (pET16) in front of <i>e2-crimson</i>	This study
pJC1-P _{<i>cg2067</i>} - <i>e2-crimson</i>	pJC1 derivative containing the promoter of <i>cg2067</i> (250 bp) fused to <i>e2-crimson</i> ; the insert includes the promoter of <i>cg2067</i> , 30 bp of the coding sequence, a stop codon, and an additional ribosome binding site (pET16) in front of <i>e2-crimson</i>	This study

able for observing rare cellular events of interest. We observed a positive correlation between the spontaneous activation of the SOS response and the spontaneous induction of the prophage CGP3, and we postulate a bona fide activation of the SOS response as a prominent trigger leading to prophage excision.

MATERIALS AND METHODS

Bacterial strains, media, and growth conditions. The bacterial strains used in this study are listed in Table 1. *C. glutamicum* ATCC 13032 was used as the wild-type strain; all strains were cultivated at 30°C. For growth experiments, a glycerin stock culture was streaked onto BHI (brain heart infusion; Difco, BD, Heidelberg, Germany) agar plates. Single colonies were used to inoculate 5 ml liquid BHI medium. After cultivation for 8 h, the preculture was used to inoculate 25 ml CGXII minimal medium (1:50) containing 4% glucose (wt/vol) as the carbon source (17). After growth overnight, fresh CGXII medium was inoculated to an optical density at 600 nm (OD₆₀₀) of 1 in 25 ml. For microtiter-scale cultivations, the Biolector microbioreactor system (m2p-labs, Heinsberg, Germany) was utilized (18) using an established protocol for *C. glutamicum* cultivation (16). *Escherichia coli* was cultivated in LB (lysogeny broth) medium and on LB agar plates at 37°C. If required, kanamycin was added to the cultivation medium at a concentration of 25 μ g/ml for *C. glutamicum* and 50 μ g/ml for *E. coli*. For induction of the SOS response, mitomycin C (Sigma-Aldrich, Seelze, Germany) was added at the appropriate concentrations at an OD₆₀₀ of 4.

Cloning techniques. For PCR amplification of DNA used for cloning, KOD HotStart polymerase (Merck Millipore, Darmstadt, Germany) was used. DreamTaq (Fisher Scientific, Schwerte, Germany) was utilized for

PCR verification of ligation reactions. Heat shock transformation of *E. coli* was performed as described previously (19). Transformation of *C. glutamicum* was performed by electroporation as described previously (20). Isolation and purification of plasmids from *E. coli* cultures was performed using plasmid isolation and purification kits from Qiagen (Qiagen, Hilden, Germany) and Thermo Scientific (Fisher Scientific, Schwerte, Germany) miniprep kits. Chromosomal DNA of *C. glutamicum* was isolated as described previously (21). DNA sequencing and oligonucleotide synthesis were performed by Eurofins MWG Operon (Ebersberg, Germany). Plasmids and oligonucleotides used in this work are listed in Table 1 and Table 2, respectively. The in-frame deletion mutant of *lexA* in the wild-type strain ATCC 13032 was constructed as described by Jochmann et al. (22).

Construction of promoter fusions. For construction of the promoter fusions of P_{*int2*}, P_{*lysin*}, and P_{*cg2067*}, 250 bp upstream of the coding sequence with an additional 10 codons and the 16-bp ribosomal binding site of pET16 were amplified using the oligonucleotide pairs int2-fwd/int2-rev, lysin-fwd/lysin-rev, and cg2067-fwd/cg2067-rev, respectively. The promoter sequences were ligated into the vector pJC1-crimson-term by restriction with BamHI and NdeI.

For construction of the *recA* promoter fusion, 260 bp upstream of the coding sequence were amplified from genomic *C. glutamicum* DNA followed by the 16-bp ribosomal binding site of pET16 using oligonucleotides PrecA_pK18_fwd and PrecA_YFP_rev. *eyfp* was amplified with oligonucleotides YFP_fwd and YFP_pK18_rev using the plasmid pEKEx2-P_{*tac*}-*eyfp* (23) as the template. The promoter fusion was generated by overlap extension PCR using oligonucleotides PrecA_pK18_fwd and PrecA_YFP_rev. XhoI and MfeI restriction sites were used to ligate

TABLE 2 Oligonucleotides used in this study

Oligonucleotide	Sequence (5'–3') ^a	Restriction site
cg2114_del_1	TCCCCCGGGGATCTAGGATCCACATGGAAGCGAACAGAG	SmaI
cg2114_del_2	TGAAGTCTGCAGCATCA	
cg2114_del_3	TGATGCTGCAGGACTTCATGTTGGCGAGTCCATGAG	
cg2114_del_4	GCTCTAGAGATCTACTGCAGCGCCACGATATGTGAGAA	XbaI
PrecA_pK18_fwd	GGAATTCAATTGTTCCGATGAAAATTCGAATT	MfeI
PrecA_YFP_rev	GCTCACCATATGTATATCTCCTTTTTTAATTCCTTAGTTTTATTGA	
YFP_fwd	AAGGAGATATACATATGGTGAGCAAGGGCGA	
YFP_pK18_rev	GGAATTCTCGAGTTATCTAGACTTGTACAGCTCGTCCAT	XhoI
divS_fwd	CTAGCTAGCTAGCGTTGGGCAAGGCTTAACT	NheI
divS_rev	ATGATATCTCCTTCTTAAAGTTTAACTTAGCTCTTTACCCGCATAAAC	
crimson_fwd	TAAACTTTAAGAAGGAGATATCATATGGATAGCAC	
crimson_rev	CTAGCTAGCTAGCAAAAGAGTTTGTAGAAACGC	NheI
int2_fwd	CGCGGATCCCGGGCGAGAGGGTGAGCGAT	BamHI
int2_rev	CGCCATATGATATCTCCTTCTTAAAGTTCAGAAGCGTGCCCTGTACCTCTCCGA	NdeI
lysin_fwd	CGCGGATCCCTTCTTTGAGGCTTGATGCCT	BamHI
lysin_rev	CGCCATATGATATCTCCTTCTTAAAGTTCATTTTTTCGGCATTGCGCCTTAAAT	NdeI
cg2067_fwd	CGCGGATCCCGAAGCTTTTGTAGTCTGTTACTGG	BamHI
cg2067_rev	CGCCATATGATATCTCCTTCTTAAAGTTCACGACCACATCTCCAACGGCTAAA	NdeI

^a Restriction sites are underlined.

the amplicon into the shuttle vector pK18mobsacB_cg1121/22. Promoter fusions of *divS* and *recN* were amplified with the oligonucleotides *divS_fwd* and *divS_rev* and the oligonucleotides *recN_fwd* and *recN_rev*, respectively, using genomic DNA as the template. Additionally, the first 10 codons were amplified along with a stop codon. The coding sequence of the fluorescent protein E2-Crimson (24) was amplified from the plasmid pAN6-*e2-crimson* with the oligonucleotides *crimson_fwd* and *crimson_rev*. Both amplicons were combined by overlap extension PCR. The restriction site NheI was used for ligation into the medium-copy-number vector pJCl.

The P_{ptsG} -*e2-crimson* promoter fusion was constructed according to Hentschel et al. (23) by amplifying 725 bp upstream of the *ptsG* start codon with oligonucleotides *PptsG_fwd* and *PptsG_rev*, introducing BamHI and NdeI restriction sites. The PCR fragment was ligated into pJCl-*e2-crimson-term* after treatment of both with BamHI and NdeI restriction enzymes.

Fluorescence microscopy. For phase contrast and fluorescence microscopy, samples were analyzed on 1 to 2% agar pads, which were placed on microscope slides and covered by a coverslip. Images were taken on a Zeiss Axioplan 2 imaging microscope equipped with an AxioCam MRM camera and a Plan-Apochromat $\times 100$ magnification, 1.4 numerical-aperture oil differential interference contrast (DIC) objective. Filter sets 46HE and 63HE were used for imaging enhanced yellow fluorescent protein (eYFP) and E2-Crimson fluorescence, respectively. Digital images were acquired and analyzed with the AxioVision 4.6 software (Zeiss, Göttingen, Germany).

Flow cytometry. Flow-cytometric measurements and sorting were performed on a FACSAria II (Becton, Dickinson, San Jose, CA) flow cytometer with 488-nm excitation by a blue solid-state laser and 633-nm excitation by a red solid-state laser. Forward-scatter characteristics (FSC) and side-scatter characteristics (SSC) were detected as small- and large-angle scatters of the 488-nm laser, respectively. eYFP fluorescence was detected using a 502-nm long-pass and a 530/30-nm band pass filter set. E2-Crimson fluorescence was detected using a 660/20-nm band pass filter set. Cells were analyzed at a threshold rate of 3,000 to 8,000 events/s and sorted onto BHI agar plates at a threshold rate of 3,000 to 4,000 events/s. Data were analyzed using FlowJo V7.6.5 (Tree Star, Inc., Ashland, OR).

Statistical analysis. Nonparametric tests for the analysis of correlation were performed with GraphPad Prism 6 (GraphPad Software, Inc., La Jolla, CA). Spearman's rank correlation coefficient (the Pearson correlation coefficient of the ranked variables) was used. A perfect (inverse) correlation takes on ρ values of ($-$)1; totally independent variables take on ρ values of 0.

Microfluidic cultivation. *C. glutamicum* was cultivated in in-house-developed microfluidic cultivation chambers (0.9 μm by 60 μm by 60 μm) arranged in parallel between 10-fold-deeper supply channels. For details on our microfluidic chip setup, see references 15 and 25.

During the experiment, CGXII minimal medium was infused continuously at 300 nl min^{-1} using a high-precision syringe pump (neMESYS; Cetoni GmbH, Korbussen, Germany) with attached disposable syringes (Omnifix-F Tuberculin, 1 ml; B. Braun Melsungen AG, Melsungen, Germany) to maintain constant environmental conditions. Cell growth and eYFP fluorescence were observed at 10-min intervals by time-lapse imaging with a fully motorized inverted Nikon Eclipse Ti microscope (Nikon GmbH, Düsseldorf, Germany). Chip cultivation was performed at 30°C using a microscope incubator system (PeCon GmbH, Erbach, Germany). The microscope was equipped with a focus assistant (Nikon PFS) to compensate for thermal drift during long-term microscopy, with a Plan Apo λ 100 \times oil Ph3 DM objective (Nikon GmbH, Düsseldorf, Germany) and a high-speed charge-coupled device (CCD) camera (Andor Clara DR-3041; Andor Technology Plc., Belfast, United Kingdom). An optical filter system (YFPHQ filter system [excitation, 490 to 550 nm; dichroic mirror, 510 nm; absorption filter, 520 to 560 nm]; AHF Analysentechnik AG, Tübingen, Germany) and a mercury light source (Intensilight; Nikon GmbH, Düsseldorf, Germany) were installed for fluorescence microscopy.

RESULTS

The prophage CGP3 is spontaneously induced in single cells. In recent studies we observed a spontaneous excision of the prophage CGP3 in a small number of *C. glutamicum* cells cultivated in shake flasks with CGXII minimal medium (5). Transcriptome analysis revealed an upregulation of CGP3 genes (cg1890 to cg2071) upon induction of the SOS response by addition of the DNA-cross-linking antibiotic mitomycin C (A. Heyer and J. Frunzke, personal communication). In an effort to create appropriate tools to monitor prophage activity, we consulted reports on previous microarray experiments to determine which genes are suitable candidates. We constructed plasmid-based promoter fusions of the CGP3 genes cg2071 (integrase, *int2*), cg1974 (putative lysin), and cg2067 (hypothetical protein) to the coding sequence of the fluorescent protein E2-Crimson. To test their function, wild-type *C. glutamicum* ATCC 13032 cells were transformed with the

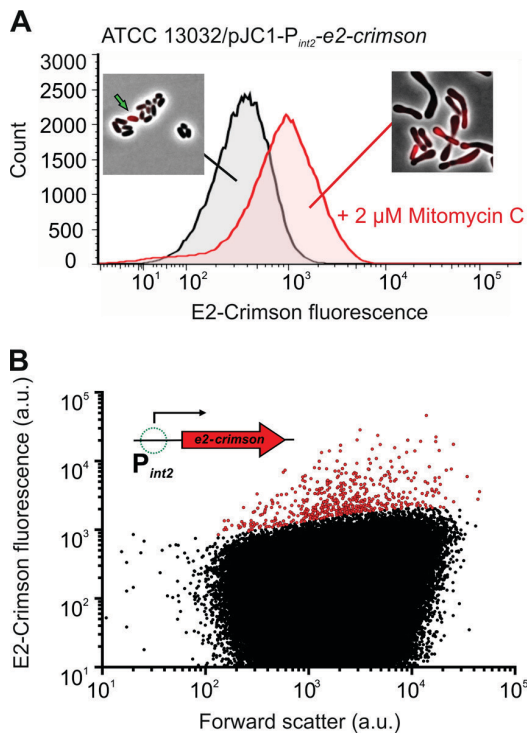


FIG 1 Utilization of prophage promoter fusions for monitoring spontaneous CGP3 induction. (A) Histogram of eYFP fluorescence of *C. glutamicum*/pJC1- P_{int2} -*e2-crimson* with 2 μ M mitomycin C (red line) and without mitomycin C (gray line) with additional fluorescence microscopy images showing the spontaneous and induced activity of P_{int2} . The insets show uninduced and induced cells carrying the plasmid pJC1- P_{int2} -*e2-crimson*. The green arrow indicates spontaneous induction of P_{int2} occurring under standard cultivation conditions. (B) Scatter plot of the strain *C. glutamicum*/pJC1- P_{int2} -*e2-crimson*. A total of 100,000 cells were analyzed for their size characteristics (forward scatter) and their fluorescent properties. Even under noninducing conditions, a small fraction of cells exhibited an increased reporter signal (red dots) in comparison to the bulk of the population (black dots). Cells were cultivated in CGXII medium plus 4% glucose and analyzed at an OD_{600} of 4.

promoter fusion constructs and treated with 2 μ M mitomycin C to induce DNA lesions and subsequently trigger the SOS response. Samples were analyzed by flow cytometry and fluorescence microscopy (shown for P_{int2}) (Fig. 1A). The treated samples exhibited a highly induced P_{int2} activity and morphological changes. The untreated cultures showed no significant P_{int2} activity, yet, in agreement with earlier studies, P_{int2} was highly induced in a small number of cells. Flow-cytometric analysis of untreated cultures revealed that a fraction of 0.01 to 0.08% of the cells exhibited a 5- to 160-fold higher P_{int2} activity than the bulk of the population (Fig. 1B). Single cells with a high fluorescent signal (phage⁺) and cells showing background fluorescence (phage⁻) were sorted onto BHI agar plates, and their survival was assessed after incubation for 24 h. As expected, the survival rate of phage⁺ cells was significantly below that of phage⁻ cells (survival rates of 23% and 96%, respectively) (Fig. 2). Thus, cells showing an increased P_{int2} activity were significantly impaired in their ability to resume growth on plates, which is likely caused by prophage excision and subsequent cell lysis.

Spontaneous P_{recA} induction in single cells. Since the host

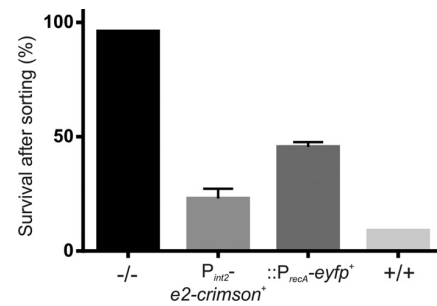


FIG 2 Viability assay of *C. glutamicum* cells which exhibit an induction of CGP3 and/or of the SOS response. Single cells were sorted onto agar plates, and the percent survival was determined as the fraction of cells able to form colonies. Nonfluorescent cells (-/-), cells with either a positive P_{recA} -*eyfp* or a positive P_{int2} -*e2-crimson* signal (+), and cells with both signals (+/+) were sorted onto separate agar plates. Colony growth was analyzed after 24 h.

SOS response is a prominent trigger of lysogenic phages, we constructed a promoter fusion of the *recA* promoter to *eyfp* and integrated it into the genome of *C. glutamicum* ATCC 13032 at the intergenic region of cg1121 and cg1122 to test for a spontaneous SOS induction. As proof of principle, the P_{recA} -*eyfp* strain was cultivated in microtiter scale and the SOS response was induced by addition of mitomycin C in increasing concentrations. A strain with a truncation of *lexA*, the repressor of SOS genes, served as a reference strain which exhibits a maximally induced SOS response (Fig. 3A, black bar). At low concentrations (15 nM and 100 nM) of mitomycin C and in the Δ *lexA* strain, P_{recA} activity showed a bimodal distribution, with the majority of cells showing a slight increase in reporter signal and a smaller fraction of cells shifted toward an even higher signal. This bimodal state was not observed at higher concentrations (500 nM and 1,000 nM mitomycin C) (Fig. 3B). We subjected cells with the integrated P_{recA} -*eyfp* promoter fusion to flow-cytometric analysis to get more detailed insight into single-cell dynamics of the SOS response in *C. glutamicum* populations. Under standard cultivation conditions, we observed a spontaneous activity, analogous to the activities of CGP3 promoters (Fig. 3C). About 0.07 to 0.2% of cells showed a 12- to 18-fold increased reporter signal (SOS⁺ cells). These SOS⁺ cells had a reduced survival rate (recovery rate of 46% after sorting on BHI agar plates) (Fig. 2). It was tempting to hypothesize that these rare events may act as a bet-hedging strategy to ensure an increased fitness under changing environmental conditions. We sorted SOS⁺ cells on agar plates with different DNA damaging conditions yet saw no increased fitness under the tested conditions (data not shown).

Spontaneous P_{recA} activity reflects a bona fide SOS response.

Next we tested whether spontaneous P_{recA} activity and reduced viability were indicative of a bona fide SOS response caused by potentially lethal DNA damage. The reporter strain harboring the integrated promoter fusion P_{recA} -*eyfp* was transformed with plasmids carrying promoter fusions of the two SOS-responsive genes *divS* and *recN*, respectively, fused to the autofluorescent reporter gene *e2-crimson*. Both genes were previously shown to be upregulated in the deletion mutant Δ *lexA* (22) or after induction with mitomycin C. Analysis of the dual reporter strain (P_{recA} -*eyfp* integrated into the genome, P_{int2} -*e2-crimson* plasmid-borne) by fluorescence microscopy and flow cytometry revealed a correlation of the P_{recA} signal to P_{divS} as well as P_{recN} signals. After gating of SOS⁺

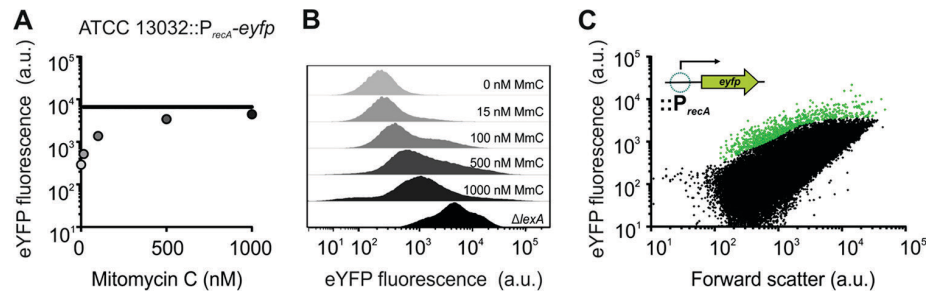


FIG 3 P_{recA} promoter fusion for the analysis of SOS induction in single cells. (A) Dose response plotted as mean eYFP fluorescence at increasing mitomycin C (MmC) concentrations. (B) Offset histogram of *C. glutamicum*:: P_{recA} -*eyfp* cells subjected to increasing concentrations of mitomycin C. *C. glutamicum* $\Delta lexA$ was used as a reference strain which exhibits maximal induction of the SOS response. (C) Scatter plot of the strain *C. glutamicum*:: P_{recA} -*eyfp* cultivated under nonstressful conditions. A total of 100,000 cells were analyzed for their size characteristics (forward scatter) and their fluorescent properties. A small fraction of cells exhibits an increased reporter signal (green dots) in comparison to the bulk of the population (black dots). Cells were cultivated in CGXII medium plus 4% glucose in the Biolector system until the stationary phase.

cells, the signals of both reporters were correlated in single cells by using Spearman's rank correlation coefficient (Fig. 4). Both promoter fusions showed a high correlation (P_{divS} , $\rho = 0.78$, $P < 0.0001$, $n = 165$; P_{recN} , $\rho = 0.85$, $P < 0.0001$, $n = 131$) at the single-cell level. The control promoter fusion P_{p1sG} -*e2-crimson* was constructed and introduced into the P_{recA} -*eyfp* strain to exclude high correlation values due to factors other than sharing the same regulation. SOS⁺ cells were gated and their P_{recA} signal correlated to the P_{p1sG} reporter signal. Both signals displayed a low correlation ($\rho = 0.36$, $P < 0.0001$, $n = 248$). Thus, the strong correlation of P_{recA} to P_{divS} and P_{recN} activities confirmed that a spontaneous P_{recA} activity in single cells leads to a bona fide induction of the downstream SOS cascade.

Time-lapse analysis of P_{recA} activation dynamics. SOS⁺ cells did not display a uniform fate, with some cells being able to survive on agar plates whereas others were not viable. For a time-resolved analysis of the SOS induction in single cells, we cultivated the P_{recA} -*eyfp* strain in an in-house-developed PDMS microfluidic system enabling spatiotemporal analysis of growing microcolonies by automated time-lapse microscopy. Single cells were seeded into the microfluidic cultivation chambers and cultivated for several generations in standard CGXII minimal medium under non-stressful conditions; images were acquired every 10 min. Again, we

observed different fates of SOS⁺ cells (see Movies S1 to S3 in the supplemental material). Some cells showed a high and continuous reporter signal together with an elongated cell morphology and growth inhibition caused by an activated SOS response (Fig. 5; also, see Movies S1 to S3 in the supplemental material). These bacteria represent cells which undergo severe DNA damage, triggering the SOS response. However, other cells merely showed a pulse of the reporter along with an unaltered growth and cell morphology (Fig. 5; also, see Movies S1 and S2 in the supplemental material). This output either represents activity due to the stochastic binding of repressor molecules or might be triggered by DNA damage which is repaired before a full-blown SOS response is initiated. Furthermore, we observed an additional cell fate which consisted of high induction of the reporter coupled with an elongated cell morphology, growth inhibition, and cell branching (see Movie S3 in the supplemental material). This is analogous to *C. glutamicum* cells which continuously overexpress *divS* under the control of the promoter P_{aceA} (26), indicating a high concentration of DivS in these cells.

Correlating prophage activity to an induced SOS response in single cells. Having established promoter fusions for the analysis of spontaneous CGP3 induction and SOS response, we combined promoter fusions of *recA* and of the prophage genes to correlate

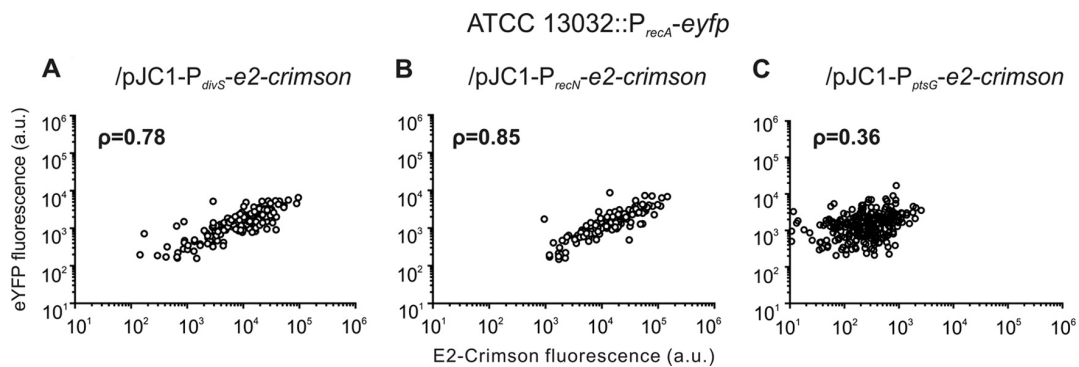


FIG 4 Correlation of P_{recA} activity to the activity of promoters of downstream SOS genes. Scatter plots of *C. glutamicum*:: P_{recA} -*eyfp*/ $pJC1$ - P_{divS} -*e2-crimson* (A), *C. glutamicum* P_{recA} -*eyfp*/ $pJC1$ - P_{recN} -*e2-crimson* (B), and *C. glutamicum* P_{recA} -*eyfp*/ $pJC1$ - P_{p1sG} -*e2-crimson* (C) are shown; *C. glutamicum* P_{recA} -*eyfp*/ $pJC1$ - P_{p1sG} -*e2-crimson* served as a control, reflecting the correlation of *recA* expression and an SOS-independent promoter. Cells with high eYFP fluorescence (spontaneous P_{recA} -*eyfp* cells) were gated and are displayed in the dot plot of eYFP fluorescence versus E2-Crimson fluorescence. Spearman's rank correlation coefficient (ρ) was calculated using GraphPad Prism 6. Cells were cultivated in CGXII medium plus 4% glucose and analyzed at an OD₆₀₀ of 4.

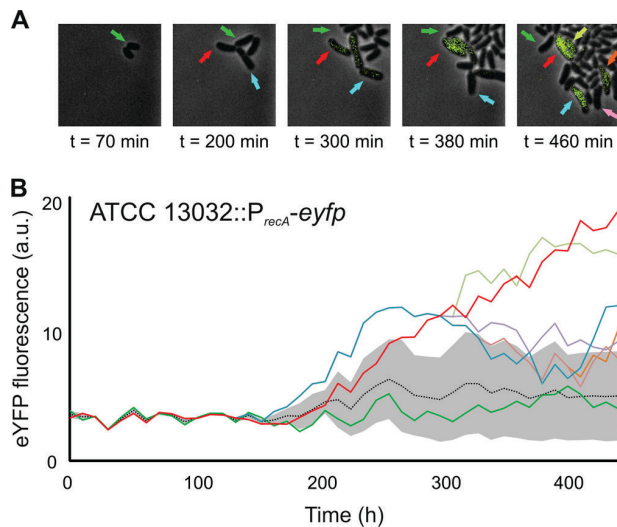


FIG 5 Fluorescence traces of P_{recA} activity in single cells observed by live cell imaging. Cells harboring the integrated P_{recA} - $eyfp$ promoter fusion were seeded into the microfluidic chip and cultivated for 24 h; a representative microcolony is shown. (A) Microscopic images of microcolony during cultivation. Single cells were analyzed for their fluorescent output and assigned a unique cell ID (colored arrow). (B) Course of fluorescence for single cells (colored lines) as well as for the entire microcolony (mean value, plotted as a dotted line; standard deviations are shown as a gray area). Single cells either showed no fluorescence (green trace), showed a high induction of P_{recA} (red and light green trace), displayed a pulsing behavior with no further promoter activity (violet and pink traces), or displayed a pulsing behavior followed by a high reporter signal (cyan and orange traces).

them at the single-cell level. To this end, the P_{recA} - $eyfp$ strain was transformed with the P_{int2} , P_{lysin} and P_{cg2067} promoter fusions to $e2$ - $crimson$. Analysis by flow cytometry again showed the occurrence of spontaneously activated cells for both types of promoter fusions. Fluorescence microscopy revealed that not all cells showed an activation of the prophage promoters when P_{recA} was active (Fig. 6). To measure the interdependence of both signals, the Spearman rank correlation coefficient was calculated for both. The highest correlation to SOS^+ cells was observed for P_{cg2067} and P_{int2} (P_{cg2067} , $\rho = 0.77$, $P < 0.0001$, $n = 687$; P_{int2} , $\rho = 0.57$, $P < 0.0001$, $n = 828$) (Fig. 6). P_{lysin} showed the lowest correlation ($\rho = 0.44$, $P < 0.0001$, $n = 790$) under the tested conditions. Even though the correlation coefficient is not able to reveal a causal link between two processes, it did show a high correlation of the promoters of $recA$ and the prophage genes. Reciprocal analysis of phage⁺ cells was performed as well and gave nearly identical values (P_{cg2067} , $\rho = 0.72$, $P < 0.0001$, $n = 119$; P_{int2} , $\rho = 0.58$, $P < 0.0001$, $n = 565$; P_{lysin} , $\rho = 0.45$, $P < 0.0001$, $n = 759$) (data not shown). This correlation suggests a link between spontaneously induced SOS response and spontaneous activity of CGP3 in single cells. Nevertheless, correlation was lower than that between P_{recA} and P_{divS}/P_{recN} , indicating that other factors besides the SOS response might influence the activity of the prophage promoters.

Impact of growth phase on spontaneous SOS and prophage activity. The P_{recA} - $eyfp/pJC1$ - P_{int2} - $e2$ - $crimson$ strain was cultivated in shake flasks, and samples were analyzed until the cells reached stationary growth phase (Fig. 7A) to eliminate the rigidity of measurements at single time points and better assess the characteristics of the reporters during growth. The P_{recA} signal showed

maximal intensity at the transition to and during the early phase of exponential growth. Activity of P_{int2} showed the same behavior. We expected this parallel activation of both promoters, if the SOS response and prophage induction are somehow linked. The number of spontaneously activated cells was measured for all time points as well (Fig. 7B). Whereas the peaks of both reporters' fluorescent output behaved similarly, the maximal number of spontaneously activated phage⁺ and SOS^+ cells showed a temporal disparity. The increase of SOS^+ cells was observed 2 h before the relative amount of phage⁺ cells increased.

DISCUSSION

The present study on the induction of lysogenic prophages was performed on a population-wide scale. It was shown that the induction of lambdoid phages is typically linked to the host's SOS response. The underlying bistable switch (13), simplified by the action of the repressor of phage genes cI , is turned toward lytic growth when the host's SOS response becomes activated. Spontaneous induction of prophages had been observed as far back as the 1950s (11), yet studies since then have not explored this phenomenon in more detail at the single-cell level. Due to the general link between the SOS response and prophage induction, it was tempting to speculate that the cause of spontaneous prophage induction lies in a spontaneously induced SOS response. The data shown in this study suggest that a small fraction of *C. glutamicum* cells grown under standard conditions spontaneously induced expression of prophage genes and that this activation is caused in part by the spontaneous activity of the SOS response in single cells.

During the cultivation of wild-type cells under standard cultivation conditions, we observed single cells that induced the SOS response spontaneously. As the occurrence of spontaneous DNA breakage has previously been reported in studies on *E. coli* (27), we tested this in *C. glutamicum*. In the *E. coli* studies, use of the SOS-inducible promoter of the cell division inhibitor gene *sulA* fused to *gfp* revealed a spontaneous SOS response in about 0.9% of cells. The rate of spontaneous SOS induction that we measured with P_{recA} - $eyfp$ lies at about 0.2%. When other LexA-regulated promoters of *C. glutamicum*, such as P_{divS} , P_{recN} , and P_{cglIAB} were used, the fraction of cells exhibiting a spontaneous SOS response lay between 0.1 and 0.5% (data not shown). Considering that further studies in *E. coli* using promoter fusions of *lexA*, *recA*, and *umuDC* showed spontaneous promoter activity in 0.09 to 3.1% of cells (28), our findings are consistent with those reported previously.

We assumed the SOS^+ cells to be impaired in their survival due to potentially lethal DNA damage. The survival rate of SOS^+ cells lay at 46%. Our microfluidic studies showed that an induction of the SOS response leads to the arrest of cell growth in some cells, probably caused by irreparable DNA damage, whereas other cells are able to resume growth after they exhibit P_{recA} activity. This activity in turn did not necessarily lead to a full-blown SOS response, as some cells showed the SOS phenotype; others, however, were either unaffected in their growth with a mere pulse of P_{recA} activity or were inhibited in their growth but able to recover from the SOS-induced inhibition of cell division. The presence of some cells showing a short pulse of reporter signal, but no growth inhibition, might hint at stochastic fluctuations in the binding of the repressor LexA or at DNA damage which is so minor that it is repaired before a full-blown SOS response is stimulated.

Studies in *E. coli* have revealed that SOS genes show a heterogeneous expression which is independent of RecA and based on

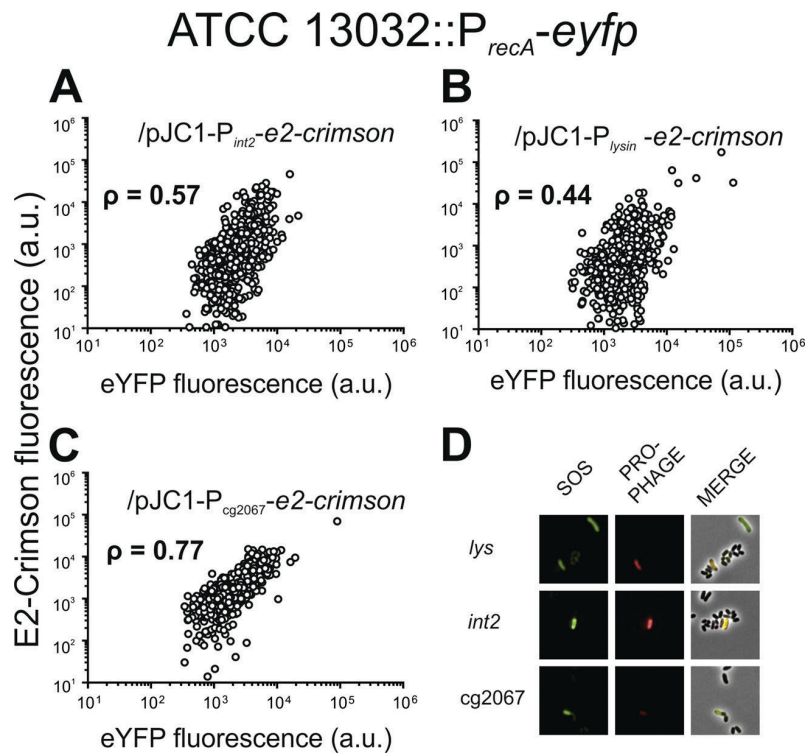


FIG 6 Correlation of P_{recA} reporter activity to the activity of CGP3 genes. Scatter plots of *C. glutamicum* P_{recA} -eyfp/pJC1- P_{int2} -e2-crimson (A), *C. glutamicum* P_{recA} -eyfp/pJC1- P_{lysin} -e2-crimson (B), and *C. glutamicum* P_{recA} -eyfp/pJC1- P_{cg2067} -e2-crimson (C) are shown. Cells with high eYFP fluorescence (SOS⁺ cells) were gated and their E2-Crimson fluorescence plotted against their eYFP fluorescence. Spearman's rank correlation coefficient (ρ) was calculated using GraphPad Prism 6. (D) Fluorescence microscopy analysis of cells on agar pads showing the spontaneous induction of SOS and prophage reporters. Cells were cultivated in CGXII medium plus 4% glucose and analyzed at an OD₆₀₀ of 4.

stochastic factors and binding affinities of LexA to SOS boxes (28). To confirm that the spontaneous induction of P_{recA} is caused by a bona fide SOS response, we transformed the P_{recA} reporter strain with plasmids carrying transcriptional fusions of *divS* and *recN* promoters, respectively. The degree of correlation gained by calculating Spearman's ranked correlation coefficient is strong (P_{divS} , $\rho = 0.78$; P_{recN} , $\rho = 0.78$). Whereas this is a strong correlation, higher values of ρ (>0.9) might be expected for causal relationships, as they are present within the SOS cascade. Even though *recA* is upregulated after cells encounter DNA damage, this damage might be repaired before the cell division inhibitor *divS* is induced, thus avoiding a premature inhibition of growth. Our microfluidic experiments showed that this might be the case, as a high number of SOS⁺ cells are not inhibited in their growth.

The same applies to the correlation values of the prophage reporters which lie below those observed for the correlation to the SOS reporters. An induced SOS response need not seal the fate of genomic excision for CGP3. Rather, an immunity to low levels of DNA damage and an induction upon accumulation or lasting presence of DNA damage would constitute a more reliable warning system telling the prophage when to "leave the sinking ship." If CGP3 were induced by every event of SOS response, the integration of the prophage would be a rather unstable situation. Thus, a threshold-based model of excision (29), as described for well-studied lambdoid phages, helps to explain the observed deviation from a perfect correlation. Nevertheless, future studies will eluci-

date the possible influence of so-far unknown regulators that play a role in the induction of CGP3. Microarray studies, for example, revealed that the putative regulator Cg2040 exhibits an inhibitory effect on a set of prophage genes when overexpressed (A. Heyer and J. Frunzke, personal communication).

Finally, we tested our dual promoter fusion strains (P_{recA} -eyfp/pJC1- P_{int2} -e2-crimson) during a standard flask cultivation experiment to analyze their expression during the course of growth. We observed that P_{recA} and P_{int2} promoters reached their peaks of activation during exponential growth phase. It is reasonable to assume that this phase of rapid cell growth gives rise to intrinsic DNA damage, which is produced by native DNA polymerases. Indeed, it has been reported that replication fork breakage is a major contributor to double-strand breaks (DSBs), which in turn activate the SOS response (30, 31). The measurement of spontaneous activation of the SOS response and prophage activity showed temporally separated peaks (Fig. 7B). As this disparity occurs in a small number of cells, it is clear that this effect would be masked in the bulk measurement of reporter output, as shown in Fig. 7A.

While the consequence of spontaneously inducing prophages has been reported for *Shewanella oneidensis* (7) and *Streptococcus pneumoniae* (8), the effects on *C. glutamicum* on a population-wide scale remain unknown. In studies by Bossi and coworkers (32), a spontaneous induction of prophages led to a competitive fitness of the population against other bacteria. Spontaneous

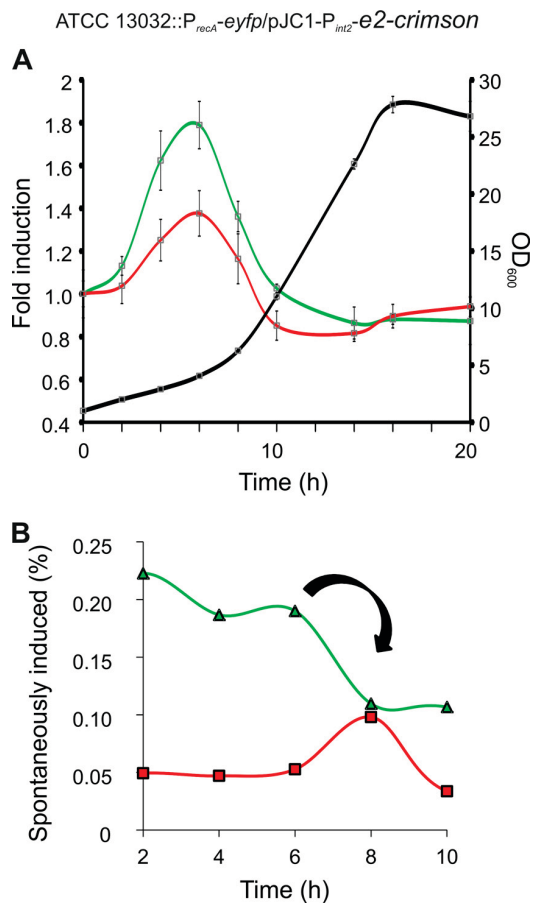


FIG 7 Analysis of activity and spontaneous activation of P_{recA} and P_{int2} during growth. *C. glutamicum* P_{recA}-eyfp/pJC1-P_{int2}-e2-crimson was cultivated in the Biolector microcultivation system. (A) OD₆₀₀ (black line) and mean eYFP (green line) and E2-Crimson (red line) fluorescence; (B) percentage of cells with a spontaneous P_{recA} (green line) and P_{int2} (red line) induction. The arrow indicates the delay between the peak for maximum spontaneous P_{recA} and maximum spontaneous P_{int2} activity in single cells. Cells were cultivated in CGXII medium plus 4% glucose.

phage release is seen as a strategy to maintain the lysogenic status of the prophage. Immunity sequences within the prophage lead to an immunity to superinfection. Interestingly, the genomic CGP3 locus possesses a restriction-modification system (*cgIIIM*, *cgIIR*, and *cgIIIM*) which might be used as a classic toxin/antitoxin module (33) to fend off infecting bacteriophages. An example of “bacterial altruism” was recently described (34) in which Shiga toxin produced by a small number of spontaneously induced prophage works as a positive selective force and benefits the population. The production of toxins by *C. glutamicum* has not been reported, but the release of DNA and proteins into the extracellular matrix as a source of nutrients for the rest of the population or as biofilm matrix for natural microbial communities is a possible scenario. Choosing irreparable or sustained DNA damage as trigger or selection marker to single out “weak individuals” would be a practical approach (35).

Future studies will aim at a more detailed investigation of the phenomenon of spontaneous prophage excision. We have

established a first link between the host’s SOS response and the excision of the genomically integrated CGP3 prophage in single bacterial cells. Further studies will assess the level at which the two phenomena are linked and which other regulatory pathways may feed into the prophage’s decision to excise from the host genome.

ACKNOWLEDGMENTS

For funding we thank the Deutsche Forschungsgemeinschaft (priority program SPP1617) and the Helmholtz Association (Young Investigator grant VH-NG-716).

REFERENCES

- Casjens S. 2003. Prophages and bacterial genomics: what have we learned so far? *Mol. Microbiol.* 49:277–300. <http://dx.doi.org/10.1046/j.1365-2958.2003.03580.x>.
- Ajinomoto Co I. 2011. Food products business. <http://www.ajinomoto.com/en/ir/pdf/Feed-useAA-Oct2011.pdf>. Ajinomoto Co., Inc., Tokyo, Japan.
- Ajinomoto Co I. 2012. Feed-use amino acids business. <http://www.ajinomoto.com/en/ir/pdf/Food-Oct2012.pdf>. Ajinomoto Co., Inc., Tokyo, Japan.
- Kalinowski J. 2005. The genomes of amino acid-producing corynebacteria, p 37–56. In Eggeling L, Bott M (ed), *Handbook of Corynebacterium glutamicum*. CRC Press, Boca Raton, FL.
- Frunzke J, Bramkamp M, Schweitzer J-E, Bott M. 2008. Population Heterogeneity in *Corynebacterium glutamicum* ATCC 13032 caused by prophage CGP3. *J. Bacteriol.* 190:5111–5119. <http://dx.doi.org/10.1128/JB.00310-08>.
- Baumgart M, Unthan S, Rückert C, Sivalingam J, Grünberger A, Kalinowski J, Bott M, Noack S, Frunzke J. 2013. Construction of a prophage-free variant of *Corynebacterium glutamicum* ATCC 13032—a platform strain for basic research and industrial biotechnology. *Appl. Environ. Microbiol.* 79:6006–6015. <http://dx.doi.org/10.1128/AEM.01634-13>.
- Gödeke J, Paul K, Lassak J, Thormann KM. 2011. Phage-induced lysis enhances biofilm formation in *Shewanella oneidensis* MR-1. *ISME J.* 5:613–626. <http://dx.doi.org/10.1038/ismej.2010.153>.
- Carrolo M, Frias MJ, Pinto FR, Melo-Cristino J, Ramirez M. 2010. Prophage spontaneous activation promotes DNA release enhancing biofilm formation in *Streptococcus pneumoniae*. *PLoS One* 5:e15678. <http://dx.doi.org/10.1371/journal.pone.0015678>.
- Flemming H-C, Neu TR, Wozniak DJ. 2007. The EPS matrix: the “house of biofilm cells.” *J. Bacteriol.* 189:7945–7947. <http://dx.doi.org/10.1128/JB.00858-07>.
- Whitchurch CB, Tolker-Nielsen T, Ragas PC, Mattick JS. 2002. Extracellular DNA required for bacterial biofilm formation. *Science* 295:1487. <http://dx.doi.org/10.1126/science.295.5559.1487>.
- Lwoff A. 1953. Lysogeny. *Bacteriol. Rev.* 17:269–332.
- Luria. 1967. Transduction studies on the role of a *rec+* gene in the ultraviolet induction of prophage lambda. *J. Mol. Biol.* 23:117–133. [http://dx.doi.org/10.1016/S0022-2836\(67\)80021-4](http://dx.doi.org/10.1016/S0022-2836(67)80021-4).
- Oppenheim AB, Kobiler O, Stavans J, Court DL, Adhya S. 2005. Switches in bacteriophage lambda development. *Annu. Rev. Genet.* 39:409–429. <http://dx.doi.org/10.1146/annurev.genet.39.073003.113656>.
- Friedberg EC, Walker GC, Siede W, Wood RD, Schultz RA, Ellenberger T. 2005. DNA repair and mutagenesis. *ASM Press*, Washington, DC.
- Grünberger A, Paczia N, Probst C, Schendzielorz G, Eggeling L, Noack S, Wiechert W, Kohlheyer D. 2012. A disposable picolitre bioreactor for cultivation and investigation of industrially relevant bacteria on the single cell level. *Lab. Chip.* 12:2060–2068. <http://dx.doi.org/10.1039/c2lc40156h>.
- Mustafi N, Grünberger A, Kohlheyer D, Bott M, Frunzke J. 2012. The development and application of a single-cell biosensor for the detection of L-methionine and branched-chain amino acids. *Metab. Eng.* 14:449–457. <http://dx.doi.org/10.1016/j.ymben.2012.02.002>.
- Keilhauer C, Eggeling L, Sahn H. 1993. Isoleucine synthesis in *Corynebacterium glutamicum*: molecular analysis of the *ilvB-ilvN-ilvC* operon. *J. Bacteriol.* 175:5595–5603.
- Kensy F, Zang E, Faulhammer C, Tan R-K, Büchs J. 2009. Validation of a high-throughput fermentation system based on online monitoring of biomass and fluorescence in continuously shaken microtiter plates. *Microb. Cell Fact.* 8:31. <http://dx.doi.org/10.1186/1475-2859-8-31>.

19. Inoue H, Nojima H, Okayama H. 1990. High efficiency transformation of *Escherichia coli* with plasmids. *Gene* 96:23–28. [http://dx.doi.org/10.1016/0378-1119\(90\)90336-P](http://dx.doi.org/10.1016/0378-1119(90)90336-P).
20. Van der Rest ME, Lange C, Molenaar D. 1999. A heat shock following electroporation induces highly efficient transformation of *Corynebacterium glutamicum* with xenogeneic plasmid DNA. *Appl. Microbiol. Biotechnol.* 52:541–545. <http://dx.doi.org/10.1007/s002530051557>.
21. Eikmanns B, Thum-Schmitz N. 1994. Nucleotide sequence, expression and transcriptional analysis of the *Corynebacterium glutamicum* *gltA* gene encoding citrate synthase. *Microbiology* 140:1817–1828. <http://dx.doi.org/10.1099/13500872-140-8-1817>.
22. Jochmann N, Kurze AK, Czaja LF, Brinkrolf K, Brune I, Hüser AT, Hansmeier N, Pühler A, Borovok I, Tauch A. 2009. Genetic makeup of the *Corynebacterium glutamicum* LexA regulon deduced from comparative transcriptomics and in vitro DNA band shift assays. *Microbiology* 155:1459–1477. <http://dx.doi.org/10.1099/mic.0.025841-0>.
23. Hentschel E, Will C, Mustafi N, Burkovski A, Rehm N, Frunzke J. 2013. Destabilized eYFP variants for dynamic gene expression studies in *Corynebacterium glutamicum*. *Microb. Biotechnol.* 6:196–201. <http://dx.doi.org/10.1111/j.1751-7915.2012.00360.x>.
24. Strack RL, Hein B, Bhattacharyya D, Hell SW, Keenan RJ, Glick BS. 2009. A rapidly maturing far-red derivative of DsRed-Express2 for whole-cell labeling. *Biochemistry* 48:8279–8281. <http://dx.doi.org/10.1021/bi900870u>.
25. Grünberger A, Probst C, Heyer A, Wiechert W, Frunzke J, Kohlheyer D. Microfluidic picoliter bioreactor for microbial single cell analysis: fabrication, system setup and operation. *J. Vis Exp.*, in press.
26. Ogino H, Teramoto H, Inui M, Yukawa H. 2008. DivS, a novel SOS-inducible cell-division suppressor in *Corynebacterium glutamicum*. *Mol. Microbiol.* 67:597–608. <http://dx.doi.org/10.1111/j.1365-2958.2007.06069.x>.
27. Pennington JM, Rosenberg SM. 2007. Spontaneous DNA breakage in single living *Escherichia coli* cells. *Nat. Genet.* 39:797–802. <http://dx.doi.org/10.1038/ng2051>.
28. Kamensék S, Podlesek Z, Gillor O, Zgur-Bertok D. 2010. Genes regulated by the *Escherichia coli* SOS repressor LexA exhibit heterogeneous expression. *BMC Microbiol.* 10:283. <http://dx.doi.org/10.1186/1471-2180-10-283>.
29. Bailone A, Levine A, Devoret R. 1979. Inactivation of prophage λ repressor in vivo. *J. Mol. Biol.* 131:553–572. [http://dx.doi.org/10.1016/0022-2836\(79\)90007-X](http://dx.doi.org/10.1016/0022-2836(79)90007-X).
30. Cox MM, Goodman MF, Kreuzer KN, Sherratt DJ, Sandler SJ, Mariani KJ. 2000. The importance of repairing stalled replication forks. *Nature* 2:37–41.
31. Rothstein R, Michel B, Gangloff S. 2000. Replication fork pausing and recombination or “gimme a break.” *Gene Dev.* 14:1–10.
32. Bossi L, Fuentes J, Mora G, Figueroa-Bossi N. 2003. Prophage contribution to bacterial population dynamics. *J. Bacteriol.* 185:6467–6471. <http://dx.doi.org/10.1128/JB.185.21.6467-6471.2003>.
33. Makarova KS, Wolf YI, Koonin EV. 2009. Comprehensive comparative-genomic analysis of type 2 toxin-antitoxin systems and related mobile stress response systems in prokaryotes. *Biol. Direct* 4:19. <http://dx.doi.org/10.1186/1745-6150-4-19>.
34. Loce JM, Loce M, Węgrzyn A, Węgrzyn G. 2012. Altruism of Shiga toxin-producing *Escherichia coli*: recent hypothesis versus experimental results. *Front. Cell Infect. Microbiol.* 2:166. <http://dx.doi.org/10.3389/fcimb.2012.00166>.
35. Watve M, Parab S, Jogdand P, Keni S. 2006. Aging may be a conditional strategic choice and not an inevitable outcome for bacteria. *Proc. Natl. Acad. Sci. U. S. A.* 103:14831–14835. <http://dx.doi.org/10.1073/pnas.0606499103>.
36. Kinoshita S, Udaka S, Shimono M. 2004. Studies on the amino acid fermentation. Part 1. Production of L-glutamic acid by various microorganisms. *J. Gen. Appl. Microbiol.* 50:331–343. <http://dx.doi.org/10.2323/jgam.3.193>.
37. Schäfer A, Tauch A, Jäger Kalinowski WJ, Thierbach G, Pühler A. 1994. Small mobilizable multi-purpose cloning vectors derived from the *Escherichia coli* plasmids pK18 and pK19: selection of defined deletions in the chromosome of *Corynebacterium glutamicum*. *Gene* 145:69–73. [http://dx.doi.org/10.1016/0378-1119\(94\)90324-7](http://dx.doi.org/10.1016/0378-1119(94)90324-7).
38. Cremer J, Eggeling L, Sahl H. 1991. Control of the lysine biosynthesis sequence in *Corynebacterium glutamicum* as analyzed by overexpression of the individual corresponding genes. *Appl. Environ. Microbiol.* 57:1746–1752.

Name of the Journal	Journal of Bacteriology
Impact Factor	2.808
Contribution to body of work	80%
1 st author	Experimental work and writing of the manuscript

Impact of Spontaneous Prophage Induction on the Fitness of Bacterial Populations and Host-Microbe Interactions

Arun M. Nanda,^a Kai Thormann,^b Julia Frunzke^a

Institut für Bio- und Geowissenschaften, IBG-1: Biotechnologie, Forschungszentrum Jülich, Jülich, Germany^a; Institut für Mikrobiologie und Molekularbiologie, Justus-Liebig-Universität Gießen, Gießen, Germany^b

Bacteriophages and genetic elements, such as prophage-like elements, pathogenicity islands, and phage morons, make up a considerable amount of bacterial genomes. Their transfer and subsequent activity within the host's genetic circuitry have had a significant impact on bacterial evolution. In this review, we consider what underlying mechanisms might cause the spontaneous activity of lysogenic phages in single bacterial cells and how the spontaneous induction of prophages can lead to competitive advantages for and influence the lifestyle of bacterial populations or the virulence of pathogenic strains.

The advancement of affordable and publicly available whole-genome sequencing platforms has given rise to sequence data on a wide range of bacterial species. These have revealed that DNA of viral origin represents a highly frequent element of bacterial genomes and can amount to a staggering 20% of the whole bacterial genome (1–3). While some of this DNA content can be accounted for by the presence of fully functional prophages, which are able to undergo a replicative, lytic life cycle, a considerable part of it is made up of prophage-like elements, phage remnants left after incomplete excision events, cryptic prophages, or genetic material acquired by horizontal gene transfer, such as genomic islands and plasmids (4) (Fig. 1). This genetic material can carry genes that influence the virulence of the bacterial host, e.g., cholera toxin (5) and Shiga toxin (6) genes, or the metabolic activities of the host. It is through this inclusion into the genetic circuitry of the microbial host that these elements may have a marked impact on host fitness (7). An important but often unnoted phenomenon is the spontaneous activation of these elements in single cells of bacterial populations even in the absence of an external trigger, a phenomenon dubbed “spontaneous prophage induction” (SPI).

As far back as the 1950s, it was observed that cultures of *Bacillus megaterium* lysogens exhibit free phages in the cultivation medium supernatant when grown under noninducing conditions (8). This spontaneous induction, often accompanied by lysis of the bacterial cell, was long seen as a potentially detrimental process for bacterial populations, as a small percentage of cells would be lost continuously. However, research in the fields of bacterial population dynamics, biofilm formation, and pathogenesis of human diseases has shed new light on the spontaneous induction of prophages.

While it is possible that SPI is merely the result of stochasticity in gene expression (genetic noise) (9) or results from a bona fide induction of the host SOS response (10), only a few studies have so far focused on the exact mechanisms underlying this phenomenon. The work performed in these studies was further supported by the advancement of single-cell analytics such as flow cytometry and time-lapse microscopy in microfluidic cultivation chambers, allowing the analysis of triggers for bacteriophages and mobile genetic elements working in a subset of bacterial populations (11–15). In this review, we set the focus on the triggering of spontaneous activity of prophages or phage remnants and the physiological consequences that this process can have for microbial popula-

tions. In the following, we use the term “spontaneous prophage induction” (SPI) not only to describe the intrinsic stability of lysogens (e.g., in a *recA* mutant background) but also for events specifically triggered in a subset of the population, e.g., during host infection or biofilm formation.

SOS-INDUCED SPI

Because an induced SOS response is responsible for the induction of many lambdoid lysogens, it was discussed by several researchers that spontaneous SOS induction in single cells might trigger the induction of prophages (10). During growth, ongoing (multifork) replication has been shown to cause sporadic DNA damage resulting in the derepression of the SOS genes (16). Recent single-cell studies revealed a small fraction of SOS-induced cells in clonal populations grown under standard conditions, and it is reasonable to infer that a prolonged induction will also lead to the activation of resident prophages (13, 17, 18).

Lwoff first described free phage appearing in the supernatant of noninduced cultures of lysogenic bacteria (8), and it was later shown that recombination-deficient *recA* mutant strains of *Escherichia coli* showed no discernible spontaneous induction of the prophage (19–21). Different parameters were shown to influence the spontaneous induction of phage λ expression in *E. coli*, such as overexpression of CI and deletion of *recA*, thus decreasing the growth rate, or exchanging glucose with glycerol, thus affecting cyclic AMP (cAMP) levels, which have an influence on the SOS response as well (22). In their recent study, Little and Michalowski found that the intrinsic switching rate of *E. coli* lambda lysogens is almost undetectably low ($<10^{-8}$ /generation) in a *recA* mutant background (21). Remarkably, the intrinsic stability very much depends on the cultivation conditions as well as on the occurrence

Accepted manuscript posted online 17 November 2014

Citation Nanda AM, Thormann K, Frunzke J. 2015. Impact of spontaneous prophage induction on the fitness of bacterial populations and host-microbe interactions. *J Bacteriol* 197:410–419. doi:10.1128/JB.02230-14.

Editor: W. Margolin

Address correspondence to Julia Frunzke, j.frunzke@fz-juelich.de.

Copyright © 2015, American Society for Microbiology. All Rights Reserved.
doi:10.1128/JB.02230-14

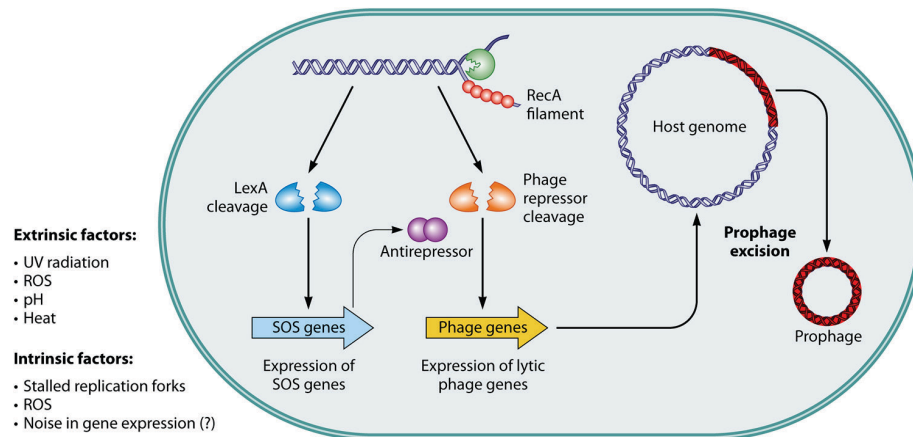


FIG 1 SOS-dependent SPI. A host of extrinsic and intrinsic factors have an influence on the host genome and can lead to spontaneous DNA lesions or stalled polymerases laying bare single-stranded DNA bound by polymerizing RecA proteins. The nucleoprotein filament in turn triggers the autocatalytic cleavage of LexA or CI-like phage repressors. Alleviation of LexA repression leads to the expression of SOS genes—initiating cell growth inhibition and DNA repair. An alternative route is the inactivation of the phage repressor by binding to antirepressor proteins. Inactivation of phage repressors leads to the derepression of the lytic promoters which facilitate the excision of the prophage from the host genome and its packaging into virions and release from the cell by holin- and lysin-mediated cell lysis.

of mutations which render the lysogen unstable. These findings emphasize that SPI has coevolved with its specific trigger (e.g., the SOS response) to optimize the switching frequency over a wide range of naturally occurring inducing conditions.

Recently, it was shown that single cells of *Corynebacterium glutamicum* undergo spontaneous SOS induction under standard cultivation conditions (13). This spontaneous induction of the SOS response is sufficient to induce key promoters within prophage CGP3, among them the genes encoding a putative integrase and lysin (13). Mutant strains lacking *recA* showed only a basal level of spontaneous CGP3 induction, which might be due to stochastic effects (see below) or mutations of the prophage. That stochasticity might play a rather minor role is also emphasized by a study by Livny and Friedman, who could show that SPI of the easily inducible H-19B prophage in almost all cases coincided with the induction of a second prophage in the same cells of Shiga toxin-producing *E. coli* (STEC) lysogens (23).

Another layer of control is added by RecA-independent and yet SOS-dependent SPI. In the case of coliphage 186, the viral Tum protein functions as an antirepressor which binds to the phage repressor, resulting in the induction of lytic growth (24, 25). Expression of *tum* itself is under the control of host LexA, and phage induction is thereby again linked to the SOS response system of the bacteria (Fig. 1). Similar mechanisms were also described for the N15 linear plasmid-prophage of *E. coli* and the Fels-2 *Salmonella enterica* phage (26, 27). Another interesting example is the induction of the CTX prophage of *Vibrio cholerae*, which encodes cholera toxin. Here, expression of the genes required for virion production is directly regulated by host LexA, which binds just upstream of the RstR phage-encoded repressor (28, 29). Repressor inactivation can also be achieved by the transcriptional regulator of the *cps* gene cluster RcsA or by the small RNA DsrA, which relieves repression of *rcaA* (30).

EXTRINSIC FACTORS

In addition to the intrinsic factors which affect genomic DNA or RecA and induce the SOS response, extrinsic factors, such as re-

active oxygen species (ROS) generated within macrophages (31–33) and UV radiation, both of which induce DNA damage, or the effects of antibiotics such as mitomycin C (MmC) (34) and fluoroquinolones (Fq) (35), should be taken into account as well. Fqs and MmC are both able to induce pneumococcal prophages in multiple strains of *Streptococcus pneumoniae* (36). In this bacterium, induction acts via RecA and yet does so in an SOS-independent manner and represents a response to the topoisomerase IV-Fq complex formed or to transcriptional regulation of phage or bacterial genes by DNA supercoiling, which is a result of Fq treatment (36). Further factors which influence the lysogenic maintenance or induction of the prophage should be taken into account as well. The effects of pH, temperature, organic carbon, and the presence of chromium (VI) and the toxic compound potassium cyanide on prophage induction were studied in the ammonia-oxidizing *Nitrospira multiformis* bacterium. Whereas increasing levels of Cr (VI) and KCN led to an increase in prophage induction, a shift toward acidic pH had the most dramatic effect (37). The neutralophile *Helicobacter pylori* B45, which inhabits the human gastric mucosa, was shown to induce its phiHP33 bacteriophage after UV irradiation and at a low pH (38, 39). The opposite relationship was observed for prophage ϕ LC3 of *Lactococcus lactis*, where a decrease in pH reduced the amount of spontaneously induced prophage (40). In their multifactorial experimental setup, the authors revealed that an increase in the levels of simultaneously acting stressors increased SPI. It is tempting to speculate that RecA and the SOS response are responsible for the prophage induction dynamics in this system, because the repressor of *L. lactis* prophage ϕ LC3 belongs to the CI-like repressor family. Indeed, earlier studies showed that changes in intracellular pH influence the stability and binding properties of LexA or CI repressor and thus influence the transcription of target genes (41, 42).

IMPACT OF STOCHASTICITY IN GENE EXPRESSION

Gene expression can be surprisingly dynamic and heterogeneous. Cell-to-cell variation, even in clonal populations of cells grown under the same conditions, has been observed in a variety of dif-

ferent organisms, from mammalian stem cells to bacteria (9, 43). Hence, a plausible mechanism for SPI is that it could result from spontaneous fluctuations in the levels of repressor such that, below a threshold level, the lytic genes would be expressed, leading to switching to the lytic state. This model does not apply in the best-studied case, phage lambda, since SPI requires RecA; in addition, phage mutants with noncleavable repressors do not show SPI, despite the likelihood that expression levels of these mutant proteins would fluctuate in the same way as in the wild type. In contrast, the unstable mutant described by Little and Michalowski likely switches by this mechanism (21). Other examples of switching also appear to result from stochastic fluctuations in gene expression. Spontaneous excision of the mobile element ICE*clc* (integrative and conjugative element encoding *clc* genes) was, for example, shown from the genome of *Pseudomonas knackmussii* B13 (12, 44). Integrative and conjugative elements reside in the host genome and are able to excise and be transferred via conjugation. The excision of ICE*clc* depends on variations in the levels of the RpoS stationary-phase sigma factor among individual cells. RpoS levels reach a threshold at which ICE*clc*-encoded excision factors are expressed, and this state is locked in these single cells, thus maintaining ICE*clc* excision in the form of a bistable state (12). In their recent study on several mycobacteriophages, which are not SOS inducible, Broussard et al. described a novel class of simple switches relying on the site-specific recombination catalyzed by integrases as a key to decision (45). They also observed spontaneous switching from lysogeny to the lytic state and speculated that this might be due to a drop in the repressor level below the threshold or to sporadic expression of the integrase gene (45).

Noise in gene expression is ubiquitous. It can provide a selective advantage by increasing phenotypic heterogeneity within a clonal population of one species or even within microbial communities (e.g., biofilms). It is therefore conceivable that several mobile genetic elements, such as ICE*clc*, pathogenicity islands (PIs), and prophages, exploit noise as a function to modulate the frequency of their spontaneous activation and transfer (Fig. 1).

IMPACT OF LYSOGENIC PROPHAGES ON THE FITNESS OF BACTERIAL POPULATIONS

In their recent review, Bondy-Denomy and Davidson summarized the general positive impact that prophages can have on a population's fitness (46). For instance, this positive impact was impressively demonstrated by the work of Wang et al., who deleted nine cryptic prophages in *E. coli* K-12 (47). These cryptic prophages are unable to propagate into infectious virus particles, and it was assumed that functions which assist their host to propagate in adverse environments were retained. The study revealed not only a decreased growth rate in the prophage-cured strain but also that it was more sensitive to antibiotics, was impaired in adaptation to osmotic stress, and showed a decrease in biofilm formation (see the next section for more details on biofilm formation). Interestingly, seven of the nine deleted prophages were shown to excise spontaneously (47). As we go on to show, this spontaneous activity of prophage elements can have a high impact on the general fitness of bacterial populations under diverse conditions.

SPI can also promote the spread of phages and increased survival of lysogens when they are grown in mixed populations. *Salmonella enterica* serovar Typhimurium harbors four to five full-size prophages, with most being able to undergo lytic devel-

opment (48–50). When clonal populations of strains carrying these prophages were cultivated, spontaneous prophage induction had no apparent consequences for the population due to its immunity to superinfection (51). However, when prophage-carrying strains and those cured of the prophages of the same origin (52) or of different origins (51) were cocultivated, a “selection regime” that forced maintenance and spread of viral DNA was set, with a portion of bacteria being killed due to lytic development of prophages and survivors undergoing lysogenic conversion. One may think of this process as lysogenic bacteria using spontaneous lytic development of their prophages as a weapon, giving them a competitive advantage against nonlysogenized cells. At the same time, the prophage uses this war to its own advantage, with the ultimate goal of spreading its DNA by lysogenic conversion of the nonlysogens (52).

The presence of inducible prophage elements can also be a selective disadvantage, as shown for *Staphylococcus aureus* in the nasopharynx. It is displaced by its relative *Streptococcus pneumoniae*, which generates H₂O₂ and is thus responsible for the formation of hyperoxides via the Fenton reaction. *S. pneumoniae* itself, however, is resistant to them (53). RecA-inducible prophages of *S. aureus* are induced, leading to cell death (54) and, ultimately, displacement of the strain. Thus, despite its positive effect, the presence of lysogenic bacteriophages may add a potential Achilles heel with respect to the fitness of the bacteria which is exploited by bacterial competitors and eventually might even be exploited by the human host.

PHAGES AFFECT MICROBIAL BIOFILM FORMATION

In nature, the vast majority of bacteria is thought to exist in surface-associated communities, commonly referred to as biofilms (55). In biofilms, the cells are encased in a matrix mainly consisting of various extracellular polymeric substances (EPS). The most prominent hallmark of cells growing in such communities is their increased tolerance of a wide range of environmental perturbations, including antibacterial and antibiotic treatments. Biofilm formation varies widely between different species but is often described as a developmental process (56). Phage-induced lysis within biofilms generally leads to an accumulation of extracellular DNA (eDNA) within the community. In concert with the high cell densities commonly occurring in biofilms, this provides a huge pool for horizontal gene transfer (reviewed in references 57 and 58).

An increasing number of studies on several bacterial species have provided evidence that (pro)phages also directly affect the progression of biofilm formation through all stages (Fig. 2). The presence of the phages can lead to biofilm dispersal resulting from cell lysis while at the same time providing the enzymes needed to degrade the extracellular matrix. On the other hand, lysis of a cellular subpopulation may provide biofilm-promoting factors such as matrix components. And finally, phages drive the diversification of the biofilm community, a major factor responsible for the overall fitness of bacterial communities (59).

All three aspects of bacterium-phage interaction in biofilm formation could be identified in *P. aeruginosa* PAO1. When grown in flow cells (hydrodynamic growth conditions), this strain undergoes an intricate biofilm developmental cycle which is strongly affected by the Pf4 filamentous bacteriophage (60). During the initial steps of biofilm formation, Pf4 activity is strongly controlled by production of the PhdA “prevent-host-death” factor

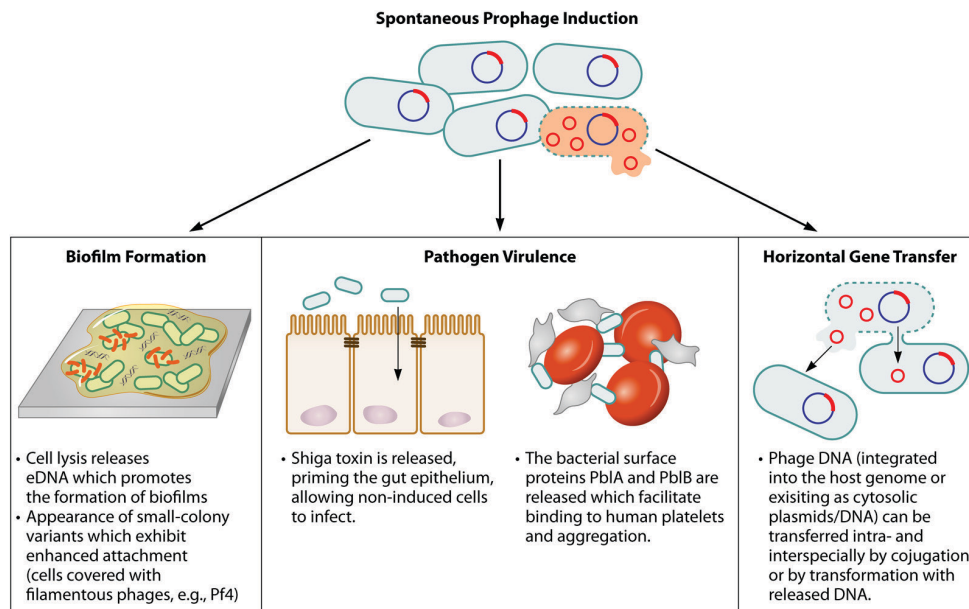


FIG 2 Impact of SPI on host physiology. Spontaneous induction of lysogenic prophages can have manifold effects, such as enhancing biofilm formation, playing a vital role in bacterial virulence or leading to horizontal gene transfer of its own DNA (including virulence factors) and of host genes.

encoded by the host (61). However, activation of the Pf4 prophage in later stages of biofilm formation (62, 63), likely due to elevated ROS levels, results in formation of a hyperinfective form of Pf4 and extensive cell lysis within the three-dimensional structures, leading to dispersal of the biofilm (62, 63). In contrast, complete loss of the prophage or overproduction of the PhdA prevent-host-death factor leads to decreased cell lysis and, notably, less-stable biofilms, a result which was attributed to the lack of eDNA as an important structural component (60, 61). Thus, it was proposed that controlled Pf4-mediated cell lysis is required for the release of biofilm-promoting factors, such as eDNA, in *P. aeruginosa* biofilm formation (64, 65). Activity of Pf4 phages coincided with formation of small-colony variants of *P. aeruginosa* PAO1, which were characterized by increased biofilm formation capacities (66). In addition, loss of the phage significantly decreased the virulence of *P. aeruginosa* PAO1 in mice, which has been attributed to phage-induced strain variations (60). This example nicely illustrates how the components of phage-host interactions are intimately linked and have evolved to benefit microbial group behaviors.

This is further exemplified in *E. coli*, in which the CP4-57, DLP12, e14, and rac cryptic prophages affect the biofilm formation of their host (47, 67). Presumably, under conditions of nutrient limitation and the presence of uncharged tRNAs, the Hha regulator activates lytic prophage genes in CP4-57 and DLP12, resulting in cell death and dispersal (68). Notably, excision of CP4-57 and its subsequent loss from the chromosome predominantly occurred in biofilm cells. These cells exhibit enhanced flagellum-mediated motility and decreased nutrient metabolism, thereby broadening the diversity of the population (67).

The diverse roles phages might play during biofilm formation are reflected in several further studies. Propagation of biofilm formation through phage-mediated lysis and eDNA release has been proposed for two other bacterial species, *Streptococcus pneumoniae* and *Shewanella oneidensis* MR-1. Spontaneous SV1-mediated

cell lysis was shown to occur in *S. pneumoniae*, and, accordingly, deletion of the SV1 phage lysin led to a decrease in cell lysis, eDNA release, and biofilm formation (69). In *S. oneidensis*, three prophages, MuSo1, MuSo2, and LambdaSo, jointly affect lysis and eDNA release, and consequently, a mutant devoid of all three phages is severely impaired in all stages of biofilm formation (70). Recent studies on this species have demonstrated that environmental iron levels are an important factor involved in inducing expression of LambdaSo in a RecA-dependent fashion during biofilm formation (71). Another highly interesting example for host-phage interactions is the lysogenic infection of *P. aeruginosa* PA14 with bacteriophage DMS3. Lysogeny results in decreased biofilm formation and bacterial swarming. Notably, this effect is dependent on the clustered regularly interspaced short palindromic repeat (CRISPR)-CAS system of the host (72).

These examples illustrate the complex interaction between (pro)phages and their hosts with respect to group behaviors such as biofilm formation. Given the fact that prophage genes are commonly among the highly regulated genes during biofilm formation and that many potential cell surface factors are encoded by prophages, it is likely that we have as yet seen only the tip of the iceberg.

SPONTANEOUS PROPHAGE ACTIVITY PROMOTES HOST VIRULENCE

A major reason we are interested in bacteria is their impact on humans. Early in the last century, d'Hérelle discovered that it is not only the relationship between humans and bacteria that is of importance but rather that bacteriophages need to be included as well (73). This seems plausible, especially when changing focus to the emergence of virulence in pathogenic bacterial strains. The formation of biofilms, which we have just covered, is in itself already an important factor for pathogen virulence. In many bacte-

rial infections, the first step is attachment and adhesion to the right host cells (74).

Once they are established within the host, the release of extracellular toxins is a hallmark of several pathogens. For example, Shiga toxin-producing *E. coli* (STEC) bacteria release Shiga toxins in the gut. The life cycle of STEC bacteria and their Stx-encoding prophages exemplifies how the spontaneous induction of prophages in a small number of cells is important for pathogenic traits (Fig. 2). The colonization of the gastrointestinal tract of ruminants was assumed to rely on the spontaneous induction of a subset of STEC serovar O157:H7 cells (75). It was proposed that the presence of a small fraction of induced STEC cells would lead to a sufficient release of Shiga toxin and thus to diarrhea, enabling the spread of the remaining uninduced lysogenic cells (23). Indeed, a basal level of spontaneous induction could be shown for Stx-encoding prophage H-19B of STEC serovar O26:H19 (23). Remarkably, the level of SPI was significantly higher than the level of induction of λ in the same strain background, suggesting that this higher frequency of SPI coevolved to meet the requirements for toxin release of the pathogenic host strain.

In Shiga toxin-producing *E. coli* (STEC) bacteria, the spontaneous induction of prophages increases the fitness of the entire bacterial population within the host environment by priming the host's epithelial cells for infection (23, 75, 76). In the proposed model, a small fraction of cells induces the Stx-encoding prophages, leading to Shiga toxin release and, in consequence, priming the gut epithelial cells by the expression and relocation of nucleolin and further receptors to the epithelial cell surface. These receptors were previously shown to bind to the bacterial surface protein intimin, thus promoting STEC colonization (77–79). In these bacteria, expression of a type 3 secretion system (T3S), which is required for colonization, was shown to be influenced by the presence of Stx-encoding prophages. Reconstitution in an *E. coli* K-12 background provided evidence for a negative impact of lysogeny (in particular, that associated with *cII*) on expression of the T3S (reduction by about 2-fold). However, the effects described in this study were rather small and their actual impact on host-microbe interaction remains to be elucidated.

Evidence for the role of SPI in other human diseases is only beginning to emerge. One example is seen in infective endocarditis, which is an inflammation of the inner lining of the heart. It is often caused by *Streptococcus mitis*. In this organism, the surface expression of ϕ SM1 prophage-encoded PblA and PblB is dependent on the presence of holin and lysin, which are expressed in the course of prophage induction (80). Upon permeabilization and lysis of the bacterial host cell, PblA and PblB are released into the culture medium, bind choline within the bacterial cell wall of unlysed cells, and mediate platelet binding and aggregation (81) (Fig. 2; deletion of *pblA* and *pblB* leads to a 40% reduction in binding). The bacterial lysin itself also plays a role in platelet binding. Through its interaction with choline, it becomes cell wall associated and can directly bind platelet fibrinogen (82). *Enterococcus faecalis* is a leading cause of hospital-acquired bacterial infections and may cause urinary tract infections, intra-abdominal infections, and infective endocarditis (83). *E. faecalis* strain V583 is polylysogenic for 7 prophage-like elements (termed V583-pp1 to V583-pp7) (Table 1). It was shown that three of these, pp1, pp4, and pp6, are important for adhesion to human platelets, which is possibly achieved by expression of the genes encoding PblA and PblB which are homologous to those of *S. mitis* (84). Thus, these

examples nicely reveal that SPI triggered lysis of a small fraction of cells, possibly promoting the adhesion of the remaining noninduced part of the population.

Besides having a direct effect on bacterial virulence, the role that spontaneous prophage activity plays in horizontal gene transfer of virulence-associated factors is of great concern (85, 86). *S. aureus* pathogenicity islands encoding toxins (SaPI) are highly mobile and packaged into small infectious particles (87, 88). SaPI-bov1 (89) and SaPI-bov2 (90) are two SaPIs which contain the *tst* gene encoding the toxic shock syndrome toxin (TSST) and the *bap* (biofilm-associated protein) gene (91), which is needed for persistence in mammary tissue (90), respectively. Once excised, both PIs are transferred due to the action of resident prophages. It was shown for both PIs that they spontaneously excise from *S. aureus* genomes. Consequently, it was postulated that, due to the spontaneous induction of resident prophages in combination with the low-level activation of SaPIs, packaging into transducible phage particles is ensured and represents a serious case of horizontal gene transfer in habitats colonized by staphylococci (92).

PHAGE-PHAGE INTERACTION

Besides the effect that phages have on their bacterial host or on human physiology, phages can also influence one another. For STEC cells, it was shown that repressor proteins of different Stx-encoding prophages mutually influence their spontaneous induction, in turn influencing the stability of the lysogenic state and, ultimately, the virulence due to Stx production (93). Another example is found in *Salmonella* species. Infection of *Salmonella enterica* with P22 or SE1 leads to a *kil*-dependent induction of the SOS response (94). This in turn activates the LexA-controlled antirepressors which bind the Gifsy phage repressors (Fig. 1) (95). The phage repressor of Gifsy-2, however, is insensitive to the antirepressors of Gifsy-1 and Gifsy-3. Rather, it is inactivated by the antirepressor of the Fels-1 prophage. This Fels-1 antirepressor is neither regulated by LexA nor involved in Fels-1 induction at all (Fels-1 induction relies on a λ CI-like repressor cleavage mechanism). Thus, the ability of prophages to influence the stability of other prophages and the properties of antirepressors with respect to recognizing noncognate substrates allow multilayered induction regulation in polylysogenic strains.

CONCLUSION

More and more studies are indicating that the spontaneous activity of prophages or prophage-like elements has a marked impact on their bacterial host and even on the host the bacteria live in. Looking back on the advances that have been made since the turn of the century, it is fascinating to think about the developments that are going to be achieved in the upcoming years. Key to research questions centering on the phenotypic heterogeneity of populations is the advancement of the single-cell analytic platforms which have become common in modern microbiology and which will see an even broader use in the upcoming years (11, 14, 96, 97). Recent studies have shown the power of flow cytometry coupled with the use of fluorescent reporters and live-cell imaging enabled by microfluidic devices in elucidating mechanisms governing the activity of foreign DNA within bacterial genomes (12, 13). Combined with classical molecular biology approaches, these recent advances in single-cell analytics shed new light on the dynamics of microbial populations and host-microbe interaction.

Spontaneous prophage activity affects the formation of bio-

TABLE 1 Spontaneously induced genetic elements discussed in this review

Species	Prophage(s)	Impact on physiology	Reference(s)	Classification	Induction
<i>Corynebacterium glutamicum</i>	CGP3	The cryptic prophage CGP3 excises and replicates in a small fraction of wild-type populations; deletion of CGP3 leads to an increase in plasmid copy no. and heterologous protein production and increased transformation efficiency	13, 99, 100	Prophage	MmC, UV
<i>Enterococcus faecalis</i>	pp1, pp4, pp6	Prophages promote platelet binding, encode PblA and PblB homologs from <i>S. mitis</i>	84	Prophage	pp1, pp4: MmC
<i>Escherichia coli</i>	Δ9 cryptic prophages	Deletion of all 9 cryptic prophages leads to a decreased growth rate, increased sensitivity to antibiotics, impaired adaptation to osmotic stress, and a decrease in biofilm formation; excision of CP4-57 in biofilms increases flagellum-mediated motility and decreases nutrient metabolism	47, 67	Cryptic prophages	e14 induced by MmC
<i>Helicobacter pylori</i>	phiHP33	Bacteriophage phiHP33 expression is induced at a low level after exposure to UV treatment or acidic pH	38	Prophage	UV radiation and acidic environment
<i>Lactococcus lactis</i>	φLC3	Nutrient availability, temp, pH, and osmolarity influence the induction of the prophage, either stabilizing the lysogenic state or inducing spontaneous induction dramatically	40	Prophage	Excised by different environmental conditions
Shiga toxin-producing <i>Escherichia coli</i>	H19-B, 933W	Induction of Stx-producing prophages leads to expression of <i>stx</i> genes and release of Shiga toxin into the surrounding area; Shiga toxin primes the gut epithelium for infection of the noninduced by expression of a type 3 secretion system	23	Prophage	UV, MmC, pressure
<i>Pseudomonas aeruginosa</i> PAO1	Pf4	The presence and activation of Pf4 at later stages are required for proper biofilm formation and survival in host systems; conversion to a hyperinfectious form enables biofilm dispersal and leads to small-colony variants with increased biofilm formation ability	60–63, 66	Prophage	
<i>Pseudomonas aeruginosa</i> PA14	DMS3	The prophage decreases biofilm formation and swarming in concert with the host's CRISPR-CAS system	72	Prophage	
<i>Salmonella enterica</i>	P22, SE1, Gifsy-1, Gifsy-2, Gifsy-3, Fels-1	The prophages of <i>S. enterica</i> influence one another; infection with P22/SE1 leads to induction of the SOS response, which in turn activates antirepressors of the Gifsy-1 and Gifsy-3 repressors; the Gifsy-2 repressor, in turn, is inactivated by the antirepressor of Fels-1 prophage, a CI-like repressor	95	Prophage	Gifsy-1, Gifsy-2, Gifsy-3, Fels-1, P22: MmC
<i>Shewanella oneidensis</i> MR-1	MuSo1, MuSo2, LamdaSO	The prophages jointly enhance biofilm formation through release of biofilm-promoting factors such as eDNA	70	Prophage	UV radiation
<i>Staphylococcus aureus</i>	80α, φ11	Induction of prophages by induction of the SOS response leads to cell lysis	54	Prophage	MmC, ciprofloxacin

(Continued on following page)

TABLE 1 (Continued)

Species	Prophage(s)	Impact on physiology	Reference(s)	Classification	Induction
<i>Staphylococcus aureus</i>	SaPIbov1, SaPIbov2	Virulence factors encoded on pathogenicity islands SaPIbov1 and SaPIbov2 are transferred by horizontal gene transfer, playing a role in acquisition of novel virulence factors	89, 90	Pathogenicity island	Spontaneous induction by Sip integrase; horizontal dissemination stimulated by SOS-induced prophages 80 α , ϕ 11, and ϕ 147
<i>Streptococcus mitis</i>	ϕ SM1	Proteins PblA and PblB are released by cell lysis; they bind to choline in the bacterial cell wall and promote binding to human platelets and aggregation	81	Prophage	ND ^a
<i>Streptococcus pneumoniae</i>	SV1	The prophage enhances biofilm formation through release of biofilm-promoting factors such as eDNA	69	Prophage	MmC

^a ND, not determined.

films and the virulence of human pathogens. It will be through studies on the evolution of prophages and bacteria and the biology underlying distinct activities, such as spontaneous excision or induced cell death, that we gain the understanding to utilize the weapons used in the ongoing war between phages and bacteria to our advantage in the form of phage therapy (98).

ACKNOWLEDGMENTS

Our work is supported by the Deutsche Forschungsgemeinschaft (SPP 1617 grant FR 2759/2-1) and by the Helmholtz Association (Young Investigator grant VH-NG-716).

Especially, we thank reviewer 3 of the *Journal of Bacteriology* for critical reading of the manuscript and for many helpful suggestions.

REFERENCES

- Canchaya C, Fournous G, Brüßow H. 2004. The impact of prophages on bacterial chromosomes. *Mol Microbiol* 53:9–18. <http://dx.doi.org/10.1111/j.1365-2958.2004.04113.x>.
- Casjens S. 2003. Prophages and bacterial genomics: What have we learned so far? *Mol Microbiol* 49:277–300. <http://dx.doi.org/10.1046/j.1365-2958.2003.03580.x>.
- Hatfull GF, Hendrix RW. 2011. Bacteriophages and their genomes. *Curr Opin Virol* 1:298–303. <http://dx.doi.org/10.1016/j.coviro.2011.06.009>.
- Dobrindt U, Hochhut B, Hentschel U, Hacker J. 2004. Genomic islands in pathogenic and environmental microorganisms. *Nat Rev Microbiol* 2:414–424. <http://dx.doi.org/10.1038/nrmicro884>.
- Waldor MK, Mekalanos JJ. 1996. Lysogenic conversion by a filamentous phage encoding cholera toxin. *Science* 272:1910–1914. <http://dx.doi.org/10.1126/science.272.5270.1910>.
- Neely MN, Friedman DI. 1998. Arrangement and functional identification of genes in the regulatory region of lambdoid phage H-19B, a carrier of a Shiga-like toxin. *Gene* 223:105–113. [http://dx.doi.org/10.1016/S0378-1119\(98\)00236-4](http://dx.doi.org/10.1016/S0378-1119(98)00236-4).
- Brown NF, Wickham ME, Coombes BK, Finlay BB. 2006. Crossing the line: selection and evolution of virulence traits. *PLoS Pathog* 2:e42. <http://dx.doi.org/10.1371/journal.ppat.0020042>.
- Lwoff A. 1953. Lysogeny. *Bacteriol Rev* 17:269–332.
- Elowitz MB, Levine AJ, Siggia ED, Swain PS. 2002. Stochastic gene expression in a single cell. *Science* 297:1183–1186. <http://dx.doi.org/10.1126/science.1070919>.
- Little JW. 1990. Chance phenotypic variation. *Trends Biochem Sci* 15:138.
- Locke JCW, Elowitz MB. 2009. Using movies to analyse gene circuit dynamics in single cells. *Nat Rev Microbiol* 7:383–392. <http://dx.doi.org/10.1038/nrmicro2056>.
- Miyazaki R, Minoia M, Pradervand N, Sulser S, Reinhard F, van der Meer JR. 2012. Cellular variability of RpoS expression underlies subpopulation activation of an integrative and conjugative element. *PLoS Genet* 8:e1002818. <http://dx.doi.org/10.1371/journal.pgen.1002818>.
- Nanda AM, Heyer A, Krämer C, Grünberger A, Kohlheyer D, Frunzke J. 25 October 2013. Analysis of SOS-induced spontaneous prophage induction in *Corynebacterium glutamicum* at the single-cell level. *J Bacteriol* <http://dx.doi.org/10.1128/JB.01018-13>.
- Nebe-von-Caron G, Stephens PJ, Hewitt CJ, Powell JR, Badley RA. 2000. Analysis of bacterial function by multi-colour fluorescence flow cytometry and single cell sorting. *J Microbiol Methods* 42:97–114. [http://dx.doi.org/10.1016/S0167-7012\(00\)00181-0](http://dx.doi.org/10.1016/S0167-7012(00)00181-0).
- Shapiro HM. 2000. Microbial analysis at the single-cell level: tasks and techniques. *J Microbiol Methods* 42:3–16. [http://dx.doi.org/10.1016/S0167-7012\(00\)00167-6](http://dx.doi.org/10.1016/S0167-7012(00)00167-6).
- Cox MM, Goodman MF, Kreuzer KN, Sherratt DJ, Sandler SJ, Mariani KJ. 2000. The importance of repairing stalled replication forks. *Nature* 404:37–41. <http://dx.doi.org/10.1038/35003501>.
- McCool JD, Long E, Petrosino JF, Sandler HA, Rosenberg SM, Sandler SJ. 2004. Measurement of SOS expression in individual *Escherichia coli* K-12 cells using fluorescence microscopy. *Mol Microbiol* 53:1343–1357. <http://dx.doi.org/10.1111/j.1365-2958.2004.04225.x>.
- Pennington JM, Rosenberg SM. 2007. Spontaneous DNA breakage in single living *Escherichia coli* cells. *Nat Genet* 39:797–802. <http://dx.doi.org/10.1038/ng2051>.
- Brooks K, Clark AJ. 1967. Behavior of λ bacteriophage in a recombination deficient strain of *Escherichia coli*. *J Virol* 1:283–293.
- Hertman I, Luria SE. 1967. Transduction studies on the role of a *rec+* gene in the ultraviolet induction of prophage lambda. *J Mol Biol* 23:117–133. [http://dx.doi.org/10.1016/S0022-2836\(67\)80021-4](http://dx.doi.org/10.1016/S0022-2836(67)80021-4).
- Little JW, Michalowski CB. 2010. Stability and instability in the lysogenic state of phage lambda. *J Bacteriol* 192:6064–6076. <http://dx.doi.org/10.1128/JB.00726-10>.
- Czyz A, Los M, Wrobel B, Wegrzyn G. 2001. Inhibition of spontaneous induction of lambdoid prophages in *Escherichia coli* cultures: simple procedures with possible biotechnological applications. *BMC Biotechnol* 1:1. <http://dx.doi.org/10.1186/1472-6750-1-1>.
- Livny J, Friedman DI. 2004. Characterizing spontaneous induction of Stx encoding phages using a selectable reporter system. *Mol Microbiol* 51:1691–1704. <http://dx.doi.org/10.1111/j.1365-2958.2003.03934.x>.
- Lamont I, Brumby AM, Egan JB. 1989. UV induction of coliphage 186: prophage induction as an SOS function. *Proc Natl Acad Sci U S A* 86:5492–5496. <http://dx.doi.org/10.1073/pnas.86.14.5492>.
- Shearwin KE, Brumby AM, Egan JB. 1998. The Tum protein of coliphage 186 is an antirepressor. *J Biol Chem* 273:5708–5715. <http://dx.doi.org/10.1074/jbc.273.10.5708>.
- Bunny K, Liu J, Roth J. 2002. Phenotypes of *lexA* mutations in *Salmonella enterica*: evidence for a lethal *lexA* null phenotype due to the Fels-2

- prophage. *J Bacteriol* 184:6235–6249. <http://dx.doi.org/10.1128/JB.184.22.6235-6249.2002>.
27. Mardanov AV, Ravin NV. 2007. The antirepressor needed for induction of linear plasmid-prophage N15 belongs to the SOS regulon. *J Bacteriol* 189:6333–6338. <http://dx.doi.org/10.1128/JB.00599-07>.
 28. Quinones M, Kimsey HH, Waldor MK. 2005. LexA cleavage is required for CTX prophage induction. *Mol Cell* 17:291–300. <http://dx.doi.org/10.1016/j.molcel.2004.11.046>.
 29. Waldor MK, Friedman DI. 2005. Phage regulatory circuits and virulence gene expression. *Curr Opin Microbiol* 8:459–465. <http://dx.doi.org/10.1016/j.mib.2005.06.001>.
 30. Rozanov DV, D'Ari R, Sineoky SP. 1998. RecA-independent pathways of lambdaoid prophage induction in *Escherichia coli*. *J Bacteriol* 180:6306–6315.
 31. Figueroa-Bossi N, Bossi L. 1999. Inducible prophages contribute to *Salmonella* virulence in mice. *Mol Microbiol* 33:167–176. <http://dx.doi.org/10.1046/j.1365-2958.1999.01461.x>.
 32. Lee K-M, Park Y, Bari W, Yoon MY, Go J, Kim SC, Lee H-I, Yoon SS. 2012. Activation of cholera toxin production by anaerobic respiration of trimethylamine N-oxide in *Vibrio cholerae*. *J Biol Chem* 287:39742–29752. <http://dx.doi.org/10.1074/jbc.M112.394932>.
 33. Wagner PL, Neely MN, Zhang X, Acheson DWK, Waldor MK, Friedman DI. 2001. Role for a phage promoter in Shiga toxin 2 expression from a pathogenic *Escherichia coli* strain. *J Bacteriol* 183:2081–2085. <http://dx.doi.org/10.1128/JB.183.6.2081-2085.2001>.
 34. Tomasz M. 1995. Mitomycin C: small, fast and deadly (but very selective). *Chem Biol* 2:575–579. [http://dx.doi.org/10.1016/1074-5521\(95\)90120-5](http://dx.doi.org/10.1016/1074-5521(95)90120-5).
 35. Piddock LJV, Wise R. 1987. Induction of the SOS response in *Escherichia coli* by 4-quinolone antimicrobial agents. *FEMS Microbiol Lett* 41:289–294. <http://dx.doi.org/10.1111/j.1574-6968.1987.tb02213.x>.
 36. López E, Domenech A, Ferrándiz MJ, Frias MJ, Ardanuy C, Ramirez M, García E, Liñares J, de la Campa AG. 2014. Induction of prophages by fluoroquinolones in *Streptococcus pneumoniae*: implications for emergence of resistance in genetically-related clones. *PLoS One* 9:e94358. <http://dx.doi.org/10.1371/journal.pone.0094358>.
 37. Choi J, Kotay SM, Goel R. 2010. Various physico-chemical stress factors cause prophage induction in *Nitrosospora multififormis* 25196—an ammonia oxidizing bacteria. *Water Res* 44:4550–4558. <http://dx.doi.org/10.1016/j.watres.2010.04.040>.
 38. Alves de Matos AP, Lehours P, Timóteo A, Roxo-Rosa M, Vale FF. 2013. Comparison of induction of B45 *Helicobacter pylori* prophage by acid and UV radiation. *Microsc Microanal* 19:27–28. <http://dx.doi.org/10.1017/S1431927613000755>.
 39. Lehours P, Vale FF, Bjursell MK, Melefors O, Advani R, Glavas S, Guegueniat J, Gontier E, Lacomme S, Alves Matos A, Menard A, Megraud F, Engstrand L, Andersson AF. 2011. Genome sequencing reveals a phage in *Helicobacter pylori*. *mBio* 2:e00239-11. <http://dx.doi.org/10.1128/mBio.00239-11>.
 40. Lunde M, Aastveit AH, Blatny JM, Nes IF. 2005. Effects of diverse environmental conditions on {phi}LC3 prophage stability in *Lactococcus lactis*. *Appl Environ Microbiol* 71:721–727. <http://dx.doi.org/10.1128/AEM.71.2.721-727.2005>.
 41. Dri AM, Moreau PL. 1994. Control of the LexA regulon by pH: evidence for a reversible inactivation of the LexA repressor during the growth cycle of *Escherichia coli*. *Mol Microbiol* 12:621–629. <http://dx.doi.org/10.1111/j.1365-2958.1994.tb01049.x>.
 42. Schuldiner S, Agmon V, Brandsma J, Cohen A, Friedman E, Padan E. 1986. Induction of SOS functions by alkaline intracellular pH in *Escherichia coli*. *J Bacteriol* 168:936–939.
 43. Levine JH, Lin Y, Elowitz MB. 2013. Functional roles of pulsing in genetic circuits. *Science* 342:1193–1200. <http://dx.doi.org/10.1126/science.1239999>.
 44. Miyazaki R, van der Meer JR. 2011. A dual functional origin of transfer in the ICE_{Edc} genomic island of *Pseudomonas knackmussii* B13. *Mol Microbiol* 79:743–758. <http://dx.doi.org/10.1111/j.1365-2958.2010.07484.x>.
 45. Broussard GW, Oldfield LM, Villanueva VM, Lunt BL, Shine EE, Hatfull GF. 2013. Integration-dependent bacteriophage immunity provides insights into the evolution of genetic switches. *Mol Cell* 49:237–248. <http://dx.doi.org/10.1016/j.molcel.2012.11.012>.
 46. Bondy-Denomy J, Davidson AR. 2014. When a virus is not a parasite: the beneficial effects of prophages on bacterial fitness. *J Microbiol* 52:235–242. <http://dx.doi.org/10.1007/s12275-014-4083-3>.
 47. Wang X, Kim Y, Ma Q, Hong SH, Pokusaeva K, Sturino JM, Wood TK. 2010. Cryptic prophages help bacteria cope with adverse environments. *Nat Commun* 1:147–147. <http://dx.doi.org/10.1038/ncomms1146>.
 48. Figueroa-Bossi N, Uzzau S, Maloriol D, Bossi L. 2001. Variable assortment of prophages provides a transferable repertoire of pathogenic determinants in *Salmonella*. *Mol Microbiol* 39:260–271. <http://dx.doi.org/10.1046/j.1365-2958.2001.02234.x>.
 49. Hooton SPT, Timms AR, Moreton J, Wilson R, Connerton IF. 2013. Complete genome sequence of *Salmonella enterica* serovar Typhimurium U288. *Genome Announc* 1:e00467-13. <http://dx.doi.org/10.1128/genomeA.00467-13>.
 50. Porwollik S, Wong RM-Y, McClelland M. 2002. Evolutionary genomics of *Salmonella*: gene acquisitions revealed by microarray analysis. *Proc Natl Acad Sci U S A* 99:8956–8961. <http://dx.doi.org/10.1073/pnas.122153699>.
 51. Bossi L, Fuentes JA, Mora G, Figueroa-Bossi N. 2003. Prophage contribution to bacterial population dynamics. *J Bacteriol* 185:6467–6471. <http://dx.doi.org/10.1128/JB.185.21.6467-6471.2003>.
 52. Gama JA, Reis AM, Domingues I, Mendes-Souares H, Matos AM, Dionisio F. 2013. Temperate bacterial viruses as double-edged swords in bacterial warfare. *PLoS One* 8:e59043. <http://dx.doi.org/10.1371/journal.pone.0059043>.
 53. Pericone CD, Park S, Imlay JA, Weiser JN. 2003. Factors contributing to hydrogen peroxide resistance in *Streptococcus pneumoniae* include pyruvate oxidase (SpxB) and avoidance of the toxic effects of the Fenton reaction. *J Bacteriol* 185:6815–6825. <http://dx.doi.org/10.1128/JB.185.23.6815-6825.2003>.
 54. Selva L, Viana D, Regev-Yochay G, Trzcinski K, Corpa JM, Lasa I, Novick RP, Penadés JR. 2009. Killing niche competitors by remote-control bacteriophage induction. *Proc Natl Acad Sci U S A* 106:1234–1238. <http://dx.doi.org/10.1073/pnas.0809600106>.
 55. Costerton JW, Lewandowski Z. 1995. Microbial biofilms. *Annu Rev Microbiol* 49:711–745. <http://dx.doi.org/10.1146/annurev.mi.49.100195.003431>.
 56. Monds RD, O'Toole GA. 2009. The developmental model of microbial biofilms: ten years of a paradigm up for review. *Trends Microbiol* 17:73–87. <http://dx.doi.org/10.1016/j.tim.2008.11.001>.
 57. Madsen JS, Burmolle M, Hansen LH, Sorensen SJ. 2012. The interconnection between biofilm formation and horizontal gene transfer. *FEMS Immunol Med Microbiol* 65:183–195. <http://dx.doi.org/10.1111/j.1574-695X.2012.00960.x>.
 58. Molin S, Tolker-Nielsen T. 2003. Gene transfer occurs with enhanced efficiency in biofilms and induces enhanced stabilisation of the biofilm structure. *Curr Opin Biotechnol* 14:255–261. [http://dx.doi.org/10.1016/S0958-1669\(03\)00036-3](http://dx.doi.org/10.1016/S0958-1669(03)00036-3).
 59. Veening J-W, Smits WK, Kuipers OP. 2008. Bistability, epigenetics, and bet-hedging in bacteria. *Annu Rev Microbiol* 62:193–210. <http://dx.doi.org/10.1146/annurev.micro.62.081307.163002>.
 60. Rice SA, Tan CH, Mikkelsen PJ, Kung V, Woo J, Way M, Hauser A, McDougald D, Webb JS, Kjelleberg S. 2009. The biofilm life cycle and virulence of *Pseudomonas aeruginosa* are dependent on a filamentous prophage. *ISME J* 3:271–282. <http://dx.doi.org/10.1038/ismej.2008.109>.
 61. Petrova OE, Schurr JR, Schurr MJ, Sauer K. 2011. The novel *Pseudomonas aeruginosa* two-component regulator BfmR controls bacteriophage-mediated lysis and DNA release during biofilm development through PhdA. *Mol Microbiol* 81:767–783. <http://dx.doi.org/10.1111/j.1365-2958.2011.07733.x>.
 62. Kirov SM, Webb JS, O'May CY, Reid DW, Woo JKK, Rice SA, Kjelleberg S. 2007. Biofilm differentiation and dispersal in mucoid *Pseudomonas aeruginosa* isolates from patients with cystic fibrosis. *Microbiology* 153(Pt 10):3264–3274. <http://dx.doi.org/10.1099/mic.0.2007/009092-0>.
 63. Webb JS, Thompson LS, James S, Charlton T, Tolker-Nielsen T, Koch B, Givskov M, Kjelleberg S. 2003. Cell death in *Pseudomonas aeruginosa* biofilm development. *J Bacteriol* 185:4585–4592. <http://dx.doi.org/10.1128/JB.185.15.4585-4592.2003>.
 64. Allesen-Holm M, Barken KB, Yang L, Klausen M, Webb JS, Kjelleberg S, Molin S, Givskov M, Tolker-Nielsen T. 2006. A characterization of DNA release in *Pseudomonas aeruginosa* cultures and biofilms. *Mol Microbiol* 59:1114–1128. <http://dx.doi.org/10.1111/j.1365-2958.2005.05008.x>.
 65. Whitchurch CB, Tolker-Nielsen T, Ragas PC, Mattick JS. 2002. Extracellular DNA required for bacterial biofilm formation. *Science* 295:1487. <http://dx.doi.org/10.1126/science.295.5559.1487>.
 66. Webb JS, Lau M, Kjelleberg S. 2004. Bacteriophage and phenotypic

- variation in *Pseudomonas aeruginosa* biofilm development. *J Bacteriol* 186:8066–8073. <http://dx.doi.org/10.1128/JB.186.23.8066-8073.2004>.
67. Wang X, Kim Y, Wood TK. 2009. Control and benefits of CP4-57 prophage excision in *Escherichia coli* biofilms. *ISME J* 3:1164–1179. <http://dx.doi.org/10.1038/ismej.2009.59>.
 68. García-Contreras R, Zhang X-S, Kim Y, Wood TK. 2008. Protein translation and cell death: the role of rare tRNAs in biofilm formation and in activating dormant phage killer genes. *PLoS One* 3:e2394. <http://dx.doi.org/10.1371/journal.pone.0002394>.
 69. Carrolo M, Frias MJ, Pinto FR, Melo-Cristino J, Ramirez M. 2010. Prophage spontaneous activation promotes DNA release enhancing biofilm formation in *Streptococcus pneumoniae*. *PLoS One* 5:e15678. <http://dx.doi.org/10.1371/journal.pone.0015678>.
 70. Gödeke J, Paul K, Lassak J, Thormann KM. 2011. Phage-induced lysis enhances biofilm formation in *Shewanella oneidensis* MR-1. *ISME J* 5:613–626. <http://dx.doi.org/10.1038/ismej.2010.153>.
 71. Binnenkade L, Teichmann L, Thormann KM. 2014. Iron triggers λ So prophage induction and release of extracellular DNA in *Shewanella oneidensis* MR-1 biofilms. *Appl Environ Microbiol* 80:5304–5316. <http://dx.doi.org/10.1128/AEM.01480-14>.
 72. Zegans ME, Wagner JC, Cady KC, Murphy DM, Hammond JH, O'Toole GA. 2009. Interaction between bacteriophage DMS3 and host CRISPR region inhibits group behaviors of *Pseudomonas aeruginosa*. *J Bacteriol* 191:210–219. <http://dx.doi.org/10.1128/JB.00797-08>.
 73. d'Hérelle F. 1917. Sur un microbe invisible antagoniste des bacilles dysentérique. *Acad Sci Paris* 165:373–375.
 74. Parsek MR, Singh PK. 2003. Bacterial biofilms: an emerging link to disease pathogenesis. *Annu Rev Microbiol* 57:677–701. <http://dx.doi.org/10.1146/annurev.micro.57.030502.090720>.
 75. Xu X, McAteer SP, Tree JJ, Shaw DJ, Wolfson EBK, Beatson SA, Roe AJ, Allison LJ, Chase-Topping ME, Mahajan A, Tozzoli R, Woolhouse MEJ, Morabito S, Gally DL. 2012. Lysogeny with Shiga toxin 2-encoding bacteriophages represses type III secretion in enterohemorrhagic *Escherichia coli*. *PLoS Pathog* 8:e1002672. <http://dx.doi.org/10.1371/journal.ppat.1002672>.
 76. Łoć JM, MŁoć Węgrzyn A, Węgrzyn G. 4 January 2013, posting date. Altruism of Shiga toxin-producing *Escherichia coli*: recent hypothesis versus experimental results. *Front Cell Infect Microbiol* <http://dx.doi.org/10.3389/fcimb.2012.00166>.
 77. Robinson CM, Sinclair JF, Smith MJ, O'Brien AD. 2006. Shiga toxin of enterohemorrhagic *Escherichia coli* type O157:H7 promotes intestinal colonization. *Proc Natl Acad Sci U S A* 103:9667–9672. <http://dx.doi.org/10.1073/pnas.0602359103>.
 78. Shimizu T, Ohta Y, Noda M. 2009. Shiga toxin 2 is specifically released from bacterial cells by two different mechanisms. *Infect Immun* 77:2813–2823. <http://dx.doi.org/10.1128/IAI.00060-09>.
 79. Tyler JS, Beeri K, Reynolds JL, Alteri CJ, Skinner KG, Friedman JH, Eaton KA, Friedman DI. 2013. Prophage induction is enhanced and required for renal disease and lethality in an EHEC mouse model. *PLoS Pathog* 9:e1003236. <http://dx.doi.org/10.1371/journal.ppat.1003236>.
 80. Siboo IR, Bensing BA, Sullam PM. 2003. Genomic organization and molecular characterization of SM1, a temperate bacteriophage of *Streptococcus mitis*. *J Bacteriol* 185:6968–6975. <http://dx.doi.org/10.1128/JB.185.23.6968-6975.2003>.
 81. Mitchell J, Siboo IR, Takamatsu D, Chambers HF, Sullam PM. 2007. Mechanism of cell surface expression of the *Streptococcus mitis* platelet binding proteins PblA and PblB. *Mol Microbiol* 64:844–857. <http://dx.doi.org/10.1111/j.1365-2958.2007.05703.x>.
 82. Seo HS, Xiong YQ, Mitchell J, Seepersaud R, Bayer AS, Sullam PM. 2010. Bacteriophage lysis mediates the binding of *Streptococcus mitis* to human platelets through interaction with fibrinogen. *PLoS Pathog* 6:e1001047. <http://dx.doi.org/10.1371/journal.ppat.1001047>.
 83. Arias CA, Murray BE. 2012. The rise of the *Enterococcus*: beyond vancomycin resistance. *Nat Rev Microbiol* 10:266–278. <http://dx.doi.org/10.1038/nrmicro2761>.
 84. Matos RC, Lapaque N, Rigottier-Gois L, Debarbieux L, Meylheuc T, Gonzalez-Zorn B, Repoila F, Lopes MDF, Serror P. 2013. *Enterococcus faecalis* prophage dynamics and contributions to pathogenic traits. *PLoS Genet* 9:e1003539. <http://dx.doi.org/10.1371/journal.pgen.1003539>.
 85. Cheetham BF, Katz ME. 1995. A role for bacteriophages in the evolution and transfer of bacterial virulence determinants. *Mol Microbiol* 18:201–208. http://dx.doi.org/10.1111/j.1365-2958.1995.mmi_18020201.x.
 86. Chen J, Novick RP. 2009. Phage-mediated intergeneric transfer of toxin genes. *Science* 323:139–141. <http://dx.doi.org/10.1126/science.1164783>.
 87. Lindsay JA, Ruzin A, Ross HF, Kurepina N, Novick RP. 1998. The gene for toxic shock toxin is carried by a family of mobile pathogenicity islands in *Staphylococcus aureus*. *Mol Microbiol* 29:527–543. <http://dx.doi.org/10.1046/j.1365-2958.1998.00947.x>.
 88. Ruzin A, Lindsay J, Novick RP. 2001. Molecular genetics of SaPII - a mobile pathogenicity island in *Staphylococcus aureus*. *Mol Microbiol* 41:365–377. <http://dx.doi.org/10.1046/j.1365-2958.2001.02488.x>.
 89. Fitzgerald JR, Monday SR, Foster TJ, Bohach GA, Hartigan PJ, Meaney WJ, Smyth CJ. 2001. Characterization of a putative pathogenicity island from bovine *Staphylococcus aureus* encoding multiple superantigens. *J Bacteriol* 183:63–70. <http://dx.doi.org/10.1128/JB.183.1.63-70.2001>.
 90. Ubeda C, Tormo MA, Cucarella C, Trotonda P, Foster TJ, Lasa I, Penadés JR. 2003. Sip, an integrase protein with excision, circularization and integration activities, defines a new family of mobile *Staphylococcus aureus* pathogenicity islands. *Mol Microbiol* 49:193–210. <http://dx.doi.org/10.1046/j.1365-2958.2003.03577.x>.
 91. Cucarella C, Solano C, Valle J, Amorena B, Í. Lasa Penadés JR. 2001. Bap, a *Staphylococcus aureus* surface protein involved in biofilm formation. *J Bacteriol* 183:2888–2896. <http://dx.doi.org/10.1128/JB.183.9.2888-2896.2001>.
 92. Ubeda C, Maiques E, Knecht E, Lasa I, Novick RP, Penadés JR. 2005. Antibiotic-induced SOS response promotes horizontal dissemination of pathogenicity island-encoded virulence factors in staphylococci. *Mol Microbiol* 56:836–844. <http://dx.doi.org/10.1111/j.1365-2958.2005.04584.x>.
 93. Serra-Moreno R, Jofre J, Muniesa M. 2008. The CI repressors of Shiga toxin-converting prophages are involved in coinfection of *Escherichia coli* strains, which causes a down regulation in the production of Shiga toxin 2. *J Bacteriol* 190:4722–4735. <http://dx.doi.org/10.1128/JB.00069-08>.
 94. Campoy S, Hervás A, Busquets N, Erill I, Teixidó L, Barbé J. 2006. Induction of the SOS response by bacteriophage lytic development in *Salmonella enterica*. *Virology* 351:360–367. <http://dx.doi.org/10.1016/j.virol.2006.04.001>.
 95. Lemire S, Figueroa-Bossi N, Bossi L. 2011. Bacteriophage crosstalk: coordination of prophage induction by trans-acting antirepressors. *PLoS Genet* 7:e1002149. <http://dx.doi.org/10.1371/journal.pgen.1002149>.
 96. Grünberger A, Paczia N, Probst C, Schendzielorz G, Eggeling L, Noack S, Wiechert W, Kohlheyer D. 2012. A disposable picolitre bioreactor for cultivation and investigation of industrially relevant bacteria on the single cell level. *Lab Chip* 12:2060–2068. <http://dx.doi.org/10.1039/c2lc40156h>.
 97. Wang P, Robert L, Pelletier J, Dang WL, Taddei F, Wright A, Jun S. 2010. Robust growth of *Escherichia coli*. *Curr Biol* 20:1099–1103. <http://dx.doi.org/10.1016/j.cub.2010.04.045>.
 98. Lu TK, Koeris MS. 2011. The next generation of bacteriophage therapy. *Curr Opin Microbiol* 14:524–531. <http://dx.doi.org/10.1016/j.mib.2011.07.028>.
 99. Baumgart M, Unthan S, Rückert C, Sivalingam J, Grünberger A, Kalinowski J, Bott M, Noack S, Frunzke J. 2013. Construction of a prophage-free variant of *Corynebacterium glutamicum* ATCC 13032 for use as a platform strain for basic research and industrial biotechnology. *Appl Environ Microbiol* 79:6006–6015. <http://dx.doi.org/10.1128/AEM.01634-13>.
 100. Frunzke J, Bramkamp M, Schweitzer JE, Bott M. 2008. Population heterogeneity in *Corynebacterium glutamicum* ATCC 13032 caused by prophage CGP3. *J Bacteriol* 190:5111–5119. <http://dx.doi.org/10.1128/JB.00310-08>.

Name of the Journal	Journal of Bacteriology
Impact Factor	2.808
Contribution to body of work	50%
1 st author	Literature research and writing of the manuscript

Assessing the Role of the SOS Response in the induction of prophage CGP3 of *Corynebacterium glutamicum*

Arun M. Nanda and Julia Frunzke*

Institute of Bio- and Geosciences, IBG-1: Biotechnology, Forschungszentrum Jülich, Germany

Summary

Taken together, we could show in this study that deletion and mutation of key SOS genes either leads to the down- or upregulation not only of SOS-regulated genes but also of prophage CGP3-encoded genes, as we had previously postulated, depending on the mutations' effect on the activity of the SOS response. We showed this by analysis of promoter fusions in the BioLector microbioreactor and by analysis of transcript abundance in the $\Delta recA$ mutant in comparison to the wild type strain. The deletion of *recA* does not, however, lead to a decrease in the number of spontaneously induced cells, as we had expected. Furthermore, we observed a high increase in *Plys*in and *PcglII*M promoter activity in the LexA_G143D strain.

*Corresponding author:

Dr. Julia Frunzke

Email: j.frunzke@fz-juelich.de

Phone: +49 2461 61-5430

Fax: +49 2461 61-2710

Keywords: bacteriophage, spontaneous induction, SOS response, FACS, mitomycin C

The gram-positive soil bacterium *Corynebacterium glutamicum* is a platform organism of biotechnology used for the industrial production of more than four million tons of amino acids, mainly L-glutamate and L-lysine, per year. Furthermore, it is a close relative of the medically relevant human pathogen *Mycobacterium tuberculosis*, causal agent of tuberculosis. Fermentations utilizing other bacteria, e.g. *Escherichia coli*, face the challenge of contamination with lytic phages. These can impact the fitness and production of the producing strain,

markedly impacting yield and leading to economic drawbacks. So far, no infectious bacteriophages have been discovered for *C. glutamicum*. The relevance of *C. glutamicum* in today's biotechnology and health sectors makes it all the more interesting to study phage-microbe relationships in this species. Whole-genome sequencing of *C. glutamicum* ATCC 13032 revealed three prophages that are integrated into its genome (CGP1-3) (Kalinowski *et al.*, 2003). Whereas CGP1 and CGP2 are probably cryptic phages, CGP3 retains the ability to excise from the

genome, as evidenced by the occurrence of circular CGP3 DNA molecules (Frunzke *et al.*, 2008).

Excision of lysogenized prophages is often triggered by activation of the host SOS response. The SOS response is a cellular response to DNA damage, which is conserved across most bacterial phyla. The single-strand binding protein RecA recognizes damaged DNA, polymerizes along it, and becomes catalytically active (RecA*). RecA* catalyzes the autoproteolysis of the central SOS repressor LexA which represses expression of target genes by binding to target motifs, so called SOS boxes. Upon cleavage, repression of the target genes is alleviated, amongst them genes for DNA repair, a putative error-prone DNA polymerase and a cell division inhibitor (Ogino *et al.*, 2008; Jochmann *et al.*, 2009). In lambdoid phages, the phage repressor mimics the catalytic center of LexA, thus undergoing cleavage upon activation of the SOS response. This leads to the transcription and expression of genes involved in prophage excision, virion assembly and ultimately cell lysis and phage release.

Previous studies have revealed that the SOS response is conserved in *C. glutamicum* as well (Jochmann *et al.*, 2009). Microarray analysis of wild type and $\Delta lexA$ cells treated with the DNA-crosslinking agent mitomycin C (MmC) revealed more than 40 genes belonging to the SOS regulon (Jochmann *et al.*, 2009). In further experiments, an expression of genes contained in the 187 kbp stretch of CGP3 DNA could be observed upon addition of MmC (Donovan *et al.*,

2015). Because it was shown that CGP3 excision occurs spontaneously in a small number of cells (Frunzke *et al.*, 2008), we analyzed the relationship of the SOS response and CGP3 induction at the single-cell level using promoter fusions to fluorescent reporter genes in combination with flow cytometry (Nanda *et al.*, 2014). We observed a high correlation between the activities of the key SOS gene *recA* to key CGP3 genes *int2* (*cg2071*) and the putative lysin *cg1974* in cells, which showed a spontaneous induction of the SOS response (Nanda *et al.*, 2014).

SOS and CGP3 promoter fusions in mutant strains

The aim of this study was to gain a deeper knowledge of the SOS response in *C. glutamicum* and its role in CGP3 induction. To this end, strains with deletions or modifications of key SOS genes were transformed with promoter fusions of SOS and CGP3 promoters. The previously described strain $\Delta lexA$ (Jochmann *et al.*, 2009; Nanda *et al.*, 2014) was utilized along with newly created strains $\Delta recA$, $\Delta recB$, $\Delta cg2040$ (Heyer, 2013), $\Delta CGP3$ (Baumgart *et al.*, 2013), and LexA_G143D. For deletion or mutation of the according genes, the gene SOEing procedure was utilized (Horton *et al.*, 1989) (see supplementary table 1 for oligonucleotides and resulting strains). Studies on *E. coli* showed that the glycine residue G85 is the substrate of the autoproteolytic cleavage reaction. Its mutation leads to the LexA non-cleavable

TABLE 1 Bacterial strains and plasmids used in this study

Strain or plasmid	Characteristics	Source or reference
Strains		
<i>E. coli</i> DH5	<i>supE44 ΔlacU169</i> (φ80 <i>lacZ</i> DM15) <i>hsdR17 recA1 endA1 gyrA96 thi-1 relA1</i>	Invitrogen
<i>C. glutamicum</i>		
ATCC13032	Biotin-auxotrophic wild type	(Kinoshita <i>et al.</i> , 2004)
ATCC 13032 Δ <i>lexA</i>	In-frame deletion of the gene <i>lexA</i> (cg2114)	(Jochmann <i>et al.</i> , 2009)
ATCC 13032 Δ <i>recA</i>	In-frame deletion of the gene <i>recA</i> (cg2141)	(Nanda <i>et al.</i> , 2014)
ATCC 13032 LexA G143D	Amino acid exchange in LexA cleavage site (glycine to aspartic acid) at position 143	This work
ATCC 13032 Δ <i>cg2040</i>	In-frame deletion of the gene <i>cg2040</i>	(Heyer, 2013)
ATCC 13032 Δ <i>CGP3</i>	In-frame deletion of the prophage CGP3 (cg1890-cg2071)	(Baumgart <i>et al.</i> , 2013)
Plasmids		
pJC1	Kan ^r , Amp ^r ; <i>C. glutamicum</i> shuttle vector	(Cremer <i>et al.</i> , 1990)
pAN6- <i>e2-crimson</i>	Kan ^r ; pAN6 derivative for expression of E2-Crimson under the control of the <i>Ptac</i> promoter	(Baumgart <i>et al.</i> , 2013)
pK19 <i>mobsacB</i>	Kan ^r , ori <i>VE. coli sacB lacZ</i>	(Baumgart <i>et al.</i> , 2013)
pJC1- <i>PrecA-e2-crimson</i>	pJC1 derivative containing the promoter of <i>recA</i> - <i>cg2141</i> (260 bp) fused to <i>e2-crimson</i> ; the insert includes the promoter of <i>divS</i> , 30 bp of the coding sequence, a stop codon, and an additional ribosome binding site (pET16) in front of <i>e2-crimson</i>	(Nanda <i>et al.</i> , 2014)
pJC1- <i>PdivS-e2-crimson</i>	pJC1 derivative containing the promoter of <i>divS</i> - <i>cg2113</i> (411 bp) fused to <i>e2-crimson</i> ; the insert includes the promoter of <i>divS</i> , 30 bp of the coding sequence, a stop codon, and an additional ribosome binding site (pET16) in front of <i>e2-crimson</i>	(Nanda <i>et al.</i> , 2014)
pJC1- <i>Pint2-e2-crimson</i>	pJC1 derivative containing the promoter of <i>int2</i> - <i>cg2070-2071</i> (250 bp) fused to <i>e2-crimson</i> ; the insert includes the promoter of <i>int2</i> , 30 bp of the coding sequence, a stop codon, and an additional ribosome binding site (pET16) in front of <i>e2-crimson</i>	(Nanda <i>et al.</i> , 2014)
pJC1- <i>Plysin-e2-crimson</i>	pJC1 derivative containing the promoter of <i>lysin</i> (250 bp) fused to <i>e2-crimson</i> ; the insert includes the promoter of <i>int2</i> , 30 bp of the coding sequence, a stop codon, and an additional ribosome binding site (pET16) in front of <i>e2-crimson</i>	(Nanda <i>et al.</i> , 2014)
pJC1- <i>PrecN-e2-crimson</i>	pJC1 derivative containing the promoter of <i>recN</i> - <i>cg1602</i> (250 bp) fused to <i>e2-crimson</i> ; the insert includes the promoter of <i>int2</i> , 30 bp of the coding sequence, a stop codon, and an additional ribosome binding site (pET16) in front of <i>e2-crimson</i>	(Nanda <i>et al.</i> , 2014)
pJC1- <i>PcgIIM-e2-crimson</i>	pJC1 derivative containing the promoter of <i>cgIIM</i> - <i>cg1996</i> (250 bp) fused to <i>e2-crimson</i> ; the insert includes the promoter of <i>int2</i> , 30 bp of the coding sequence, a stop codon, and an additional ribosome binding site (pET16) in front of <i>e2-crimson</i>	This work
pJC1- <i>PdnaE2-e2-crimson</i>	pJC1 derivative containing the promoter of <i>dnaE2</i> - <i>cg0738</i> (250 bp) fused to <i>e2-crimson</i> ; the insert includes the promoter of <i>int2</i> , 30 bp of the coding sequence, a stop codon, and an additional ribosome binding site (pET16) in front of <i>e2-crimson</i>	This work

phenotype (Ind⁻) (Lin and Little, 1988). In *C. glutamicum* we mutated the conserved glycine residue G143 by point mutation to obtain the LexA_G143D mutant (GGT → GDT).

At the onset of the experiments, we expected mutants of key SOS genes to have an effect on the LexA-regulated promoter fusions of P_{recA} and P_{divS} . Furthermore, if the SOS response is a causal trigger or plays an integral part in the induction of CGP3 genes, the promoter fusions P_{int2} and P_{lysin} should be affected as well, showing the highest activity in strains with an activated SOS response and a decreased activity in strains with an impaired SOS response.

As expected, strains with mutations in key players of the SOS response ($\Delta recA$, $\Delta lexA$, LexA_G143D) were impaired in their growth (data not shown), caused by the cell's inability to repair damaged DNA or resolve stalled replication forks (Cox *et al.*, 2000). $\Delta lexA$ displayed the highest growth inhibition, $\Delta recA$ reached a 25% lower final OD₆₀₀ than the wild type strain and LexA_G143D showed a reduced growth rate during the logarithmic growth phase, but reached a comparable final OD₆₀₀ compared to the wild type strain (data not shown).

It had been shown previously that overexpression of the CI-like phage regulator Cg2040 regulates its own promoter and influences the transcription of neighboring genes (Heyer, 2013). A deletion of *cg2040* influenced a small number of genes, none of them known to be involved in the SOS response or CGP3 induction. Nevertheless, the deletion strain was utilized to check for effects on the SOS

response or induction of CGP3, which might have been missed in previous studies. The $\Delta cg2040$ strain showed no significant change in reporter output for any of the promoter fusions tested in this study - with or without addition of MmC - in comparison to the wild type strain. Therefore it can safely be assumed that the putative regulator plays no role in *recA*, *divS*, *int2* or *lysin* regulation.

No significant increase was observed for P_{recA} , P_{divS} and P_{int2} in the strain $\Delta CGP3$ in which the entire prophage CGP3 was deleted (Figure 1). In case of the SOS-responsive genes this comes as no surprise, because we did not expect elements encoded on the prophage CGP3 to feed back onto the regulation of the SOS response. The activity of P_{lysin} was increased in the deletion strain after addition of MmC (maximum induction ~36 in comparison to ~25 in the wild type) (Figure 2, Table 2). This hints at potentially SOS-regulated regulatory elements encoded on the prophage playing a role in stabilizing its lysogenic state. Upon deletion of these putative elements, P_{lysin} and perhaps other prophage-induction-related genes are activated.

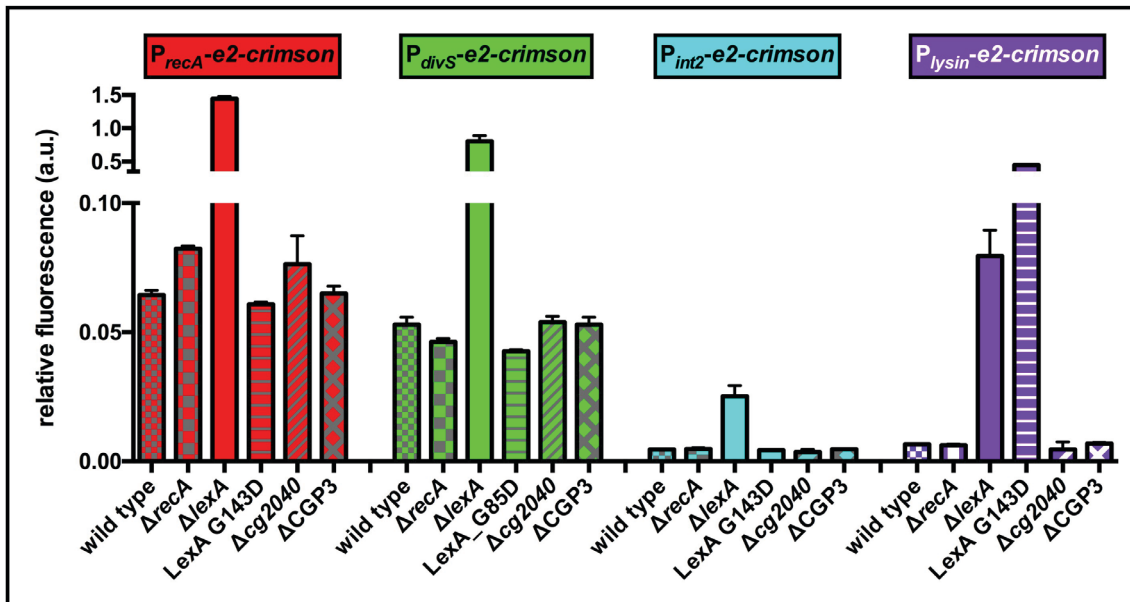


Figure 1: Average fluorescent output of the promoter fusions pJC1- P_{recA} -e2-crimson (red), pJC1- P_{divS} -e2-crimson (green), pJC1- P_{int2} -e2-crimson (cyan), and pJC1- P_{lysIn} -e2-crimson (purple). The cells were cultivated in the BioLector microbioreactor system and the average relative fluorescence intensity measured during a period of 4 hours in the stationary growth phase.

Activity of P_{recA}

Addition of MmC induced P_{recA} activity 14-fold (Table 2), which is expected as P_{recA} is repressed by LexA and the SOS response leads to $recA$ transcription. We observed a 22-fold induction of P_{recA} when $lexA$ was deleted and thus the SOS response is activated constitutively. Deletion of $recA$ leads to a slightly increased basal transcription of $recA$ (increased by a factor of 1.3). SOS induction, however, is reduced by 40%. Whereas increased P_{recA} is counterintuitive in the SOS-inhibited $\Delta recA$ strain, this might be a cellular response to not sufficiently activating the SOS response to a basal level. Under SOS-inducing conditions, however, the activity behaves as expected. The LexA_G143D mutation decreases basal transcription by 10% and MmC-induced induction by 20%. Removing $recA$ or inhibiting the SOS response by

mutation of LexA should lead to a decrease in P_{recA} output under SOS-inducing conditions, which we could readily observe.

Activity of P_{divS}

As observed for P_{recA} , addition of MmC led to an eleven-fold increase in $divS$ promoter activity, which could be further elevated by addition of MmC (15-fold induction). The SOS-inhibiting strains $\Delta recA$ and LexA_G143D showed a slight decrease in basal transcription of 10% and 20%, respectively. After addition of MmC, the maximum induction of P_{divS} merely reached 30% in $\Delta recA$ and 40% in LexA_G143D. The activity of the $divS$ promoter – which is a *bona fide* down-stream target of the SOS response – is highly impacted by the SOS-inhibiting mutants under SOS-inducing conditions but not as much under standard cultivation conditions, whereas activity of

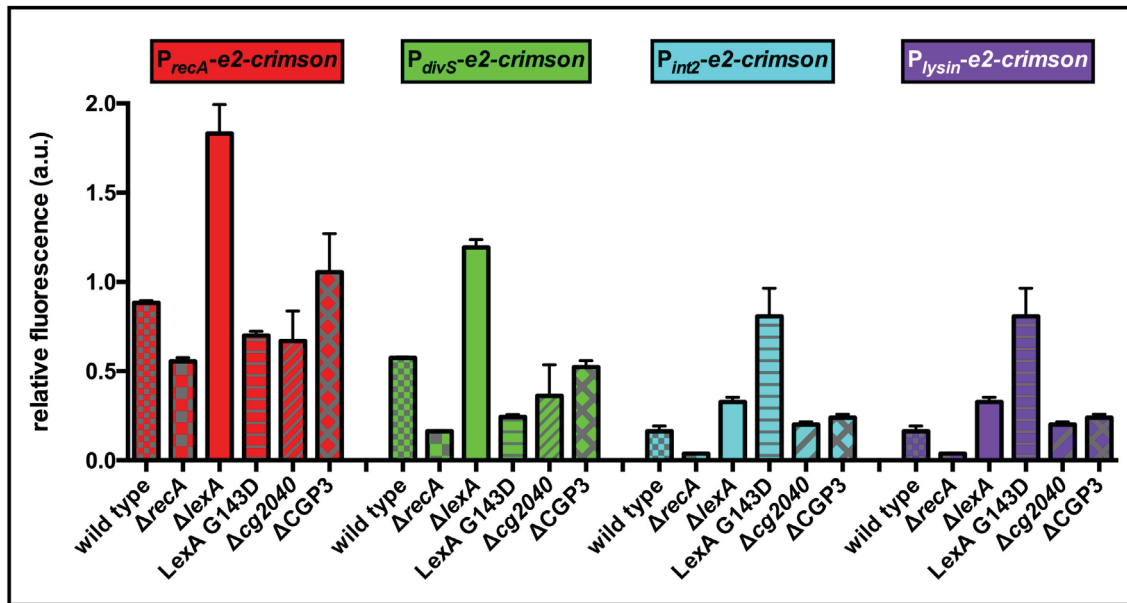


Figure 2: Average fluorescent output of the promoter fusions $pJC1$ - P_{recA} -e2-crimson (red), $pJC1$ - P_{divS} -e2-crimson (green), $pJC1$ - P_{int2} -e2-crimson (cyan), and $pJC1$ - P_{lysIn} -e2-crimson (purple). At an OD_{600} of ~ 4 $2\mu M$ of MmC was added to the cultivation chambers. The cells were cultivated in the BioLector microbioreactor system and the average relative fluorescence intensity measured during a 4 hour period in the stationary growth phase.

the *recA* promoter is less impacted. Therefore, we can assume that the cell has a certain capacity for increasing the transcription of its key SOS gene *recA* under circumstances when a functional SOS response can not be fully induced. Basal transcription of *divS*, however, is not affected by this process, as would be expected, because a dysregulation of *divS* transcription could have potentially lethal effects due to its growth-inhibiting properties.

Activity of P_{int2}

Because we had shown previously that P_{int2} activity correlates positively to an induced SOS response (Nanda *et al.*, 2014), the ten-fold induction of P_{int2} by MmC came as no surprise. The highest induction was seen in the $\Delta lexA$ strain where basal transcription was increased nearly six-fold and SOS-

induced induction showed a fold change of 16 compared to 10 in the wild type strain. In the SOS-inhibited strain $\Delta recA$ the basal activity was unchanged, yet MmC-inducibility was impaired and only reached 60%. This reinforces our hypothesis that the SOS response plays an integral part in CGP3 induction, yet other unknown factors influence it as well.

Activity of P_{lysIn}

P_{lysIn} showed the highest SOS-inducibility of all tested reporters in this study with a 25-fold induction. Maximum induction in the $\Delta lexA$ strain was also the highest of all tested reporters (50-fold induction). Furthermore, deletion of *recA* highly influenced the SOS-inducibility of P_{lysIn} without affecting its basal transcription. These findings show that CGP3 *lysIn* is highly induced by the SOS response and

links the SOS response to CGP3 induction even more than our previous studies showed, which found the single-cell correlation between *recA* and *lysin* to be lower than that for *int2*. Surprisingly, the highest induction of all tested reporters

under any circumstances was found in the LexA_G143D strain, where P_{lysin} activity was induced by more than 120-fold. This high increase in the mutant strain is addressed later in further detail (see section 'Effects of the G143D mutation in LexA').

TABLE 2 Fold change in promoter activity with and without addition of MmC. All activities were referenced to values for the wild type without addition of MmC to calculate fold changes.

Strain	<i>PrecA</i>		<i>PdivS</i>		<i>Pint2</i>		<i>Plysin</i>	
	-	+	-	+	-	+	-	+
WT	1	14	1	11	1	10	1	25
Δ <i>lexA</i>	22	28	15	23	5.5	16	12	50
Δ <i>recA</i>	1.3	9	0.87	3	1	6	1	6
LexA_G85D	0.94	11	0.80	5	0.9	6	68	122
Δ <i>cg2040</i>	1.2	10	1	7	0.8	4	0.7	11
Δ CGP3	1	16	0,9	10	1	8	1	36

Effect of the mutations and deletions on spontaneous P_{recA} activity

We previously showed that P_{recA} is spontaneously induced under non-SOS-inducing conditions. Therefore, we tested whether this spontaneous activity could be abolished by mutation of LexA or deletion of *recA*. To this end, we analyzed cultures of wild type, Δ *recA* and LexA_G143D strains with the P_{recA} -*e2-crimson* promoter fusion by flow cytometry and analyzed the percentage of induced cells and the total fluorescent output of the analyzed cells (Figure 3). After inoculation in CGXII minimal media at an OD_{600} of 1 in Flowerplates®, the cultures were agitated until cultures reached an OD_{600} of ~4. Samples were then analyzed in the BD FACSaria II flow cytometer. Surprisingly, under non-inducing conditions, a deletion

of *recA* not only leads to an increased P_{recA} activity (1.5-fold induction) but also to an increased number of cells with an induced P_{recA} activity (35% compared to 1% in wild type). By transforming the Δ *recA* strain with a plasmid carrying a copy of the wild type *recA* gene under control of its native promoter, we were able to complement the growth phenotype (Supplementary Figure 1). The LexA_G143D strain, however, showed the expected smaller number of spontaneously SOS-induced cells (0.8% compared to 1% in wild type) and a lower total fluorescence of the analyzed cells (94%). Because both the Δ *recA* and LexA_G143D strains not only showed a significant difference in P_{recA} and P_{lysin} activity but also in the amount of spontaneously induced cells, different hypotheses can be explored: i) RecA and LexA have separate domains for normal and

spontaneous SOS induction. ii) Manipulation of RecA and LexA influence so far unknown components, which have an effect on the normal and spontaneous induction of the SOS response.

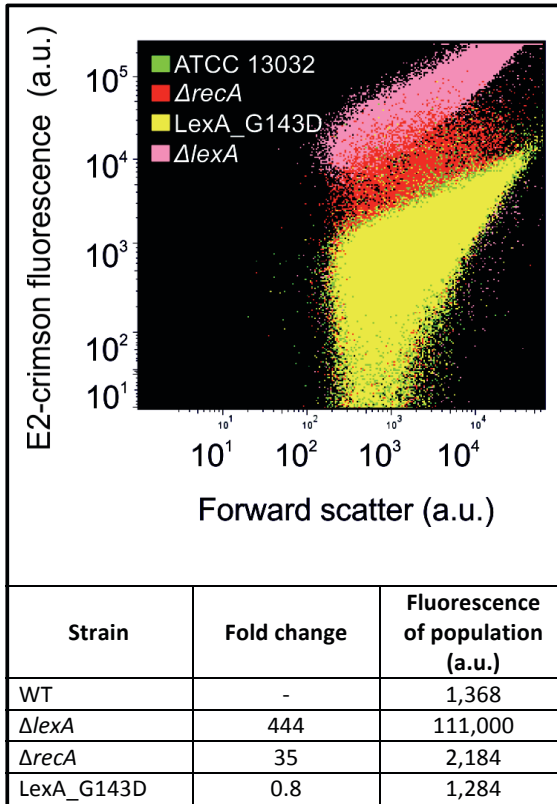


FIGURE 3 Comparison of spontaneous induction of P_{recA} -*e2-crimson* in wild type (green), $\Delta recA$ (red), and LexA_G143D (yellow) mutant strains. $\Delta lexA$ (pink) is shown as a reference for maximum induction of the SOS response. Cells were cultivated in the BioLector microbioreactor system, samples removed at an OD_{600} of 4 and analyzed in the BD FACSArialII flow cytometer.

Effects of the G143D mutation in LexA

The G143D mutation we introduced in LexA led to a high increase of P_{lysin} promoter activity. We tested the activity of other known SOS-responsive promoter fusions in the LexA_G143D strain to assess whether the observed activities are an isolated case

for P_{lysin} or affect other genes of the SOS stimulon as well. *cglIM* codes for a putative DNA methyltransferase (Schäfer, 1997) that is part of a putative restriction modification system whose deletion is necessary for curing the prophage CGP3 (Baumgart *et al.*, 2013), *recN* is a homolog of the *E. coli* protein *recN* which belongs to the SMC family of proteins (Hirano, 1995) and is involved in the repair of double-strand by loading of RecA protein onto single-stranded DNA, and *dnaE2* is a homolog of the *M. tuberculosis* gene *dnaE2*, which encodes an error-prone DNA polymerase (PolIV) that plays a role in the DNA repair machinery and mutagenesis of the SOS response (Boshoff, 2003).

Analysis in the flow cytometer revealed heightened activities for P_{lysin} , P_{cglIM} , and for P_{recN} . P_{recA} and P_{dnaE2} showed a low induction of the promoter fusion, comparable to the induction seen in the wild type strain (Figure 4). The dynamics of the reporter output were observed during cultivation in the BioLector microbioreactor system (Figure 5). P_{lysin} and P_{cglIM} had a two- to three-fold higher activity than the other tested promoter fusions in the wild type and LexA_G143D strains (0.15 a.u. compared to 0.05-0.09 a.u.). The activity of P_{lysin} exceeded that of P_{cglIM} during the logarithmic growth phase and displayed a two-fold increased activity during stationary growth. P_{recN} , P_{recA} and P_{dnaE2} started with activities of 0.05-0.09. In the stationary growth phase P_{dnaE2} and P_{recA} showed similar activities with P_{recN} showing an elevated activity of 0.15.

Taken together, the three promoter fusions

P_{lysin} , P_{cglIM} , and P_{recN} showed a significantly elevated activity compared to that in the wild type strain (Figure 5) or the activities of P_{recA} and P_{dnaE2} . *lysin* and *cglIM* are both encoded on CGP3, whereas the other genes are encoded outside of the prophage region. Because we observed that the LexA_G143D strain had a generally reduced SOS response (Figures 1-3), which we introduced by altering the cleavability of LexA, a higher induction of genes would not hint at an increased level of LexA cleavage, but rather at a weaker binding of LexA to the respective SOS box. The SOS box consensus motif TcGAA(a/c)AnnTGTtCGA that was elucidated for *C. glutamicum* in Jochmann *et al.* is a highly variable motif (Jochmann *et al.*, 2009). In the case of *lysin*, *cglIM* and *recN*, the LexA_G143D mutation might have altered the binding properties of LexA to the corresponding SOS boxes, thus shifting the equilibrium between bound and free state towards free state and increasing transcription from this promoter. So far, no SOS box has been described for the promoter of *lysin*.

The level of P_{lysin} activity in the LexA_G143D strain is markedly higher than that in the $\Delta lexA$ strain. For other SOS-responsive promoters, such as P_{recA} or P_{divS} , $\Delta lexA$ displays the highest possible induction of the SOS response in our experiments. Because P_{lysin} activity is 2-5 times higher in LexA_G143D than in $\Delta lexA$, it is conceivable that an additional mode of induction alongside the SOS response exists.

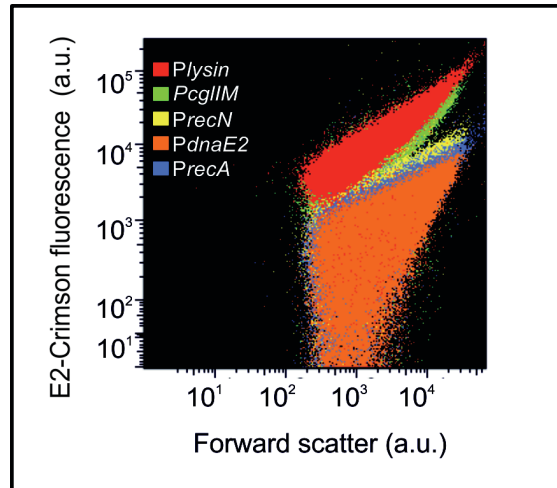


FIGURE 4 Comparison of promoter activity of P_{lysin} , P_{cglIM} , P_{recN} , P_{dnaE2} , and P_{recA} in the LexA_G143D mutant strain. Cells were cultivated in the BioLector microbioreactor system, samples removed at an OD_{600} of ~ 4 and then analyzed in the BD FACSSerialII flow cytometer.

Microarray analysis

Because we observed that the $\Delta recA$ strain does not show a reduced SOS activity but rather an increased basal and spontaneous induction, we compared the transcriptome of the mutant and wild type strain under standard and SOS-inducing conditions. Analogous to previous studies in *C. glutamicum* (Jochmann *et al.*, 2009) we cultivated wild type and $\Delta recA$ cells in shake flasks in CGXII minimal medium with 4% glucose and isolated total RNA before and 30 minutes after addition of 0.6 μM MmC. mRNA isolation, generation of hybridization probes and handling of resulting data was performed as described previously (Vogt *et al.*, 2014). Results of the transcriptome analysis can be found in Supplementary Table 1-5.

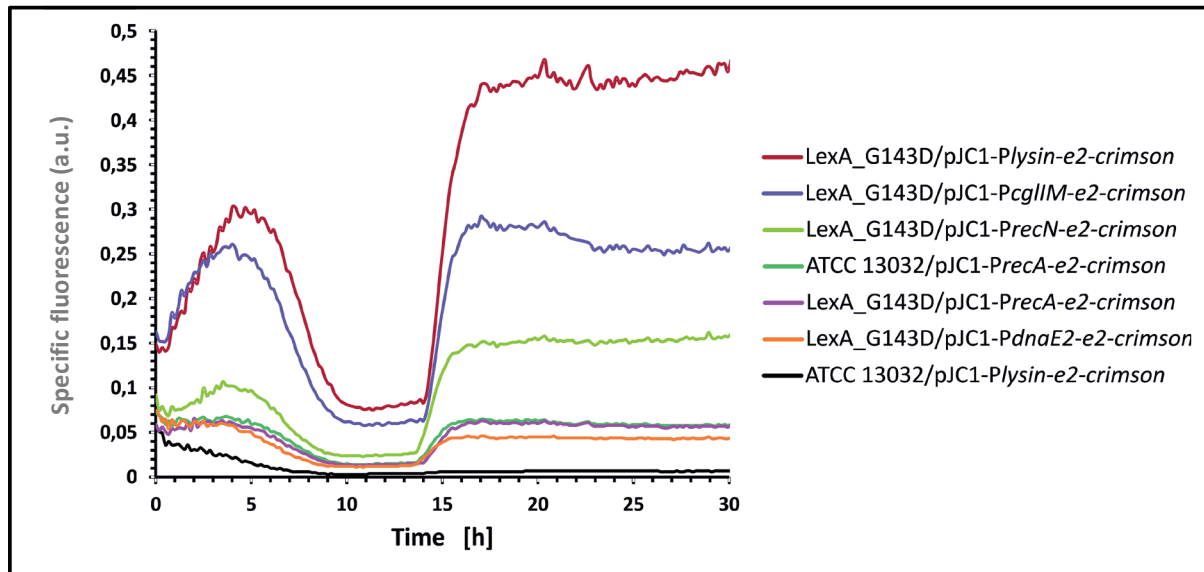


FIGURE 5 Comparison of promoter activity of P_{lysIn} , $P_{cgIII-M}$, P_{recN} , P_{dnaE2} , and P_{recA} in the LexA_G143D mutant strain during long-term cultivation. Cells were cultivated in the BioLector microbioreactor system in CGXII minimal medium with 4% glucose.

Upon addition of MmC we expected a lower abundance of transcripts of genes of the MmC stimulon or LexA regulon in the $\Delta recA$ strain. We readily observed this in our experiments where the transcripts of LexA-regulated components of the SOS response *recA*, *lexA*, *uvrA*, *recX*, *recN*, *nrdR*, and *divS* showed a two- to ten-fold higher amount of transcripts in the wild type strain (Supplementary Table 1). Further genes of interest with a lower transcript abundance include *cg2064*, which encodes a putative DNA topoisomerase I omega-protein. It has been shown in previous studies in *E. coli* that the DNA topoisomerase I *topA* is required for the transcription of genes of the SOS response (Liu *et al.*, 2011). The operon *cg0713-cg0714* encodes a hypothetical protein and a putative polymerase that is involved in DNA repair. Additionally, a number of genes that are encoded in the genomic region of CGP3 are downregulated (Suppl. Table 3). These include genes that were previously described as being up-regulated after addition of MmC or deletion of *lexA*.

Furthermore, six genes were down-regulated in the $\Delta recA$ strain that showed no differential regulation in the aforementioned studies. These included three hypothetical proteins, two putative secreted proteins and a ATP-binding subunit of a putative ATPase with chaperone activity. Appropriately, the mRNA levels of the CGP3-encoded genes were lower in $\Delta recA$ than in the wild type strain, concurrent with our observations that a deletion of *recA* leads to a decreased activity of CGP3-encoded promoters.

The CGP3 gene *cg2048* is of particular interest because it showed the opposite behavior of the other differentially regulated genes CGP3 genes (Suppl. Table 3). It was up-regulated in both conditions with a three-fold increased mRNA level before and 1.35-fold elevated transcript levels 30 minutes after addition of MmC. This gene is annotated as a hypothetical protein. It is a paralog of the down-regulated *cg2062*, which is similar to the plasmid-encoded protein PXO2.09. A BLAST

of the translated sequence of cg2048 reveals high similarities to hypothetical proteins. It shares a 44% identity to a putative conjugation-related ATPase from *Lactobacillus equi* and 43% sequence identity to a lipopolysaccharide biosynthesis protein and a putative polysaccharide biosynthesis protein from *Pseudomonas putida*.

Enzymes involved in the cell's metabolism were downregulated. The first two genes of the *benABCD* operon, *benB* (cg2638 - benzoate dioxygenase small subunit), and *benA* (cg2637 - benzoate 1,2-dioxygenase α subunit aromatic ring hydroxylation dioxygenase A) (Suppl. Table 5), as well as the first gene of the *benKE* operon, *benK1* (cg2642 - putative benzoate transport protein) (Suppl. Table 4), and *adhA* (Zn-dependent alcohol dehydrogenase) (Suppl. Table 1) were downregulated. The phosphofruktokinase *pfkB(fruK)* (cg2119) and its regulator *fruR* (cg2118 - transcriptional regulator of sugar metabolism) were downregulated as well. It is unclear, whether this downregulation of genes involved in metabolism is a specific RecA-mediated effect or a more general effect, e.g. as seen in *Pseudomonas aeruginosa* where the addition of the SOS-inducing antibiotic ciproflaxin downregulates a large number of genes involved in metabolism (Cirz *et al.*, 2006).

Amongst the genes with the highest differential regulation after addition of MmC were cg3329, encoding a conserved protein with homology to the tRNA-splicing ligase RtcB, with an mRNA level of 3.62 (Suppl. Table 2). RtcB mediates the ligation

of broken tRNA-like stem-loop structures in case of tRNA breakage (Tanaka and Shuman, 2011). The flavohemoprotein *hmp* (cg3141) that is involved in nitrate and nitrite metabolism (Platzen *et al.*, 2014) had an average of 2.17 and the cold shock protein *cspB* (cg0938) had an average mRNA level of 1.94 (Suppl. Table 1). The transposase fragments *tnp17b* (cg0427) and *tnp17c* (cg0428) were both up-regulated in $\Delta recA$. Because the cell's capacity to sense DNA damage and induce the SOS response is impaired, it is conceivable that the DNA damage which can not be repaired is sensed by a RecA-independent mechanism and leads to the up-regulation of the transposase fragments.

Interestingly, a lot of genes of putative transporters were upregulated in the $\Delta recA$ strain (Suppl. Table 4), amongst them *oppC* (cg2183) and *oppD* (cg2184) that encode an ABC-type peptide transport system, an ABC-type Mn/Zn import system *znuC2* (cg0043), putative ABC-type iron-siderophore transporters (cg0053, cg0777, cg0778), and a putative secondary Na⁺/glutamate symporter (cg3080). The genes cg0421 (*wzx* - putative translocase of a cell surface polysaccharide), cg1982 (putative ATPase with chaperone activity), and cg2893 (putative cadaverine transporter, multidrug efflux permease) were downregulated. cg2983 was not the only transporter putatively involved in the trafficking of toxic compounds found in this study, however, with cg1696 (putative antibiotic efflux permease), cg2349 (putative ATPase component of ABC transporter for antibiotics), and cg1288 (put. multidrug efflux permease) upregulated in $\Delta recA$.

Regulation of *cg1288* by LexA has previously been shown (Jochmann *et al.*, 2009). The efflux of antibiotics from the cell is one general mechanism that is employed by bacterial cells to circumvent the toxic effects of xenobiotic compounds (Wright, 2005). Another mechanism consists of the inactivation of the toxic compounds by modification or group transfer (Wright, 2005). A range of putative enzymes that are differentially regulated and potentially have the modifying or transfer activity include a flavin-containing monooxygenase (*cg3195*), a hydrolase or acyltransferase of the α/β hydrolase superfamily (*cg1295*), a homoserine O-acetyltransferase (*cg0961*), a reductase that is related to diketogulonate reductase (*cg0031*), and an oxidoreductase (*cg2919*). If *C. glutamicum* possesses a cellular response to antibiotic stress, it is conceivable that this stress is sensed indirectly by the SOS response. Possibly, RecA or a cleavage target of its activated form (e.g. LexA) is involved in the up-regulation of transporters and modifying enzymes to circumvent the effects of toxic compounds. Upon deletion of *recA*, the corresponding genes are no longer transcribed, leading to the down-regulation we observe in the $\Delta recA$ strain. However, we also observe an up-regulation of some genes putatively involved in the toxicity evasion mechanism. It is conceivable, that the cell senses the accumulating DNA damage in the $\Delta recA$ strain by a RecA-independent mechanism. In response to this, the genes are transcribed.

Taken together, we could show in this study that deletion and mutation of key SOS genes not only influences SOS-regulated

genes but also prophage CGP3-encoded genes, as we had previously postulated, depending on the mutations' effect on the activity of the SOS response. These findings were obtained by a targeted approach, utilizing promoter fusions of key SOS and CGP3 genes as well as by utilizing a more global approach in the form of analyzing transcript abundance in wild type and $\Delta recA$ cells before and after the addition of MmC. Surprisingly, the deletion of *recA* does not lead to a decrease in the number of spontaneously induced cells. However, the RecA-dependent activation of the SOS response is impaired as well as induction of CGP3. Furthermore, we observed a very high increase in P_{lys} and P_{cgIII} promoter activity in the LexA_G143D strain, which merits further studies on the nature of this increase and the effects that changing the catalytic center of LexA have.

The SOS response in *C. glutamicum* and its effect on the lysogenic prophage CGP3 requires further studies to potentially find the causal effect behind spontaneous SOS and CGP3 induction.

We had previously suggested that the SOS response is not the causal trigger for CGP3 induction but plays a role in it (Nanda *et al.*, 2014). This study furthers our understanding of the relationship between the SOS response and CGP3 induction. While it is not a causal relationship, the SOS response plays a large role in the dynamics of stabilizing and inducing the prophage CGP3.

References

- Baumgart, M., Unthan, S., Rückert, C., Sivalingam, J., Grünberger, A., Kalinowski, J., *et al.* (2013) Construction of a prophage-free variant of *Corynebacterium glutamicum* ATCC 13032 - a platform strain for basic research and industrial biotechnology. *Appl Environ Microbiol* **79**: 6006–15.
- Cirz, R.T., O'Neill, B.M., Hammond, J. a, Head, S.R., and Romesberg, F.E. (2006) Defining the *Pseudomonas aeruginosa* SOS response and its role in the global response to the antibiotic ciprofloxacin. *J Bacteriol* **188**: 7101–10
- Cox, M.M.M., Goodman, M.M.F., Kreuzer, K.N.K., Sherratt, D.J., Sandlerk, S.J., and Mariani, K.J. (2000) The importance of repairing stalled replication forks. *Nature* **404**: 37–41.
- Cremer, J., Eggeling, L., and Sahm, H. (1990) Cloning the *dapA dapB* cluster of the lysine-secreting bacterium *Corynebacterium glutamicum*. *Mol Gen Genet MGG* **5**: 478–480
- Donovan, C., Heyer, A., Pfeifer, E., Polen, T., Wittmann, A., Krämer, R., *et al.* (2015) A prophage-encoded actin-like protein required for efficient viral DNA replication in bacteria. *Nucleic Acids Res* **43**: 5002–5016
- Frunzke, J., Bramkamp, M., Schweitzer, J.-E., and Bott, M. (2008) Population heterogeneity in *Corynebacterium glutamicum* ATCC 13032 caused by prophage CGP3. *J Bacteriol* **190**: 5111–9
- Heyer, A. (2013) Characterization of a novel phage-encoded actin-like protein and the function of the ChrSA two-component system in *Corynebacterium glutamicum*. PhD thesis, Heinrich-Heine-University Düsseldorf
- Horton, R., Hunt, H., Ho, S., Pullen, J., and Pease, L. (1989) Engineering hybrid genes without the use of restriction enzymes: gene splicing by overlap extension. *Gene* **77**: 61–68.
- Jochmann, N., Kurze, A.K., Czaja, L.F., Brinkrolf, K., Brune, I., Hüser, A.T., *et al.* (2009) Genetic makeup of the *Corynebacterium glutamicum* LexA regulon deduced from comparative transcriptomics and in vitro DNA band shift assays. *Microbiology-Sgm* **155**: 1459–1477
- Kalinowski, J., Bathe, B., Bartels, D., Bischoff, N., Bott, M., Burkovski, A., *et al.* (2003) The complete *Corynebacterium glutamicum* ATCC 13032 genome sequence and its impact on the production of l-aspartate-derived amino acids and vitamins. *J Biotechnol* **104**: 5–25
- Kinoshita, S., Udaka, S., and Shimono, M. (2004) Studies on the amino acid fermentation. Part 1. Production of L-glutamic acid by various microorganisms. *J Gen Appl Microbiol* **50**: 331–343.
- Lin, L.L., and Little, J.W. (1988) Isolation and characterization of noncleavable (Ind-) mutants of the LexA repressor of *Escherichia coli* K-12. *J Bacteriol* **170**: 2163–73.
- Liu, I.-F., Sutherland, J.H., Cheng, B., and Tse-Dinh, Y.-C. (2011) Topoisomerase I function during *Escherichia coli* response to antibiotics and stress enhances cell killing from stabilization of its cleavage complex. *J Antimicrob Chemother* **66**: 1518–24
- Nanda, A.M., Heyer, A., Krämer, C., Grünberger, A., Kohlheyer, D., and Frunzke, J. (2014) Analysis of SOS-induced spontaneous prophage induction in *Corynebacterium glutamicum* at the single-cell level. *J Bacteriol* **196**: 180–8
- Ogino, H., Teramoto, H., Inui, M., and Yukawa, H. (2008) DivS, a novel SOS-inducible cell-division suppressor in *Corynebacterium glutamicum*. *Mol Microbiol* **67**: 597–608
- Platzen, L., Koch-Koerfges, A., Weil, B., Brocker, M., and Bott, M. (2014) Role of flavohaemoprotein Hmp and nitrate reductase NarGHJ1 of *Corynebacterium glutamicum* for coping with nitrite and nitrosative stress. *FEMS Microbiol Lett* **350**: 239–48
- Tanaka, N., and Shuman, S. (2011) RtcB is the RNA ligase component of an *Escherichia coli* RNA repair operon. *J Biol Chem* **286**: 7727–31
- Vogt, M., Haas, S., Klaffl, S., Polen, T., Eggeling, L., Ooyen, J. van, and Bott, M. (2014) Pushing product formation to its limit: metabolic engineering of *Corynebacterium glutamicum* for L-leucine overproduction. *Metab Eng* **22**: 40–52
- Wright, G.D. (2005) Bacterial resistance to antibiotics: enzymatic degradation and modification. *Adv Drug Deliv Rev* **57**: 1451–70

Name of the Journal	to be submitted
Impact Factor	-
Contribution to body of work	80%
1 st author	Experimental work and writing of the manuscript

Spatiotemporal Microbial Single-Cell Analysis Using a High-Throughput Microfluidics Cultivation Platform

Alexander Grünberger,[†] Christopher Probst,[†] Stefan Helfrich, Arun Nanda, Birgit Stute, Wolfgang Wiechert, Eric von Lieres, Katharina Nöh, Julia Frunzke, Dietrich Kohlheyer^{*}

Forschungszentrum Jülich GmbH, IBG-1: Biotechnology, Jülich 52425, Germany

Received 2 February 2015; Revised 26 May 2015; Accepted 19 August 2015

Grant sponsor: German Federal Ministry of Education and Research, Grant number: 031A095A

Grant sponsor: Helmholtz Association, Grant number: VH-NG-1029

Grant sponsor: DFG, Grant number: KO 4537/1–2

Additional Supporting Information may be found in the online version of this article.

*Correspondence to: Dietrich Kohlheyer, Forschungszentrum Jülich GmbH, IBG-1: Biotechnology, Jülich 52425, Germany. E-mail: d.kohlheyer@fz-juelich.de

The first two authors contributed equally to this work.

Published online 00 Month 2015 in Wiley Online Library (wileyonlinelibrary.com)

DOI: 10.1002/cyto.a.22779

© 2015 International Society for Advancement of Cytometry

• Abstract

Cell-to-cell heterogeneity typically evolves due to a manifold of biological and environmental factors and special phenotypes are often relevant for the fate of the whole population but challenging to detect during conventional analysis. We demonstrate a microfluidic single-cell cultivation platform that incorporates several hundred growth chambers, in which isogenic bacteria microcolonies growing in cell monolayers are tracked by automated time-lapse microscopy with spatiotemporal resolution. The device was not explicitly developed for a specific organism, but has a very generic configuration suitable for various different microbial organisms. In the present study, we analyzed *Corynebacterium glutamicum* microcolonies, thereby generating complete lineage trees and detailed single-cell data on division behavior and morphology in order to demonstrate the platform's overall capabilities. Furthermore, the occurrence of spontaneously induced stress in individual *C. glutamicum* cells was investigated by analyzing strains with genetically encoded reporter systems and optically visualizing SOS response. The experiments revealed spontaneous SOS induction in the absence of any external trigger comparable to results obtained by flow cytometry (FC) analyzing cell samples from conventional shake flask cultivation. Our microfluidic setup delivers detailed single-cell data with spatial and temporal resolution; complementary information to conventional FC results. © 2015 International Society for Advancement of Cytometry

• Key terms

single-cell analysis; microfluidics; time-lapse microscopy; *C. glutamicum*

While unraveling and understanding population heterogeneity, high throughput is of utmost importance to derive statistically reliable data, since many cellular phenomena occur with a very low probability per time unit. These rare events and population heterogeneity may be highly dynamic and often have evolved allowing isogenic populations, for example, by division of labor and bet-hedging strategies, to cope with more complex and dynamic environments. In bet-hedging strategies, a very small phenotypic subpopulation can be essential for the fate of the total population in particular under fluctuating environmental conditions. In division of labor strategies, specialized phenotypic subpopulations can have severe impact on the populations overall performance, for example with respect to growth or infection. To correctly understand this cellular heterogeneity, spatial and temporal resolution at the single-cell level, ideally during controlled perturbation studies, has gained much attention in the last few years (1,2). Therefore, simple agarose pad approaches have been frequently used to investigate single-cell growth (3,4) and single-cell lag phase behavior (5). In addition to agarose pads with limited environmental control (6,7),

ORIGINAL ARTICLE

matured and user-friendly microbial single-cell culture and analysis systems are not yet available as standard analytics. However, progress in the field of microfluidics is promising (1,8,9).

Microfluidic single-cell devices in which single cells and colonies can be cultivated over long time periods under well-defined environmental conditions have been developed (8–11). Inside microstructures, individual cells can then be monitored by automated time-lapse microscopy (12–14), allowing new insights into single-cell physiology, behavior and lineage which are typically obscured by conventional bulk technologies.

By high-density large scale integration, microfluidic devices with improved throughput have been reported, for example, for single-cell analysis of various yeast strains (15) and bacteria (16,17). The latter and similar devices often operate with very special cultivation geometries that do not harbor the whole isogenic microcolony but only a fraction, thereby providing incomplete lineage information. Moreover, many of these devices were applied for the cultivation of one specific organism only, thus limiting a wide application range.

Over the last few years, we have developed a microbial single-cell cultivation technology with a strong focus on practical applicability and versatility. The present report describes a disposable, microfluidic cultivation device for the analysis of isogenic microbial microcolonies under well-controlled environmental conditions. Its beneficial and practical usability as a generic high-throughput microbial single-cell analysis tool is presented. Its functionality is demonstrated by analyzing the model organism and industrially applied bacterium *Corynebacterium glutamicum*. Detailed single-cell data and analysis plots of *C. glutamicum* are shown to highlight the broad analysis capability, rather than interpreting the biological phenomena in detail. In addition, the identification of single SOS (*recA*) expressing cells is demonstrated utilizing an fluorescent reporter to transform an intracellular signal into a detectable readout.

In comparison to many previously published single-cell cultivation systems, our platform combines several unique technological features and fulfills the following important characteristics:

- Single use,
- Full microcolony growth providing complete lineage information,
- Single-cell resolution since cellular growth is geometrically restricted to monolayers,
- Spatial as well as temporal resolution due to image-based time-lapse microscopy,
- High throughput (>100,000 cells/cultivation),
- Excellent micro-environmental control by continuous media perfusion,
- Cell growth under mainly diffusive mass transport with negligible convection and

- Applicable to various bacteria (In the present study we cultivated *Corynebacterium glutamicum*. Experimental data on *Escherichia coli* and *Gluconobacter oxydans* will be published elsewhere.).

MATERIALS AND METHODS

Device Fabrication and Setup

Polydimethylsiloxane (PDMS) microfabrication was carried out to manufacture single-use microfluidic devices with integrated 10 μm high supply channels and cultivation chambers with a height of 1 μm . A 100 mm silicon wafer was spin-coated separately with two layers of SU-8 photoresist, processed by photolithography. Profilometer measurements were performed regularly to validate SU-8 structure heights during wafer fabrication. This silicon wafer served as a reusable mold during subsequent PDMS casting. Thermally cured and separated PDMS chips were treated with oxygen plasma and permanently bonded to 170 μm thick glass slides just before the experiments. Manually punched inlets and outlets were connected with tubing (Tygon S-54-HL, ID = 0.25 mm, OD = 0.76 mm, VWR International) via dispensing needles (dispensing tips, ID = 0.2 mm, OD = 0.42 mm, Nordson EFD). SU-8 and PDMS fabrication is common to date and a very detailed fabrication protocol can be found elsewhere (18,19).

Flow Characterization

Microscopic flow profile characterization was performed by infusing fluorescently labeled microspheres with diameters of 200 nm (yellow-green fluorescent 505/515 nm; catalogue number: F8811) and of 1 μm (blue fluorescent 350/440 nm; catalogue number: F8815, Molecular Probes, Invitrogen). 1 μm spheres were utilized to visualize the cell inoculation and trapping process. 200 nm spheres were used to emulate diffusive mass transport during cultivation conditions. Prior to microsphere injection, all microfluidic channels were primed with a 0.1% BSA solution (buffer: dH₂O, pH = 7.0) at 700 nl/min for 60 min to minimize unspecific microspheres adhesion. All microsphere suspensions (2% solids) were diluted 1:1000 in 0.1% BSA solution. The exposure time during fluorescence microscopy was 10 s to capture complete flow trajectories. Further details can be found in the time-lapse imaging section.

Bacterial Strains and Pre-Cultivation

C. glutamicum ATCC 13032 was used for general cultivation experiments. *C. glutamicum*/pJC1-P_{recA}-e2-crimson was used when screening for spontaneously induced SOS. Here, an e2-crimson protein is co-expressed with *recA* resulting in fluorescent cells when *recA* is induced. Detailed information on the construction of *C. glutamicum*/pJC1-P_{recA}-e2-crimson is given in (20).

CGXII was used as standard mineral medium for *C. glutamicum* cultivations consisting of (per liter): 20 g (NH₄)₂SO₄, 5 g urea, 1 g K₂HPO₄, 1 g KH₂PO₄, 0.25 g MgSO₄·7H₂O, 42 g 3-morpholinopropanesulfonic acid (MOPS), 10 mg CaCl₂, 10 mg FeSO₄·7H₂O, 10 mg

MnSO₄·H₂O, 1 mg ZnSO₄·7H₂O, 0.2 mg CuSO₄, 0.02 mg NiCl₂·6H₂O, 0.2 mg biotin, and 0.03 mg of protocatechuic acid. The medium was adjusted to pH 7 and 4% glucose (w/v) was added as a carbon source. All chemicals were purchased from Carl Roth and Sigma Aldrich. The medium was autoclaved and sterile-filtered (0.22 μm pore size) to prevent clogging of the microfluidic channels by particles and cell agglomerates.

Cells were pre-cultured as 20 mL cultures in 100 mL baffled Erlenmeyer flasks on a rotary shaker at 120 rpm orbital shaking at 30°C. A first pre-culture in BHI (Brain-heart infusion, Becton Dickinson, USA) complex medium was inoculated into a second pre-culture in CGXII mineral medium, which was finally inoculated at OD₆₀₀ = 0.05 into CGXII mineral medium, the main culture.

Microfluidic Cultivation

Fluid flow into the microfluidic chip was controlled with a fourfold NeMESYS syringe pump (Cetoni GmbH, Germany). A detailed setup protocol can be found in (18,19). Prior to microfluidic cultivation, the microfluidic chip was purged with fresh and sterile-filtered CGXII medium at 400 nL/min for 10 min.

Afterwards, the chip was infused with bacterial suspension for single-cell inoculation as described in full detail recently (21). Bacterial suspensions were withdrawn from the main culture at the exponential growth phase (OD₆₀₀ between 0.5 and 1). As soon as sufficient single cells were inoculated into the microfluidic cultivation chambers, solely CGXII medium was infused at 400 nL/min throughout the entire cultivation.

Time-Lapse Imaging

Experiments were carried out using an inverted time-lapse live cell microscope (Nikon TI-Eclipse, Nikon Instruments, Germany) equipped with a 100× oil immersion objective (CFI Plan Apo Lambda DM 100X, NA 1.45, Nikon Instruments, Germany) and a temperature incubator (PeCon GmbH, Germany). Phase contrast and fluorescence time-lapse images of growing microcolonies were captured every 10–20 min using an ANDOR LUCA R DL604 CCD camera. Fluorescence images were recorded with an exposure time of 200 ms using a 300 watt Xenon light source (Lamda DG-4, Sutter Instruments, USA) at maximum intensity and appropriate optical filters (excitation: HQ 600/37, dichroic: DM630, emission: HQ 675/67; AHF Analysentechnik AG, Germany).

Image Analysis and Data Visualization

Time-lapse movies of monolayer growth chambers were analyzed using a custom, specialized workflow implemented as an ImageJ/Fiji plugin (22). Cell identification was performed using a segmentation procedure tailored to detect individual rod-shaped cells in crowded populations. Detected cells were subsequently tracked throughout all image sequences using an adapted single particle tracking approach as implemented in TrackMate (23). This image analysis approach allowed the extraction of measurable quantities of individual cells, for example, cell number, cell area, mean single cell fluo-

rescence, as well as derived quantities, for example the growth rate. All data sets were subsequently processed using the analysis and visualization software “Vizardous” (24). Vizardous assists the user with analysis and interpretation tasks for single-cell data in an interactive, configurable and visual way by augmenting lineage trees with time-resolved cellular characteristics.

For detailed growth rate analysis (Figs. 3 and 4), specific chambers were selected that contained only 1 or 2 cells at the beginning of the experiment. For SOS-response studies (Fig. 7), all inoculated chambers were considered for analysis.

To determine growth rates of isogenic microcolonies (Fig. 4), the number of cells in each colony was counted up to a colony size of approximately 130 cells. The maximum growth rate μ_{\max} [1/h] was then estimated from the plot Ln(Cell number) vs. time by fitting an exponential function to the cell number increase applying the method of least squares (25), as depicted in the insert in Figure 4 a.

The analysis of spontaneously induced SOS expression in cells (Figs. 6 and 7b) was performed as follows: First, the contour of each cell was determined. Second, the mean fluorescence intensity of the cell was determined. Third, spontaneously induced cells were determined from fluorescence vs. cell area plots. Spontaneously induced *C. glutamicum* cells exhibiting a fivefold higher mean fluorescence than non-induced cells were classified as SOS positive (SOS+). Results of microfluidic high-throughput screening experiments (Fig. 7c) were obtained by determining the total fluorescence intensity of fluorescing cells. Non-fluorescing cells were not further analyzed. The average final cell number of 750 cells per cultivation chamber was applied to derive the percentage of SOS+ cells.

Flow Cytometry (FC)

FC was performed on an Aria II (Becton Dickinson, San Jose, USA) flow cytometer with 633 nm excitation by a red solid-state laser. E2-Crimson fluorescence was detected using a 660/20 nm band-pass filter. About 100,000 cells were analyzed to determine SOS response at different time points. Cells with a fluorescence output 12- to 18-fold higher than the average were counted as SOS+ cells (Supporting Information 3). The different gating during FC and MGC analysis are related to technical differences of the optical systems. For FC measurements (FACSaria II, BD), the PMT voltage was adjusted to obtain a good dynamic range of the fluorescent signal. During MGC cultivation the fold change of SOS positive cells was significantly lower. However, the stop of cellular growth and changes in morphology observed via time-lapse imaging are in agreement with an induction of the SOS response.

Computational Fluid Dynamics

Computational fluid dynamics (CFD)-based analysis was performed using COMSOL multiphysics (Comsol Multiphysics GmbH, Germany) with the model geometry shown in Fig. 1d. The underlying mesh is described in more detail in Supporting Information 1. The incompressible stationary flow was modeled by the Navier-Stokes equation [Eqs. 1 and 2]:

ORIGINAL ARTICLE

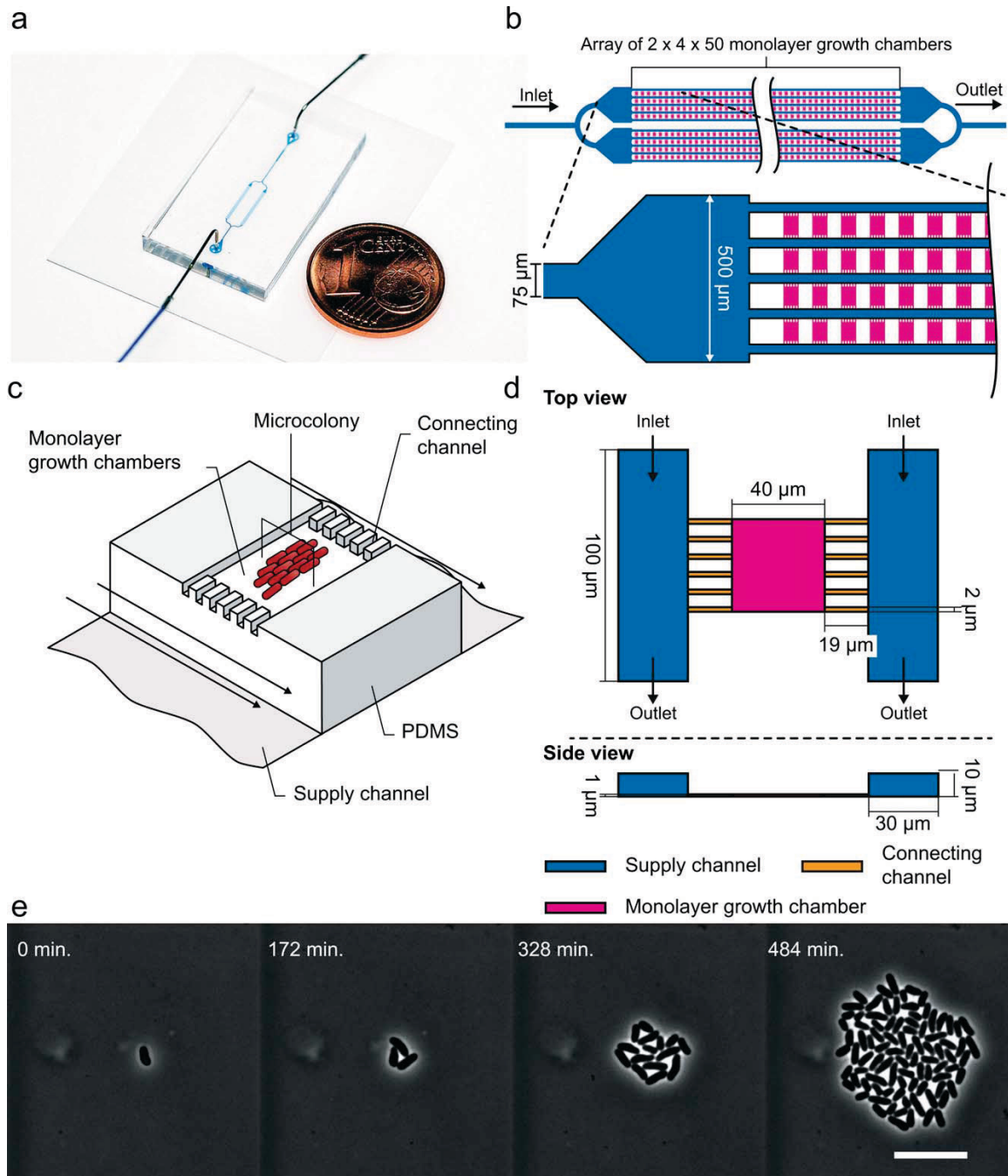


Figure 1. (a) Microfluidic PDMS glass device for high-throughput single-cell cultivation and analysis. (b) 2D CAD design of microfluidic channels with arrays of MGC arranged in parallel (c) 3D dimensional illustration of a single MGC highlighting the different depths of the channels. (d) Geometry of the MGC used for the CFD simulations. (e) Growing microcolonies of up to 750 cells can be observed for several hours depending on the organism and media used; here *C. glutamicum* (scale bar 10 μm).

$$\rho(\vec{u} \cdot \nabla)\vec{u} = \nabla \cdot \left[-pI + \mu(\nabla \vec{u} + (\nabla \vec{u})^T) \right] \quad (1)$$

$$\rho \nabla \cdot \vec{u} = 0 \quad (2)$$

with \vec{u} the velocity, p the pressure, I the identity matrix, $(\nabla \vec{u})^T$ the transpose of $\nabla \vec{u}$, $\mu = 0.0012$ Pa s the dynamic viscosity of a 4% glucose-water solution (w/v); $\rho = 1016.5$ kgm⁻³ the fluid density of a 4% glucose-water (w/v) solution. The velocity at the two supply channel inlets was 0.002 ms⁻¹ which corresponds to a volumetric flow rate of 40 nL min⁻¹. On chip a total flow rate of 400 nL min⁻¹ is equally distributed among 10 supply channels.

The transport of glucose (dc/dt) was described by the time dependent convection-diffusion equation [Eq. (3)]:

$$\frac{\partial c}{\partial t} = -\vec{u} \cdot \nabla c + \nabla \cdot (D \nabla c) \quad (3)$$

with c the molecule concentration of glucose, $D = 0.67 \cdot 10^{-9}$ m² s⁻¹ the diffusion coefficient of glucose and \vec{u} the velocity field given by the solved Navier Stokes equation. The starting concentration of the glucose solution was 244 mol/m³.

RESULTS

Device Layout and Principle

The present microfluidic system is intended for high-throughput single-cell cultivation and analysis of growing isogenic microcolonies. The device consists of a PDMS glass chip with the approximate size of a postage stamp (20 mm × 15 mm × 3 mm) (length × width × height) with incorporated microfluidic channels (Fig. 1a). The chip has one inlet channel that supplies medium, incorporates 400 monolayer growth chambers (MGC) (2 × 4 arrays of 50 MGCs) and has a single outlet channel (Fig. 1c). Each MGC (40 μm × 40 μm × 1 μm) can accommodate a single microcolony of approximately 750 individual bacteria (Fig. 1d). The uniform height of 1 μm restricts microcolony growth to a defined cell monolayer (Fig. 1e). MGCs are arranged between two tenfold deeper supply channels (10 μm × 30 μm) (height × width) with laterally interconnected micrometer sized connecting channels (19 μm × 2 μm × 1 μm) (length × width × height) as depicted in Figure 1c and 1d.

Throughout standard cultivation, medium is fed continuously at nearly identical flow rates into each supply channel and thus negligible pressure difference occurs across the MGC perpendicular to the flow. However, during the primary inoculation phase, the volume flow rates in the parallel supply channels are unequal, resulting in a perpendicular pressure difference and thus fluid convection supporting direct cell transport into the MGC.

Flow Tracer Analysis

To optically visualize laminar stream lines and diffusive mass transport conditions, the microfluidic chip was characterized experimentally using fluorescent microspheres. 1 μm microspheres with a comparable diameter to that of typical bacteria cells were infused into the fully wetted chip to visual-

ize the cell trapping process. As shown, few 1 μm microspheres were randomly trapped and remained inside the MGC throughout the course of the experiment (bright spots in Fig. 2a). Our inoculation procedure utilizes a nanoliter sized air bubble entrapped right before each fivefold channel branching (Fig. 1b), thereby sealing single channels temporarily modifying the flow conditions (21). This induces pressure differences across the MGCs and convective flow through the cultivation chambers, facilitating active cell transport into the chambers. Within two minutes the air bubble disappears by diffusion through the permeable PDMS and normal flow conditions with balanced flow rates through all supply channels are restored.

Once sufficient cells are trapped in the MGC in a realistic cultivation, the growth phase is initiated by changing the medium from the cell suspension to cultivation medium. During this cultivation phase, both parallel media streams have nearly identical volume flow rates, resulting in diffusive mass transport conditions with negligible convective flow inside the MGCs. This diffusive mass transport was experimentally validated by supplementing the fluid with 200 nm fluorescent microspheres which exhibited diffusive migration only, as indicated by the random fluorescence flow traces (Fig. 2a).

Computational Fluid Dynamics

CFD simulations were performed to gain essential knowledge on flow velocities, mass transport and nutrition supply. For CFD simulations, a flow rate of 40 nL/min per supply channel was configured. This corresponds to a total medium flow rate of 400 nL/min equally distributed between 2 × 5 parallel supply channels (see Fig. 1b). The visualized simulations show a homogenous parabolic velocity profile inside the parallel supply channels (Fig. 2b). In contrast to this, the flow inside the MGC is negligibly low in the y -direction (Fig. 2b) and x -direction (Fig. 2c) during cultivation conditions. It has to be noted, that the present CFD simulation geometry does not perfectly match the experimental configuration. On chip (Fig. 1b) some supply channels are connected to MGCs at both sides, whereas the simulation was based on a fully symmetrically and single MGC configuration. In reality this little asymmetry might induce inhomogeneous flow rates through the 10 supply channels. In fact, very detailed CFD simulations (not presented in the present manuscript) using the realistic chip geometry showed slightly inhomogeneous differences, with channel to channel differences as high as 4% maximum. However, the same simulations revealed that inside the MGCs diffusion was absolutely dominating and no convection could be determined. This can be mainly explained by the low flow rates and the high hydrodynamic resistance difference between the 10 fold deeper supply channel and the shallow MGCs. Furthermore, derived cell growth rates inside the chambers did not show particular phenotypes related to certain MGC locations on chip.

A medium switch was simulated to acquire characteristic nutrition supply rates under potentially changing medium conditions. Within 2 s after the change from no glucose to

ORIGINAL ARTICLE

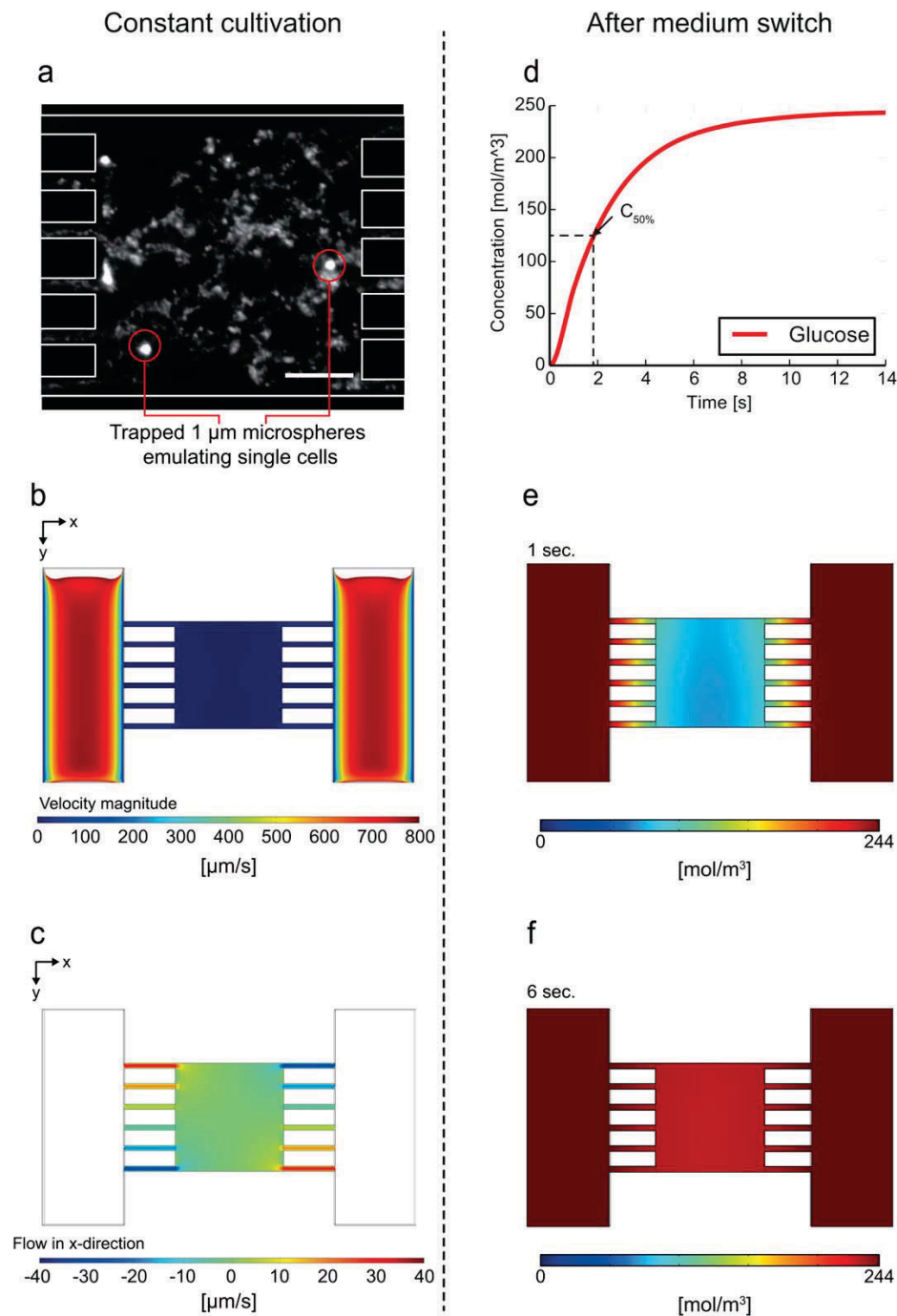


Figure 2. Characterization of fluid flow and concentration profiles inside an MGC: (a) Fluorescence traces of 200 nm microspheres show diffusive migration behavior inside a single MGC during cultivation conditions (scale bar 10 μm). Two 1 μm microspheres were trapped inside the MGC during a cell trapping emulation. (b) CFD simulations revealed laminar parabolic flow inside the supply channels (velocity magnitude). (c) Inside the MGC convective flow is negligible low with the highest velocity inside the connecting channels. (d) Simulations chart of nutrient supply after a sudden medium change from no glucose to 244 mol/m^3 glucose in the supply streams. (e + f) Glucose concentration profile during simulations revealed fast medium changes within seconds.

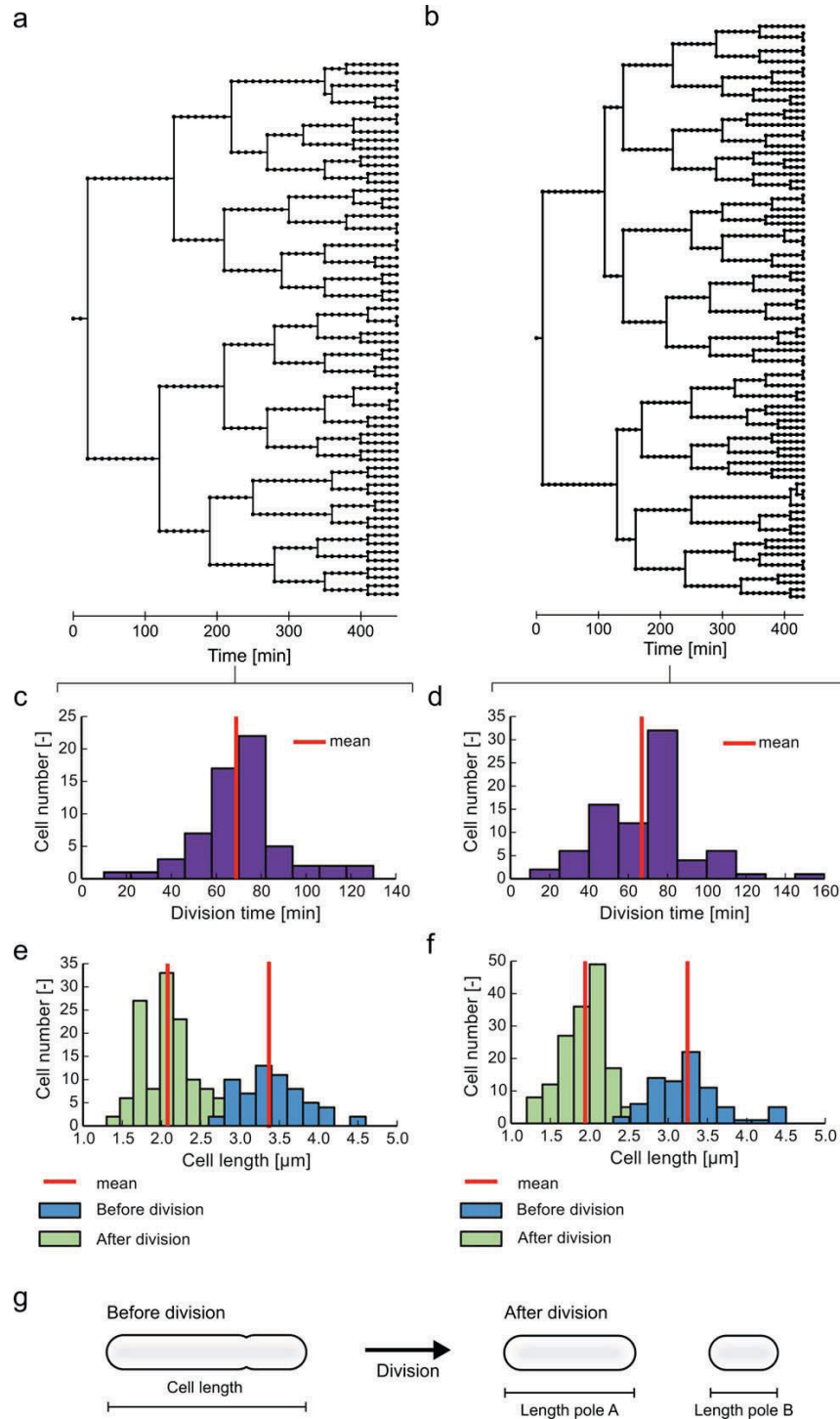


Figure 3. Heterogeneity analysis of two clonal *C. glutamicum* microcolonies: (a, b) Lineage trees showing the overall growth and division behavior. (c, d) Division time distribution for $t_{d, \text{average c}} = 68.87 \pm 20.56$ min and $t_{d, \text{average d}} = 66.88 \pm 24.06$ min. (e, f) Cell length distribution before ($L_{\text{before, average e}} = 3.37 \pm 0.44$ μm , $L_{\text{before, average f}} = 3.25 \pm 0.46$ μm) and after division ($L_{\text{after, average e}} = 2.08 \pm 0.33$, $L_{\text{after, average f}} = 1.94 \pm 0.35$ μm) derived from lineage trees. (g) Description of morphology related parameters: Cell length before division; cell length of pole A and pole B after division. [Color figure can be viewed in the online issue, which is available at wileyonlinelibrary.com.]

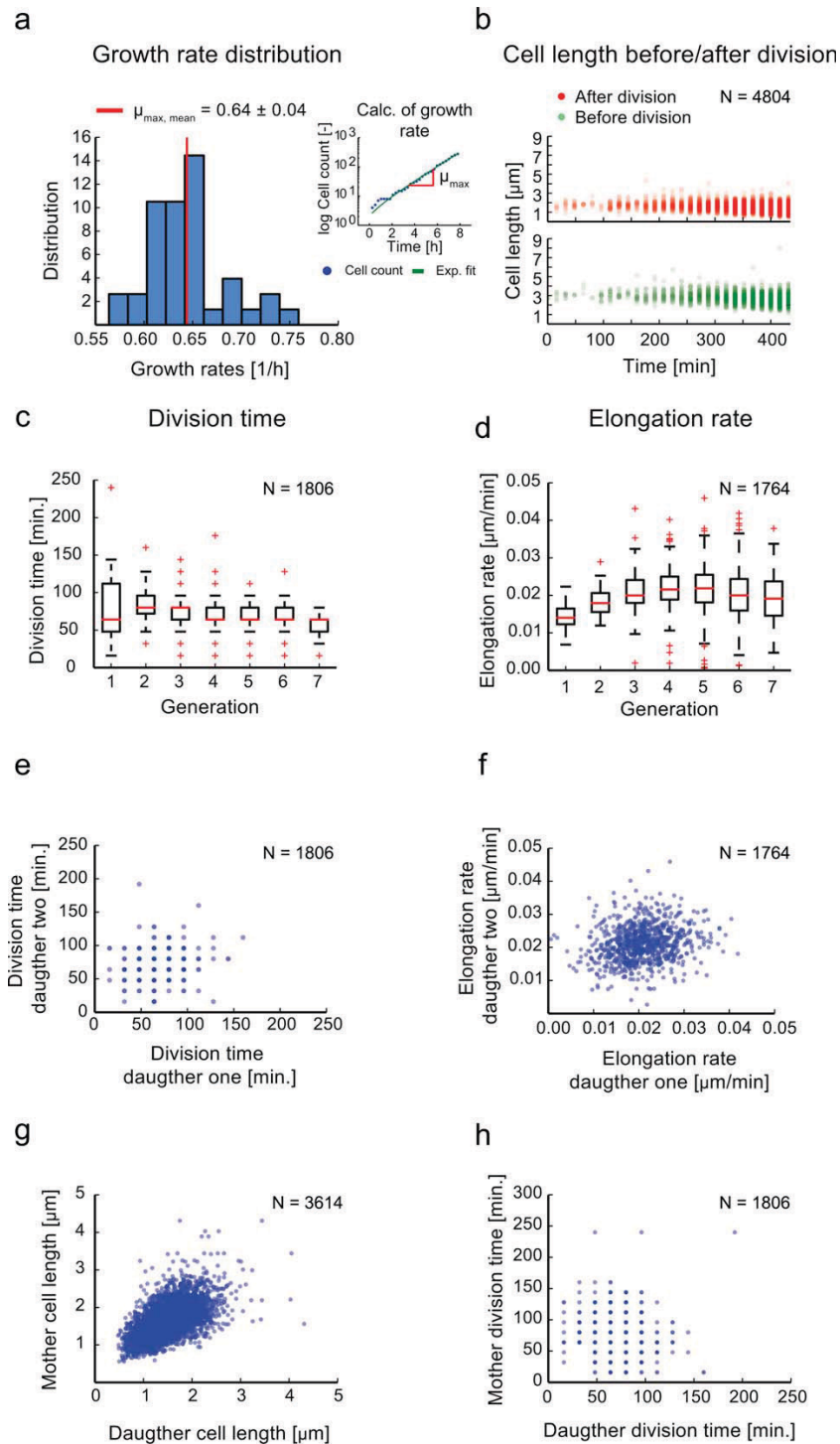


Figure 4. High-throughput single-cell analysis of several microcolonies ($N_{\text{col.}} = 37$) and a total cell number of 4,804 cells: (a) Growth rate distribution plot from each analyzed colony with a mean of $\mu_{\max, \text{mean}} = 0.64 \pm 0.04$ 1/h and an average division time of $t_{\text{d, average}} = 64.81 \pm 3.95$ min. (b) Cell length before and after division over the entire cultivation period. (c) Box plot of the division time over the cell generations ($N_{\text{gen.}} = 7$). (d) Box plot of elongation rates over the cell generations ($N_{\text{gen.}} = 7$). (e) Scatter plot of division times of daughter cell one and daughter cell two. (f) Scatter plot of elongation times of daughter cell one and daughter cell two. (g) Scatter plot of the newborn mother cell length vs. cell length of the related next generation daughter cells. (h) Scatter plot of mother cell division time vs. division time of the related next generation daughter cells.

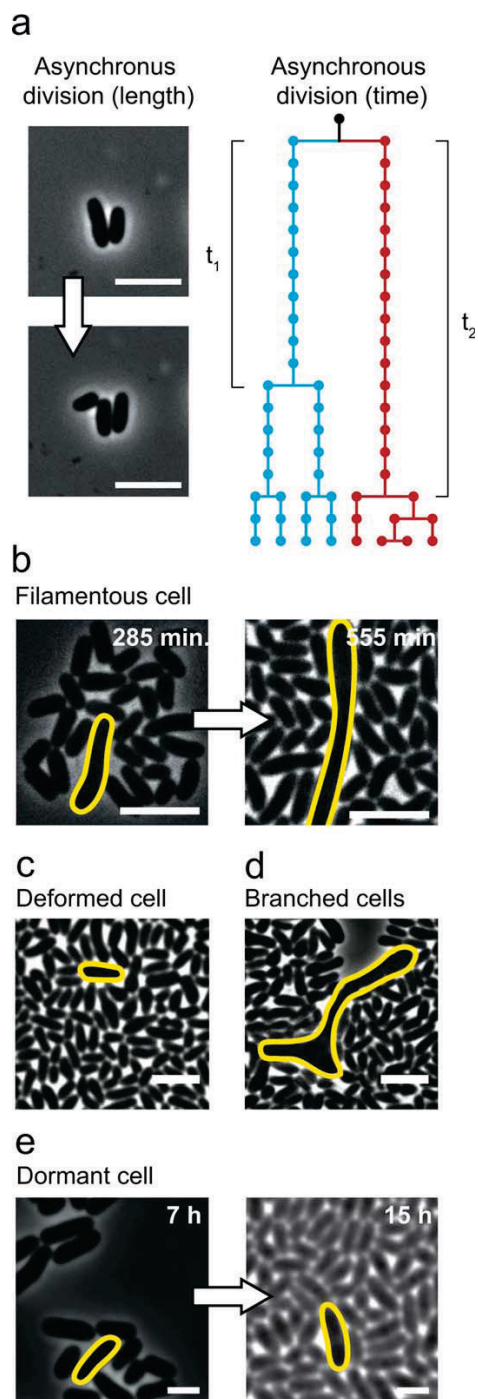


Figure 5. Overview of rare events during *C. glutamicum* cultivation in MGC: (a) Asynchronous division resulting in different cell lengths and division times (scale bar 5 μm), (b) filamentous cell growth (scale bar 5 μm), (c) deformed (scale bar 5 μm), (d) branched cells (scale bar 5 μm), and (e) dormant cells (scale bar 2.5 μm). [Color figure can be viewed in the online issue, which is available at wileyonlinelibrary.com.]

244 mol/m³ glucose delivered by the supply flow (Fig. 2d), the glucose concentration at the MGC center reached 50% of its maximum concentration value by diffusive mass transfer (Fig. 2e). A homogenous and nearly constant glucose distribution was achieved within 6 s only (Fig. 2f).

Microbial Single-Cell Analysis of Isogenic Microcolonies

An exemplary in-depth analysis was performed on two separate *C. glutamicum* ATCC 13032 colonies with single-cell resolution. By cell identification and tracking, lineage trees could be generated as shown in Figures 3a and 3b. Furthermore, characteristic single-cell growth and morphological parameters were extracted, in particular, division time distributions (Figs. 3c and 3d), as well as cell length before and after each division event (Figs. 3e and 3f). All distributions showed Gaussian behavior, with few outliers exceeding 3 times the standard deviation. To further support these findings, further analyzes were performed. Length characteristics were derived as illustrated in Figure 3g.

37 colonies containing a total of 4804 cells were further analyzed to gather single-cell data from higher cell numbers and the results are depicted in Figure 4. Based on this data, an average and maximum growth rate of $\mu_{\text{max;mean}} = 0.64 \pm 0.04$ 1/h (Fig. 4a) was calculated based on the exponentially inclining cell number and an average division time of $t_{\text{d,average}} = 64.81 \pm 3.95$ min. Furthermore, a length analysis of all single cells was conducted, deriving cell length before and cell length directly after each division event over the entire cultivation period of approximately 7 hours and is shown in Figure 4b.

Utilizing the available spatial and temporal information from time-lapse imaging of 4804 cells, the division time (Fig. 4c) and the elongation rate (Fig. 4d) were plotted against the cell generations, respectively, to analyze more complex circumstances and dynamics of morphology and division parameters. The cellular division time appears to be fairly stable over several generations while in contrast the single-cell elongation rates [$\mu\text{m}/\text{min}$] increase by approximately 50% on average during the first four generations before reaching a moderately constant value for the following generations.

The relationship between two related daughter cells and their individual division times is plotted in Figure 4e while individual daughter elongation rates are shown in Figure 4f. No correlation can be found for the two cases; division times and the elongation rates of two related daughters appear to be normally distributed.

Moreover, a correlation analysis was performed to determine if mother cells with long division times (or cell length) have daughter cells with short division times (or cell length) (Figs. 4g and 4h). The results show a strong linear correlation between the mother cell length and daughter cell length (Fig. 4g). In contrast, the mother division time does not correlate with the daughter division times but shows a normal distribution (Fig. 4h). A detailed division analysis and statistical tests of the corresponding histograms were additionally performed

ORIGINAL ARTICLE

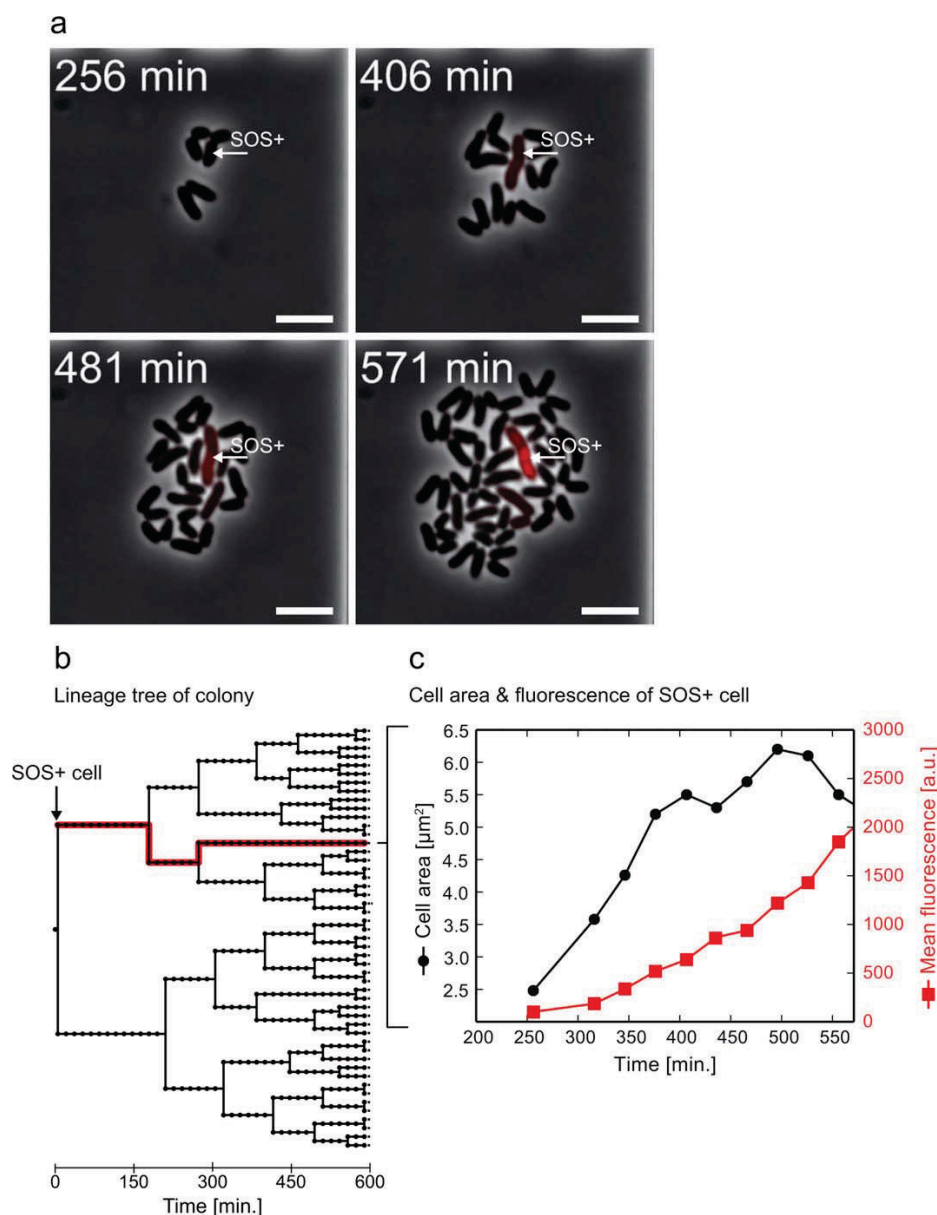


Figure 6. Dynamic SOS response of *C. glutamicum* (scale bars $5 \mu\text{m}$): (a) *C. glutamicum* colony containing one single cell exhibiting spontaneously induced SOS response during cultivation; (b) corresponding lineage tree showing the homogeneous growth, except one cell that stops growing; (c) corresponding mean fluorescence and cell area vs. time illustrating cellular dynamics. [Color figure can be viewed in the online issue, which is available at wileyonlinelibrary.com.]

for each of the 37 colonies separately. The results are shown in Table 1.

Identifying Rare Cellular Events in *C. glutamicum*

As evident from Figures 3 and (4), cell length and division behavior (both parameters are directly accessible from phase contrast image data) of *C. glutamicum* varied signifi-

cantly between individual cells. With our MGC setup, we were able to identify several exceptional outliers and rare events, namely (Fig. 5): a) asynchronous division resulting in two daughter cells of uneven length, b) cellular filamentation, c) deformed cells, d) branched cells and e) dormant cells. These rare events typically appeared with very low probability per time unit.

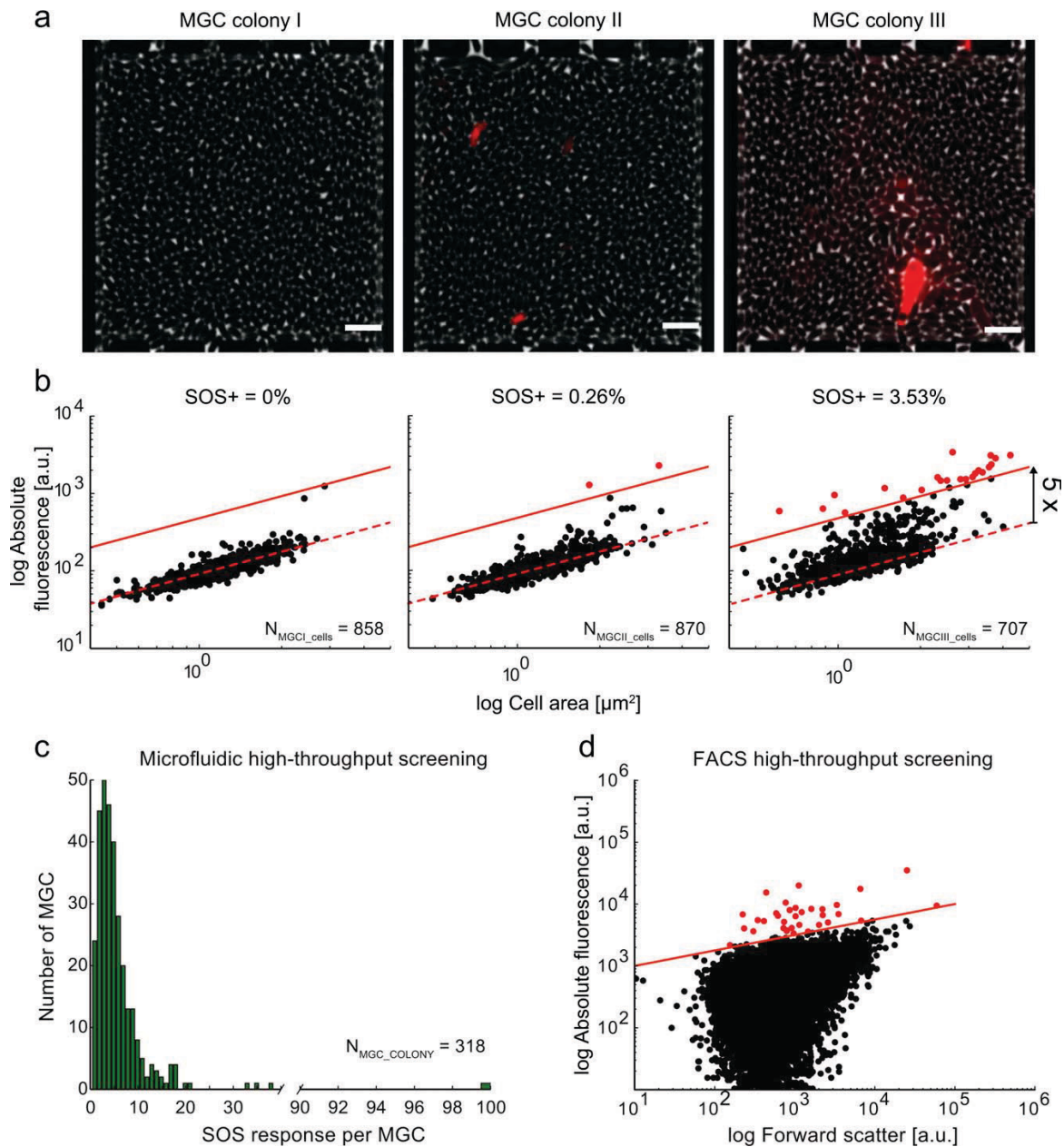


Figure 7. SOS response (SOS+) quantification during microfluidic single-cell cultivation: (a) images of three final clonal colonies (scale bar 25 μm); (b) corresponding total fluorescence vs. cell area scatter plots; dashed line corresponds to the background fluorescence, parallel straight line corresponds to the fivefold higher fluorescence threshold; (c) distribution of SOS+ cells over 318 separate MGC microcolonies in total; (d) for comparison, scatter plot derived from flow FC and shaking flask cultivations.

Dynamics of Spontaneously Induced SOS in Single *C. glutamicum* Cells

In addition to screening for more obvious phenotypes with unusual division behavior and morphology, our technology was used to screen for individual cells undergoing cellular

SOS response, which is not directly detectable by phase contrast microscopy. Thus, a genetically encoded reporter system which is able to perceive a cell's response to DNA damage was used (further denoted as "SOS reporter"). In response to DNA damage, RecA binds ssDNA, catalyzes the

ORIGINAL ARTICLE

Table 1. Cellular characteristics of 37 analyzed *C. glutamicum* colonies

COLONY #	MEAN LENGTH BEFORE [μM]	STANDARD DEVIATION [μM]	MEAN LENGTH AFTER [μM]	STANDARD DEVIATION [μM]	MEAN ELONGATION RATE [$\mu\text{M}/\text{MIN}$]	STANDARD DEVIATION [$\mu\text{M}/\text{MIN}$]	BIMODALITY ^a	DIP TEST VALUE (D)
1	2.83	0.54	1.60	0.43	0.021	0.006	No	0.143
2	2.57	0.49	1.42	0.39	0.020	0.005	No	0.113
3	3.03	0.40	1.71	0.36	0.023	0.005	No	0.130
4	2.70	0.41	1.56	0.34	0.019	0.005	No	0.167
5	2.84	0.44	1.58	0.36	0.021	0.005	No	0.139
6	2.57	0.56	1.37	0.42	0.019	0.006	No	0.137
7	2.25	0.55	1.15	0.37	0.016	0.006	No	0.118
8	2.38	0.53	1.28	0.39	0.017	0.005	No	0.130
9	2.32	0.61	1.20	0.42	0.016	0.006	No	0.117
10	3.07	0.50	1.73	0.39	0.024	0.006	Marginal	0.080
11	2.62	0.36	1.47	0.34	0.020	0.004	Marginal	0.076
12	2.72	0.38	1.49	0.34	0.022	0.004	No	0.152
13	2.66	0.44	1.45	0.37	0.006	0.016	No	0.111
14	2.84	0.42	1.57	0.34	0.021	0.006	No	0.162
15	3.15	0.69	1.79	0.44	0.023	0.009	No	0.211
16	3.04	0.56	1.72	0.45	0.023	0.006	No	0.116
17	2.97	0.66	1.67	0.49	0.021	0.008	No	0.196
18	2.67	0.51	1.45	0.37	0.020	0.007	No	0.107
19	2.61	0.66	1.41	0.47	0.020	0.006	Marginal	0.088
20	2.69	0.58	1.44	0.43	0.020	0.007	No	0.111
21	2.75	0.58	1.49	0.49	0.020	0.005	No	0.100
22	2.71	0.59	1.53	0.47	0.020	0.008	Marginal	0.135
23	2.65	0.36	1.47	0.34	0.021	0.005	No	0.079
24	2.76	0.52	1.49	0.40	0.021	0.005	No	0.172
25	2.75	0.53	1.54	0.39	0.022	0.005	No	0.140
26	2.78	0.67	1.54	0.51	0.021	0.006	No	0.184
27	2.56	0.35	1.40	0.25	0.020	0.005	No	0.113
28	2.49	0.46	1.35	0.41	0.019	0.004	No	0.110
29	2.61	0.50	1.39	0.40	0.021	0.005	Marginal	0.096
30	2.82	0.61	1.56	0.53	0.021	0.006	Marginal	0.097
31	4.14	1.95	2.23	0.94	0.017	0.006	No	0.143
32	2.68	0.45	1.45	0.41	0.021	0.004	No	0.103
33	2.83	0.49	1.61	0.41	0.022	0.006	Marginal	0.097
34	3.02	0.48	1.74	0.39	0.023	0.006	No	0.136
35	2.87	0.46	1.59	0.38	0.023	0.006	No	0.141
36	2.79	0.58	1.78	0.49	0.021	0.008	No	0.148
37	2.97	0.47	1.66	0.37	0.023	0.006	No	0.174

Values are given for the mean cell-length before/after division and the mean elongation rate, as well as the respective standard deviations. Furthermore, results of bimodality are given for the distribution of the elongation rate in each colony and the *D*-value (Dip test value).

^aBimodality of elongation rate histograms was computed according to Hartigan's dip test (The Dip Test of Unimodality) (26).

autoproteolytic cleavage of the repressor LexA and thus leads to its own activation (20) (further denoted as "SOS+ cells"). The cellular SOS response is then transformed into an optically detectable readout – an intracellular fluorescence signal. Hence, the SOS reporter gives a visual output for the transcription of the gene encoding the single-strand binding protein RecA. For detailed information and characterization of the used strain, the reader is referred to Nanda et al. (20).

During microfluidic cultivation of *C. glutamicum*/pJC1-*P_{recA}-e2-crimson* under identical cultivation conditions as previously reported, phase contrast microscopy images again

revealed few rare morphologically deformed and filamentous phenotypes. Figure 6a shows a time-lapse image sequence of an isogenic *C. glutamicum*/pJC1-*P_{recA}-e2-crimson* colony in which an individual cell stopped cellular division but continued elongating for several hours, while all other cells grew normally as expected (Fig. 6b). At the same time, only this specific elongated cell exhibited a constantly increasing SOS reporter fluorescence for several hours. The dynamics of the specific SOS event are visualized in the corresponding cell size (measured here using the projected cell area) and single-cell mean fluorescence vs. time chart (Fig. 6c).

High-Throughput Screening of SOS+ Cells

Instead of analyzing all available 3055 time-lapse images separately recorded during 12 hours of *C. glutamicum*/pJC1- P_{recA} -*e2-crimson* cultivation, only the final still images of each microcolony were screened for spontaneously induced SOS+ cells in the following analysis. Three exemplary clonal microcolonies from the identical microfluidic cultivation are shown in Figure 7a. The corresponding scatter plots are given in Figure 7b. In more detail: MGC microcolony I ($N_{MGC_{I_cells}} = 858$) contained no SOS+ cell (0%), MGC microcolony II ($N_{MGC_{II_cells}} = 870$) contained two SOS+ cells (0.26%) and MGC microcolony III ($N_{MGC_{III_cells}} = 707$) contained 25 SOS+ cells (3.53%) as shown by the parallel lines drawn at fivefold higher threshold fluorescence than the fitted dashed line in the fluorescence vs. area plots for the entire population. Clearly, the number of SOS+ cells directly depends on the selected gating, as shown in more detail in Supporting Information 2.

Overall, the complete screening on all MGC microcolonies ($N_{MGC_COLONY} = 318$) revealed that between 0.07% and 0.49% of all cells ($N_{total_cells} \approx 318 \times 750 = 238,500$) were SOS+ (Fig. 7c and Supporting Information 2). Our findings are in good agreement with results obtained by offline FC analysis after conventional shaking flask cultivations of *C. glutamicum*/pJC1- P_{recA} -*e2-crimson* (Fig. 7d) in which the percentage of SOS+ cells was between 0.05% and 1.25% ($N_{total} = 10^6$) (20). This value highly depends on the gating and number of cells analyzed, as illustrated in more detail in Supporting Information 3.

DISCUSSION

Currently, most of the single-cell results are derived from FC and time-lapse microscopy. During live cell microscopy, cells are often cultivated on simple agarose pads (6) to observe growing microcolonies over time and extract specific cellular parameters from subsequent off-line image analysis. In addition to the required automated time-lapse microscopy, agarose pads are simple enough that they can be prepared in practically any microbiology lab. However, agarose pads very quickly reach their experimental limitations, since there is nearly no method of controlling the micro-environment during the course of the experiment.

When single cells have to be cultivated for longer time periods over many generations inside well-controllable environments, there is practically no alternative to microfluidic single-cell cultivation technology. This becomes even more evident when single-cell cultivation inside dynamic environments is desired. Unfortunately, microfluidics technology is not generally available in most laboratories, since advanced fabrication facilities and expert knowledge are required to build tailor-made devices. Successfully applied systems fulfilling the demands of a microbiologist, especially applicability as well as simplicity, are typically developed by highly interdisciplinary project consortia. In the present work, we used a fairly simple microfluidic platform technology for various applications and strains in microbial single-cell analysis.

The presented chip incorporates several hundred MGCs inside a single device. The high degree of parallelization enables the generation of statistically reliable information, a prerequisite for investigation at the single-cell level. One minor bottleneck is automated microscopy, which currently restricts the analysis throughput. We analyze about 100 MGCs during a typical experiment, which we found to be a good compromise between throughput, time resolution and image analysis effort for most fast-growing microorganisms.

Previous versions of our microfluidic MGC device layout were successfully applied in several research projects (7,12,20,21,26–29). The two adjacent supply streams continuously deliver fresh medium and remove any by-products and secreted metabolites, while the MGC interior fluid volume is replenished solely by diffusion, which was confirmed experimentally by fluorescent microspheres and by CFD simulations. This configuration enables cells to be cultivated under optimal conditions (initial rate conditions) inside the MGCs under the absence of any convection or shear stress. Environmental changes can be implemented within seconds simply by infusing a different medium. The availability of (in particular low-abundance) specific medium compound (for example, N, P sources and micronutrients) and oxygen supply is currently under investigation utilizing more advanced microfluidic setups with integrated fluid control and comprehensive modeling and simulation work.

C. glutamicum was chosen as a model organism due to its high relevance for biotechnological applications (in particular, in industrial biotechnology) and its relation to the pathogenic relative *Mycobacterium tuberculosis* (30). Several other studies on *C. glutamicum* reported cell-to-cell heterogeneity within isogenic populations, revealing differences in cellular viability, membrane potential and growth (31), amino acid productivity (12) and spontaneous prophage induction (20,32); offering a wide range of applications ideal to verify and validate our new system.

The described results and plots on *C. glutamicum* in the present report were mainly derived to demonstrate the broad analysis spectrum at the single-cell level instead of focusing on the biological phenomena themselves. We basically investigated *C. glutamicum* at four different levels of detail, namely:

- I. The high spatial and temporal resolution due to monolayer cultivation in combination with image-based microscopy favors the generation of complete lineage trees, shown for two clonal colonies as an example in Figure 3. Such lineage trees give expressive impressions of evolving microcolonies but this format is limited to a few generations only. Related distribution charts then give a direct impression of the obvious population heterogeneity.
- II. We analyzed 37 microcolonies with respect to growth rate distributions enabling a closer view of the growth rate variability of clonal populations (Fig. 4a). In total, 4,804 cells were analyzed to investigate specific cellular parameters over the entire cultivation period or over cell generations, deriving cellular dynamics on a long time

ORIGINAL ARTICLE

scale (Figs. 4b–4d). The large variance of single-cell elongation rates (Fig. 4d) is currently under further investigation. One reason for this could be the influence of the increasing colony size and thus the physical effects of neighboring cells on each other.

- III. During cultivation of *C. glutamicum*, several special phenotypes were identified, as illustrated in Figure 5. These events were observed in less than 1% of all cells. Once a specific phenotype of interest was identified, all the microcolonies can be screened systematically. One explanation for the observed dormant cells and cells with elongated morphology could be the spontaneous induction of the SOS response in the absence of any external trigger but triggered by DNA damage (20,33). Therefore, we focused in particular on elongated cells with impaired growth and division behavior and additionally utilized a genetically encoded fluorescence reporter which transformed an intracellular signal, the SOS activity, into a detectable readout. This allowed the dynamics of intracellular parameters to be traced both on the individual cell and population level (Fig. 6).
- IV. All final time-lapse images were screened for SOS+ cells (Fig. 7a). Due to the low numbers of SOS+ cells, 318 microcolonies were analyzed to derive reliable data. As illustrated in cell size vs. fluorescence scatter plots, our single cell data agree well with FC data. Our results revealed that 0.07–0.5% of *C. glutamicum* cells expressed spontaneously induced SOS under standard cultivation conditions which is in good agreement with results from conventional FC analysis (SOS+ cells = 0.07–1.25%) and shake flask cultivation (Fig. 7d). These findings confirm that the MGC cultivation conditions used in the present study have no significant impact on cellular physiology. Notably, MGC cultivations allowed the identification of the growth of SOS+ cell clusters originating from a common mother cell (Fig. 7a - colony III). This crucial information remains hidden if solely FC is performed.

The investigations into dynamic single-cell division are of high interest, for example for the investigation of single-cell lag phase behavior after changes in different environmental conditions. Roostaltu et al. (34) monitored the dilution of green fluorescent protein (GFP) due to cell growth and division by FC. They found a bimodal distribution of the isogenic population of growing and non-growing cells when the cells were transferred from stationary phase to fresh medium conditions.

In a similar approach, Kotte et al. (35) used a fluorescent membrane-intercalating dye to follow the dilution of the cellular fluorescence due to cell growth over time with FC. They determined the number and growth rate of the growing cell fraction upon a shift to a new carbon source and also found a bimodal distribution of growing and non-growing cells.

These two examples applying FC and fluorescence dilution methods revealed highly interesting bet-hedging strategies as a result of stochastic switching or responsive diversification. Despite this, the more complex dynamics and

lineage behavior could not be resolved solely by FC. Using our MGC with time-lapse imaging and a controlled medium switch, this bet-hedging strategy could be directly investigated without any fluorescence stains that may affect cell metabolism. In particular, the growth dynamics and lineage information would be directly accessible, allowing more accurate interpretations of the bimodal distribution at the single-cell level and functionally at population level. Furthermore, critical cellular phenomena such as cell lysis would also be directly observable. This is not possible with FC.

In contrast, dynamic large-scale processes, such as monitoring the synthesis of a destabilized green fluorescent protein (GFP) (36) under changing environmental reactor conditions could be difficult to investigate with the current MGC setup. Whereas FC can be connected to real bioprocesses, the MGC cannot mimic complex dynamic bioprocesses yet. This needs further development, for example the possibility of performing batch cultivation, as shown by Dai et al. (37), or the implementation of integrated valves and pumps to create and control dynamic flow profiles (15).

We further want to emphasize that our method is not limited to one specific microorganism and can be applied for various other microorganisms. Currently, the limiting step for widespread use in microbiology and biotechnology is the demand for automatic image analysis tools. Most of the organisms have different specific characteristics in division behavior and cell morphology, which typically require tailor-made image analysis algorithms.

CONCLUSIONS

The presented microfluidic technology allows the systematic single-cell analysis of clonal microbial populations and screening for rare cellular events with high statistical reliability, an important prerequisite for systematic cell-to-cell heterogeneity studies.

Using conventional cultivation technology in combination with FC enables a snapshot analysis of rare events. However, the history, cell lineages and cellular dynamics cannot be investigated. The MGC has proven useful for investigating single-cell growth and dynamic behavior such as spontaneous SOS response and interestingly revealed both spontaneously induced single cells as well as spontaneously induced cell clusters. We propose that such technology will find its place in microbiology as a complimentary technique next to conventional FC. This may offer new insights into the mechanisms of rare bacterial cellular events.

Future applications of these techniques for cultivation and analysis at the single-cell level will expand our understanding of cell-to-cell heterogeneity in various biological processes, ranging from antibiotic screening (38) and adaptation processes (39–41) to new insights for applied fields such as food microbiology (42). Particularly for the investigation of cellular processes in the early exponential and lag phase (43), suitable tools are still lacking. The MGCs offer a novel technique for future investigation of these phenomena.

ACKNOWLEDGMENTS

Microfabrication was performed at the Helmholtz Nano-electronic Facility (HNF) of Forschungszentrum Jülich GmbH. The authors thank HNF for its support. They also acknowledge support with image analysis from Karin Bokelmann and Charaf Eddine Azzouzi.

LITERATURE CITED

- Fritzsche FSO, Dusny C, Frick O, Schmid A. Single-cell analysis in biotechnology, systems biology, and biocatalysis. *Annu Rev Chem Biomol Eng* 2012;3:129–155.
- Hol FJH, Dekker C. Zooming in to see the bigger picture: Microfluidic and nanofabrication tools to study bacteria. *Science* 2014;346:1251821.
- Niven GW, Morton JS, Fuks T, Mackey BM. Influence of environmental stress on distributions of times to first division in *Escherichia coli* populations, as determined by digital-image analysis of individual cells. *Appl Environ Microb* 2008; 74:3757–3763.
- Schaechter M, Williamson JP, Hood JR, Koch AL. Growth, cell and nuclear divisions in some bacteria. *J Gen Microbiol* 1962;29:421–434.
- Niven GW, Fuks T, Morton JS, Rua SACG, Mackey BM. A novel method for measuring lag times in division of individual bacterial cells using image analysis. *J Microbiol Methods* 2006;65:311–317.
- Young JW, Locke JCW, Altinok A, Rosenfeld N, Bacarian T, Swain PS, Mjolsness E, Elowitz MB. Measuring single-cell gene expression dynamics in bacteria using fluorescence time-lapse microscopy. *Nat Protoc* 2012;7:80–88.
- Dusny C, Grünberger A, Probst C, Wiechert W, Kohlheyer D, Schmid A. Technical bias of microcultivation environments on single cell physiology. *Lab Chip* 2015;15:1822–1834.
- Grünberger A, Wiechert W, Kohlheyer D. Single-cell microfluidics: Opportunity for bioprocess development. *Curr Opin Biotechnol* 2014;29:15–23.
- Dusny C, Schmid A. Microfluidic single cell analysis links boundary environments and individual microbial phenotypes. *Environ Microbiol* 2014;17:1839–1856.
- Weaver WM, Tseng P, Kunze A, Masaali M, Chung AJ, Dudani JS, Kittur H, Kulkarni RP, Di Carlo D. Advances in high-throughput single-cell microtechnologies. *Curr Opin Biotechnol* 2014;25:114–123.
- Vasdekis AE, Stephanopoulos G. Review of methods to probe single cell metabolism and bioenergetics. *Metab Eng* 2015;27:115–135.
- Mustafi N, Grünberger A, Mahr R, Helfrich S, Nöh K, Blombach B, Kohlheyer D, Frunzke J. Application of a genetically encoded biosensor for live cell imaging of L-valine production in pyruvate dehydrogenase complex-deficient *Corynebacterium glutamicum* strains. *Plos One* 2014;9:e85731.
- Jaqaman K, Loerke D, Mettlen M, Kuwata H, Grinstein S, Schmid SL, Danuser G. Robust single-particle tracking in live-cell time-lapse sequences. *Nat Methods* 2008; 5:695–702.
- Elfving A, LeMarc Y, Baranyi J, Ballagi A. Observing growth and division of large numbers of individual bacteria by image analysis. *Appl Environ Microb* 2004;70:675–678.
- Dénervaud N, Becker J, Delgado-Gonzalo R, Damay P, Rajkumar AS, Unser M, Shore D, Naef F, Maerkl SJ. A chemostat array enables the spatio-temporal analysis of the yeast proteome. *Proc Natl Acad Sci USA* 2013;110:15842–15847.
- Ullman G, Wallden M, Marklund EG, Mahmutovic A, Razinkov I, Elf J. High-throughput gene expression analysis at the level of single proteins using a microfluidic turbidostat and automated cell tracking. *Philos T R Soc B* 2013;368:20120025.
- Moffitt JR, Lee JB, Cluzel P. The single-cell chemostat: An agarose-based, microfluidic device for high-throughput, single-cell studies of bacteria and bacterial communities. *Lab Chip* 2012;12:1487–1494.
- Grünberger A, Paczia N, Probst C, Schendzielorz G, Eggeling L, Noack S, Wiechert W, Kohlheyer D. A disposable picoliter bioreactor for cultivation and investigation of industrially relevant bacteria on the single cell level. *Lab Chip* 2012;12:2060–2068.
- Grünberger A, Probst C, Heyer A, Wiechert W, Frunzke J, Kohlheyer D. Microfluidic picoliter bioreactor for microbial single-cell analysis: Fabrication, system setup, and operation. *J Vis Exp* 2013;82:e50560.
- Nanda AM, Heyer A, Krämer C, Grünberger A, Kohlheyer D, Frunzke J. Analysis of SOS-induced spontaneous prophage induction in *Corynebacterium glutamicum* at the single-cell level. *J Bacteriol* 2014;196:180–188.
- Probst C, Grünberger A, Braun N, Helfrich S, Noh K, Wiechert W, Kohlheyer D. Rapid inoculation of single bacteria into parallel picoliter fermentation chambers. *Anal Methods* 2015;7:91–98.
- Schneider CA, Rasband WS, Eliceiri KW. NIH Image to ImageJ: 25 years of image analysis. *Nat Meth* 2012;9:671–675.
- Schindelin J, Arganda-Carreras I, Frise E, Kaynig V, Longair M, Pietzsch T, Preibisch S, Rueden C, Saalfeld S, Schmid B, and others. Fiji: An open-source platform for biological-image analysis. *Nat Meth* 2012;9:676–682.
- Helfrich S, Azzouzi CE, Probst C, Grünberger A, Wiechert W, Kohlheyer D, Nöh K. Vizardous: Interactive visualization and analysis of microbial populations with single cell resolution. *Bioinformatics* 2015; doi:10.1093/bioinformatics/btv468.
- Grünberger A, van Ooyen J, Paczia N, Rohe P, Schendzielorz G, Eggeling L, Wiechert W, Kohlheyer D, Noack S. Beyond growth rate 0.6: *Corynebacterium glutamicum* cultivated in highly diluted environments. *Biotechnol Bioeng* 2013;110:220–228.
- Binder D, Grünberger A, Loeschcke A, Probst C, Bier C, Pietruszka J, Wiechert W, Kohlheyer D, Jaeger K-E, Drepper T. Light-responsive control of bacterial gene expression: Precise triggering of the lac promoter activity using photocaged IPTG. *Integr Biol* 2014;6:755–765.
- Unthan S, Grünberger A, van Ooyen J, Gäggs J, Heinrich J, Paczia N, Wiechert W, Vizardous: Interactive visualization and analysis of microbial populations with single cell resolution. *Biotechnol Bioeng* 2014;111:359–371.
- Probst C, Grünberger A, Wiechert W, Kohlheyer D. Microfluidic growth chambers with optical tweezers for full spatial single-cell control and analysis of evolving microbes. *J Microbiol Meth* 2013;95:470–476.
- Helfrich S, Pfeifer E, Krämer C, Sachs CC, Wiechert W, Kohlheyer D, Nöh K, Frunzke J. Live cell imaging of SOS and prophage dynamics in isogenic bacterial populations. *Mol Microbiol* 2015; doi:10.1111/mmi.13147.
- Varela C, Rittmann D, Singh A, Krumbach K, Bhatt K, Eggeling L, Besra GS, Bhatt A. MmpL genes are associated with mycolic acid metabolism in mycobacteria and corynebacteria. *Chem Biol* 2012;19:498–506.
- Neumeier A, Hubschmann T, Muller S, Frunzke J. Monitoring of population dynamics of *Corynebacterium glutamicum* by multiparameter flow cytometry. *Microb Biotechnol* 2013;6:157–167.
- Frunzke J, Bramkamp M, Schweitzer JE, Bott M. Population heterogeneity in *Corynebacterium glutamicum* ATCC 13032 caused by prophage CGP3. *J Bacteriol* 2008; 190:5111–5119.
- Ogino H, Teramoto H, Inui M, Yukawa H. DivS, a novel SOS-inducible cell-division suppressor in *Corynebacterium glutamicum*. *Mol Microbiol* 2008;67:597–608.
- Roostalu J, Joers A, Luidalepp H, Kaldalu N, Tenson T. Cell division in *Escherichia coli* cultures monitored at single cell resolution. *BMC Microbiol* 2008;8:68.
- Kotte O, Volkmer B, Radzikowski JL, Heinemann M. Phenotypic bistability in *Escherichia coli*'s central carbon metabolism. *Mol Syst Biol* 2014;10:736–736.
- Brognaux A, Han S, Sorensen S, Lebeau F, Thonart P, Delvigne F. A low-cost, multiplexable, automated flow cytometry procedure for the characterization of microbial stress dynamics in bioreactors. *Microb Cell Fact* 2013;12:100.
- Dai J, Yoon SH, Sim HY, Yang YS, Oh TK, Kim JF, Hong JW. Charting microbial phenotypes in multiplex nanoliter batch bioreactors. *Anal Chem* 2013;85:5892–5899.
- Dawson CC, Intapa C, Jabra-Rizk MA. “Persisters”: Survival at the cellular level. *Plos Pathog* 2011;7:e1002121.
- Fritz G, Megerle JA, Westermayer SA, Brick D, Heermann R, Jung K, Rädler JO, Gerland U. Single cell kinetics of phenotypic switching in the arabinose utilization system of *E. coli*. *Plos One* 2014;9:e89532.
- Acar M, Mettetal JT, Oudenaarden A. Stochastic switching as a survival strategy in fluctuating environments. *Nat Genet* 2008;40:471–475.
- Boulineau S, Tostevin F, Kiviet DJ, ten Wolde PR, Nghe P, Tans SJ. Single-cell dynamics reveals sustained growth during diauxic shifts. *PLoS One* 2013;8:e61686.
- Aguirre JS, Monis A, García de Fernando GD. Improvement in the lag phase estimation of individual cells that have survived mild heat treatment. *Int J Food Sci Technol* 2014;49:884–894.
- Bridson EY, Gould GW. Quantal microbiology. *Lett Appl Microbiol* 2000;30:95–98.

Name of the Journal	Cytometry Part A
Impact Factor	2.928
Contribution to body of work	10%
4 th author	Microbiological experimental work and analyzing of the data

4 Discussion

4.1 Mechanisms underlying the spontaneous induction of the *C.*

glutamicum prophage CGP3

Bacterial genomes are littered with DNA of prophagal origin (Casjens, 2003). Genome analyses have shown that up to 20% of a bacteria's genome can be of viral origin (Casjens *et al.*, 2000). Therefore, it is not far-fetched that this DNA can have a marked impact on the bacteria's physiology. Not only are novel genes and functions introduced into the host (Canchaya *et al.*, 2004), but also the excision and integration dynamics of the prophage DNA itself influence the host as well (Dobrindt *et al.*, 2004). Therefore it is of utmost importance for the survival of individual bacteria to tightly control the stability of their lysogenic prophages.

Nevertheless, work performed by Lwoff and coworkers revealed that there is free phage DNA in the supernatant of bacterial cultures that are cultivated under standard laboratory conditions (Lwoff, 1953). Therefore, spontaneous excision of prophages and consequent lysis of the bacterial cell seems unavoidable. Indeed, later studies found that *E. coli* cells display spontaneous activity of their prophages and foreign DNA in a small fraction of cells (Hertman and Luria, 1967). This spontaneous activation is of importance for various biological functions, such as bacterial pathogenicity (e.g. Shiga-toxin producing *E. coli*) (Loś *et al.*, 2012) or biofilm formation (*P. aeruginosa*) (Webb *et al.*, 2003; Rice *et al.*, 2008). The mechanisms underlying these processes not been studied extensively thus far, making it all the more interesting to elucidate them.

In this work, the role of the SOS response in promoting the spontaneous induction of prophage CGP3 was characterized in *C. glutamicum*. *C. glutamicum* and its prophage CGP3 represent an interesting model to study the relationship between host and bacteriophage in terms of spontaneous prophage induction for many reasons. On one hand, *C. glutamicum* is a close relative of *Mycobacterium tuberculosis* (Stackebrandt *et al.*, 1997), the causal agent of tuberculosis in humans. Findings from studies on *C. glutamicum* can be studied in *M. tuberculosis*, as well, to eventually find novel targets for treatment of patients suffering from a tuberculosis infection. On the other hand, *C. glutamicum* is one of the most widely used and thus important bacteria in White Biotechnology, and so far no known infectious bacteriophages have been described for it. Whereas fermentations with the commonly used bacteria *E. coli* can and often do suffer from infection with bacteriophages (Łoś, 2004), *C. glutamicum* does not have this drawback. Thus, studying the physiology of the resident prophage CGP3 - that at some point was successful in infecting *C. glutamicum* - and assessing the effects that this cryptic phage has on its host, is of great interest (Frunzke *et al.*, 2008). Furthermore, studies on CGP3 and the mechanisms that i) keep it in its lysogenic form and ii) make *C. glutamicum* hard to infect may prove valuable when addressing the aforementioned challenges faced in industrial cultivation of *E. coli* strains.

4.2 Spontaneous SOS response

Lambdoid phages such as Phage λ are induced by the SOS response (Oppenheim *et al.*, 2005). When the integrity of the bacterial genome is compromised, the *ssb* protein RecA is

activated (RecA*) and induces the SOS response (Friedberg *et al.*, 2005). RecA* acts as a co-protease of the repressor LexA, the master regulator of the SOS response, which undergoes autoproteolytic cleavage (Little, 1984). However, RecA* recognizes other substrates as well, amongst them the phage repressor CI in *E. coli*. Its cleavage leads to the expression of genes required for the lytic life cycle and the excision of phage λ from the genome (Oppenheim *et al.*, 2005).

In this work, a relationship between the host SOS response and the induction of prophage CGP3 of *C. glutamicum* was established (Nanda *et al.*, 2014). Spontaneous P_{recA} activity was observed in about 0.2% of the bacterial population. A high positive correlation was observed for the promoter of *recA* and down-stream SOS-responsive promoters. Thus, we conclude that the spontaneous activity of P_{recA} leads to a *bona fide* induction of the SOS response, excluding promoter noise as the source of the observed spontaneous P_{recA} activity in most cells. Earlier studies revealed that spontaneously occurring DNA breakage leads to an induction of SOS-regulated genes (in this case the cell division inhibitor P_{sulA}) (Pennington and Rosenberg, 2007). Owing to rapid growth during the logarithmic growth phase, polymerases stall more frequently at replication forks, leading to their inactivation (Cox, 2000), thus accumulating regions of single-stranded DNA that are sufficient to induce the SOS response (Higuchi, 2003; McInerney and O'Donnell, 2007). Indeed, we see an increased activity of P_{recA} during the logarithmic growth phase in *C. glutamicum*. What should not be neglected, however, is the possibility of the observed spontaneous events having occurred during the stationary phase of pre-cultivation or during the lag phase after inoculation in fresh medium. Cells which are not able to resume growth would remain in the dormant and P_{recA} -activated state. It has been described for

Salmonella enterica serovar Typhimurium that a transient accumulation of metal ions, specifically iron, takes place during the stationary growth phase and in turn leads to an increase of reactive oxygen species due to the Fenton reaction (Rolfe *et al.*, 2012). Likewise, the uptake of iron has been linked to spontaneous RecA-dependent induction of the *Shewanella oneidensis* prophage λ So (Binnenkade *et al.*, 2014). The effect iron has on the SOS response in *C. glutamicum* has been tested. Interestingly, these studies showed that a shift of wild type *C. glutamicum* cells from iron-limited minimal medium into iron-supplemented minimal medium leads to a high rate of spontaneous activity of the P_{recA} promoter fusion (Pfeifer, 2013).

4.3 Spontaneous induction of CGP3

We demonstrated that strains lacking SOS activity ($\Delta recA$) are impaired in their ability to induce prophagal promoters of CGP3, and that a constitutively elevated SOS induction ($\Delta lexA$) leads to an increased activity of the promoters.

In the $::P_{recA-eyfp}$ strain transformed with promoter fusions of CGP3-encoded genes *int2* or *lysin* we observe a correlation between both reporter signals at the single cell level, albeit to a lower degree than for signals of P_{recN} or P_{divS} , which are regulated by the SOS response. This indicates that the SOS response is not the sole or causal trigger for CGP3 induction, yet implies its role in feeding into the mechanism of prophage induction. It is conceivable that the SOS response induces prophagal antirepressors that lead to an activation of prophage genes, as it is described for *Salmonella enterica* (Lemire *et al.*, 2011). A first step to validating the hypothesis lies in finding repressors of CGP3 genes. Putative genes could be deleted or over-expressed to assess their effect on prophage

dynamics. Furthermore, promising candidates could then be used as an epitope for affinity chromatography experiments. A less directed and more global approach can be taken as well, e.g. by comparing the proteomes of cells which are grown to minimally and maximally induce their prophage and searching for putative regulatory proteins.

A putative candidate for further studies is the sigma factor SigH (Busche *et al.*, 2012). SigH triggers expression of the genes *uvrA* (cg1560), *uvrC* (cg1790), both involved in nucleotide-excision repair, *uvrD3* (cg1555), which encodes a DNA helicase similar to UvrD proteins, and a gene cluster putatively involved in alkylated DNA repair (cg0184-cg0186). SigH and *uvrA* are both controlled by LexA, as evidenced by the presence of SOS boxes in their promoter regions, thus linking SigH to the SOS response even more tightly and presenting it as a central regulator of this response (Busche *et al.*, 2012). In *S. aureus* the alternative sigma factor H has a stabilizing effect on the prophage by expression of the SigH-controlled integrase, which is responsible for reintegration of excised prophages (Tao *et al.*, 2010). However, no CGP3 genes were shown to be under control of SigH (Busche *et al.*, 2012). To further investigate the possibility of SigH acting as a higher level regulator that influences CGP3 excision and integration dynamics, a deletion mutant of SigH and its direct SOS targets might provide insights into the underlying regulatory dynamics.

Further hints towards the complexity of CGP3 regulation were found. In *E. coli*, the phage repressor CI represses phage λ . *C. glutamicum* possesses a Cro/CI-type regulator (Cg2040), however it shows no significant change in the induction of CGP3 genes when deleted or overexpressed (Heyer, 2013). Likewise, the reported studies show no influence of the potential prophage repressor on CGP3 induction. A point mutation within the cleavage

site of LexA in *C. glutamicum*, analogous to a LexA non-cleavable mutation in *E. coli* (Ind⁻), behaves similarly to the $\Delta recA$ strain, as expected. However, it exhibits a surprisingly high activity of the LexA-regulated P_{lysin} and P_{cglIM} promoters, indicating a RecA-independent mode of induction for CGP3 genes in *C. glutamicum*. Because the $\Delta lexA$ and $\Delta recA$ strains exhibit the expected loss-of-function and gain-of-function phenotypes in regards to the SOS response, and the LexA_G143D mutant exhibits an inhibited SOS response with simultaneous induction of CGP3 genes, so far unknown RecA-independent roles in repressing genes for LexA can be stipulated.

To test this hypothesis, different approaches can be chosen. The promoter regions of *lysin* or *cglIM* and other known LexA targets, such as *recA*, can be utilized in electrophoretic mobility shift assays using purified LexA and LexA_G143D to analyze putatively altered binding properties of both. In a more global approach, the promoter sequences of interest can be immobilized by biotinylation and incubated with crude extracts of wild type and LexA_G143D strains cultivated under SOS-inducing and non-inducing conditions, thus finding novel DNA-binding proteins involved in the SOS response and CGP3 induction.

As another global approach, the transcriptome of the LexA_G143D strain can be compared to that of the wild type strain before and after addition of mitomycin C. To analyze effects, which do not act on the level of transcription but rather on the level of translation, protein extracts of both strains would then be subjected to 2D-PAGE and subsequent analysis by MALDI.

4.4 The fate of cells with a SI of the SOS response and CGP3

FACS analysis reveals a divergent fate for cells with either an elevated P_{recA} or P_{int2} activity or with a high activity of both promoter fusions. Roughly 50% of cells with an induced SOS response, and 75% of cells with an induced prophage, are unable to resume growth on cultivation plates. Cells with a high activity of both promoters only have a viability of 10% (Nanda, 2014). Further analysis of the $::P_{recA}-eyfp$ strain in a microfluidic cultivation system confirm this finding (Julia Frunzke, personal communication). However, the FACS results can not be confirmed for the CGP3 promoter fusions when cultivated in the microfluidic cultivation setup (data not shown). The signal output of the CGP3 promoter fusions is generally lower than for the P_{recA} promoter fusions. Therefore, it is likely that spontaneous activity observed in the flow cytometer is not seen in the microfluidic setup. This leads to observed cases of CGP3 promoter activity in single cells representing rather high activities. In this scenario, low, pulsing activities of CGP3 promoters, without a growth inhibition, is not seen. To test whether a low signal intensity is indeed the source of this observation, the CGP3 promoters can be cloned to drive expression of the autofluorescent protein *venus*, which is currently being utilized in combination with the P_{recA} promoter, and be integrated into the genome. *venus* is a third generation derivative of YFP which has useful properties for dynamic measurements, such as a higher signal output and a faster maturation time (Nagai *et al.*, 2002).

A pulsing behavior is observed for the $P_{recA}-eyfp$ reporter signal in cells with normal growth behavior, as well as a continuous signal in cells with inhibited growth or an alleviation of this signal in cells that resumed growth (Nanda, 2014). Pennington *et al.* observed a spontaneous induction of the $P_{sulA}-gfp$ promoter fusion, as well (Pennington

and Rosenberg, 2007). In their studies, 35% of P_{sulA} -active cells in *E. coli* are able to resume growth. Removal of *sulA* reveals that growth inhibition after spontaneous SOS induction is not necessarily caused by irreparable DNA damage but might reflect a state of senescence (Fonville *et al.*, 2010). Cellular senescence describes the process of a cell's response to exogenous or endogenous stress. In this context, describing the reported findings as senescence makes sense. As the bacterial cell tries to either compensate the encountered DNA damage by arresting its cell cycle and inducing repair mechanisms or by completely halting its growth, ultimately leading to cell stasis, the survival of unfit cells is decreased (Campisi and d'Adda di Fagagna, 2007; Pennington and Rosenberg, 2007). Assessing the age of individual cells and measuring their spontaneous SOS response complete with cell fate (repair and growth or growth inhibition) over the course of many generations will allow us to estimate the effect of cellular aging on the growth of *C. glutamicum*. The tools necessary for experiments towards this end are present and rely on cultivation in specialized microfluidic chambers (Wang, 2010; Grünberger, 2012) and the visual tracking and separation of the bacteria under study (Helfrich, 2015).

Whether the growth inhibition of cells with a continuous reporter output, as observed in our studies, is caused by cell death or if these cells are in a dormant state can not be tested in this system. Using a mutant strain lacking the repressor of cell division DivS a better estimation of how much lethal DNA damage is encountered by cells during the exponential growth phase can be gained, especially when coupled to cellular dyes such as PI, Syto 9 and DiOC₂(3) (Neumeyer *et al.*, 2013), which act as an indicator of a cell's metabolic status and viability. Further breaking down the cellular fate into DivS- and RecA-

dependent growth inhibition will shed light on the involvement of the SOS response in this process.

Taken together, the use of dual promoter fusion strains will prove helpful in resolving the sequence of SOS and CGP3 induction. Furthermore, the cell's fate after the induction of either event can be monitored and categorized. The activity of promoter fusions, and their temporal dynamics along with growth rates of the corresponding cells, will help in painting a more detailed picture of the induction mechanics of CGP3.

So far, the link between an activity of the chosen CGP3-encoded genes to the excision of CGP3 has not been established. To this end, a *C. glutamicum* strain combining the CGP3 promoter fusions (Nanda *et al.*, 2014) and a genomically integrated *tetO* array together with a plasmid-based YFP-TetR fusion (Frunzke *et al.*, 2008) should be constructed. Using microfluidic cultivation, the correlation of CGP3 promoter activity and of CGP3 excision can be analyzed.

4.5 Global response to a deletion of *recA*

Because the spontaneous induction of the SOS response is not impaired in the $\Delta recA$ strain, the transcript levels of $\Delta recA$ were compared to those of *C. glutamicum* ATCC 13032 before and after the addition of MmC to gain further insights into the SOS response pathway of *C. glutamicum*. We observed that LexA-regulated genes were significantly down-regulated in the deletion mutant, as well as CGP3-encoded genes, which we had previously postulated to be indirectly controlled by the SOS response (Nanda *et al.*, 2014).

Genes of enzymes that are involved in metabolic processes were down-regulated in $\Delta recA$, which might be specific to the deletion of *recA* or a general response to MmC, as

seen in *Pseudomonas aeruginosa* where addition of the SOS-inducing antibiotic ciprofloxacin down-regulates a large number of genes involved in metabolic processes (Cirz *et al.*, 2006).

Many mechanisms exist in various bacteria to avoid the effects of xenobiotic compounds, amongst them the efflux, enzymatic degradation or modification of the toxic compound (Wright, 2005; Nishino and Yamaguchi, 2008; Nikaido, 2010). Interestingly, a high number of transporters, as well as genes putatively involved in group transfer and modification of toxic compounds are up-regulated in the $\Delta recA$ strain. These might pose a part of a drug evasion mechanism of *C. glutamicum*. Various antibiotic resistance mechanisms are known for *Corynebacteria* species, among them efflux systems and transferases. These include the resistance towards streptomycin, spectinomycin and tetracyclines, mediated by resistance genes on the R-plasmids pTET3 in *C. glutamicum* LP-6 (Tauch *et al.*, 2002), streptomycin, spectinomycin and sulfonamide resistance on pCG4 in *C. glutamicum* 31830 (Tauch *et al.*, 2003) and chloramphenicol resistance mediated by the plasmid pXZ10145 in *C. glutamicum* 1014 (Na *et al.*, 1991). Furthermore, penicillin binding proteins (PBP) have been found in sequence analyses of *C. glutamicum*. The deletion of four high-molecular-weight PBPs were shown to increase sensitivity to β -lactam antibiotics (Valbuena *et al.*, 2007). Additionally, the genome of *C. glutamicum* possesses potential β -lactamase genes (Kalinowski, 2005). Considering that cell wall damage mediated by β -lactam antibiotics is sensed by the cell and elicits an SOS response in *E. coli* (Miller, 2004), the up-regulation of the multitude of potential drug export and metabolizing enzymes in our studies provide an interesting question as to unknown

compounds able to induce the SOS response and potential novel pathways of evading cellular stress in *C. glutamicum*.

The work presented in this thesis has studied the relationship between the SOS response and the spontaneous induction of prophage CGP3. Single-cell reporters for SOS and CGP3 activity were constructed and tested in combination, and it was shown, that both have a high activity in a small subset of cells under normal cultivation conditions. The results outlined in this thesis paint the picture that intrinsic, spontaneous DNA damage is closely involved in spontaneous activation of the *C. glutamicum* prophage CGP3 at the single-cell level. On a population-wide level, key players of the SOS response were deleted and the effects on CGP3 induction assessed. Whereas constitutive SOS induction led to a high induction of CGP3 genes, a reduction of SOS response led to a decrease in CGP3 gene activity. Furthermore, a gain-of-function mutation of the transcriptional repressor LexA surprisingly led to a high increase in CGP3 gene activity.

This thesis has underlined the intricacies of the SOS pathway in *C. glutamicum* and its accompanying activation of the prophage CGP3. It has laid the groundwork for future studies regarding spontaneous prophage induction in *C. glutamicum*, the activity of prophage CGP3, and the SOS regulon of *C. glutamicum*.

5 References

- Ajinomoto Co., I. (2011) Food products business. <http://www.ajinomoto.com/en/ir/pdf/Feed-useAA-Oct2011.pdf>.
- Ajinomoto Co., I. (2012) Feed-Use amino acids business. <http://www.ajinomoto.com/en/ir/pdf/Food-Oct2012.pdf>.
- Baumgart, M., Unthan, S., Rückert, C., Sivalingam, J., Grünberger, A., Kalinowski, J., *et al.* (2013) Construction of a prophage-free variant of *Corynebacterium glutamicum* ATCC 13032 for use as a platform strain for basic research and industrial biotechnology. *Appl Environ Microbiol* **79**: 6006–15.
- Binnenkade, L., Teichmann, L., and Thormann, K.M. (2014) Iron triggers λ So prophage induction and release of extracellular DNA in *Shewanella oneidensis* MR-1 biofilms. *Appl Environ Microbiol* **49**.
- Bossi, L., Fuentes, J., Mora, G., and Figueroa-Bossi, N. (2003) Prophage Contribution to Bacterial Population Dynamics. *J Bacteriol* **185**: 6467–6471.
- Brooks, K., and Clark, A. (1967) Behavior of λ Bacteriophage in a Recombination Deficient Strain of *Escherichia coli*. *J Virol* **1**: 283–293.
- Brown, N.F., Wickham, M.E., Coombes, B.K., and Finlay, B.B. (2006) Crossing the Line: Selection and Evolution of Virulence Traits. *PLoS Pathog* **2**: e42.
- Brüssow, H. (2012) What is needed for phage therapy to become a reality in Western medicine? *Virology* **434**: 138–142.
- Brüssow, H., Canchaya, C., and Hardt, W.-D. (2004) Phages and the Evolution of Bacterial Pathogens: from Genomic Rearrangements to Lysogenic Conversion. *Microbiol Mol Biol Rev* **68**: 560–602.
- Busche, T., Silar, R., Pičmanová, M., Pátek, M., and Kalinowski, J. (2012) Transcriptional regulation of the operon encoding stress-responsive ECF sigma factor SigH and its anti-sigma factor RshA, and control of its regulatory network in *Corynebacterium glutamicum*. *BMC Genomics* **13**: 445.
- Campisi, J., and d’Adda di Fagagna, F. (2007) Cellular senescence: when bad things happen to good cells. *Nat Rev Mol Cell Biol* **8**: 729–740.
- Canchaya, C., Fournous, G., and Brüssow, H. (2004) The impact of prophages on bacterial chromosomes. *Mol Microbiol* **53**: 9–18.
- Carrolo, M., Frias, M.J., Pinto, F.R., Melo-Cristino, J., and Ramirez, M. (2010) Prophage spontaneous activation promotes DNA release enhancing biofilm formation in *Streptococcus pneumoniae*. *PLoS One* **5**: e15678.
- Casjens, S. (2003) Prophages and bacterial genomics: what have we learned so far? *Mol Microbiol* **49**: 277–300.
- Casjens, S., Palmer, N., Vugt, R. van, Huang, W.M., Stevenson, B., Rosa, P., *et al.* (2000) A

- bacterial genome in flux: the twelve linear and nine circular extrachromosomal DNAs in an infectious isolate of the Lyme disease spirochete *Borrelia burgdorferi*. *Mol Microbiol* **35**: 490–516.
- Cirz, R.T., O’Neill, B.M., Hammond, J. a, Head, S.R., and Romesberg, F.E. (2006) Defining the *Pseudomonas aeruginosa* SOS response and its role in the global response to the antibiotic ciprofloxacin. *J Bacteriol* **188**: 7101–10.
- D’Herelle, F. (1917) Sur un microbe invisible antagoniste des bacilles dysentériques. *CR Acad Sci Paris* **165**: 373–375.
- d’Herelle, F. (1931) Bacteriophage as a Treatment in Acute Medical and Surgical Infections. *Bull N Y Acad Med* **7**: 329–348.
- D’Herelle, F. (2007) On an invisible microbe antagonistic toward dysenteric bacilli: brief note by Mr. F. D’Herelle, presented by Mr. Roux. *Res Microbiol* **158**: 553–554.
- Dobrindt, U., Hochhut, B., Hentschel, U., and Hacker, J. (2004) Genomic islands in pathogenic and environmental microorganisms. *Nat Rev Microbiol* **2**: 414–24.
- Erill, I., Campoy, S., and Barbé, J. (2007) Aeons of distress: an evolutionary perspective on the bacterial SOS response. *FEMS Microbiol Rev* **31**: 637–56.
- Fonville, N.C., Bates, D., Hastings, P.J., Hanawalt, P.C., and Rosenberg, S.M. (2010) Role of RecA and the SOS Response in Thymineless Death in *Escherichia coli*. *PLoS Genet* **6**: e1000865.
- Freeman, V.J. (1951) Studies on the virulence of bacteriophage-infected strains of *Corynebacterium diphtheriae*. *J Bacteriol* **61**: 675–688.
- Friedberg, E.C., Walker, G.C., Siede, W., Wood, R.D., Schultz, R.A., and Ellenberger, T. (2005) DNA Repair and Mutagenesis. *Washington, DC Am Soc Microbiol* .
- Frunzke, J., Bramkamp, M., Schweitzer, J.-E., and Bott, M. (2008) Population Heterogeneity in *Corynebacterium glutamicum* ATCC 13032 caused by prophage CGP3. *J Bacteriol* **190**: 5111–9.
- Grünberger, A., Paczia, N., Probst, C., Schendzielorz, G., Eggeling, L., Noack, S., *et al.* (2012) A disposable picolitre bioreactor for cultivation and investigation of industrially relevant bacteria on the single cell level. *Lab Chip* **12**: 2060–2068.
- Grünberger, A., Probst, C., Helfrich, S., Nanda, A., Stute, B., Wiechert, W., *et al.* (2015) Spatiotemporal microbial single-cell analysis using a high-throughput microfluidics cultivation platform. *Cytom Part A* **87**: 1101-15.
- Grünberger, A., Wiechert, W., and Kohlheyer, D. (2014) Single-cell microfluidics: opportunity for bioprocess development. *Curr Opin Biotechnol* **29**: 15–23.
- Hatfull, G., and Hendrix, R. (2011) Bacteriophages and their Genomes. *Curr Opin Virol* **1**: 298–303.
- Hertman, I., and Luria, S.E. (1967) Transduction Studies on the Role of a *rec+* Gene in the Ultraviolet Induction of Prophage Lambda. *J Mol Biol* **23**: 117–133.

- Heyer, A. (2013) Characterization of a novel phage-encoded actin-like protein and the function of the ChrSA two-component system in *Corynebacterium glutamicum*. **Heinrich-Heine-University Düsseldorf** <http://juser.fz-juelich.de/record/135092>.
- Horvath, P., and Barrangou, R. (2010) CRISPR/Cas, the Immune System of Bacteria and Archaea. *Science* **327**: 167–170.
- Jochmann, N., Kurze, A.K., Czaja, L.F., Brinkrolf, K., Brune, I., Hüser, A.T., *et al.* (2009) Genetic makeup of the *Corynebacterium glutamicum* LexA regulon deduced from comparative transcriptomics and in vitro DNA band shift assays. *Microbiology* **155**: 1459–1477.
- Kalinowski, J. (2005) The genomes of amino acid-producing *corynebacteria*, p. 37–56. In L. Eggeling and M. Bott (ed.),. In *Handbook of Corynebacterium glutamicum*.
- Lemire, S., Figueroa-Bossi, N., and Bossi, L. (2011) Bacteriophage Crosstalk: Coordination of prophage induction by trans-acting antirepressors. *PLoS Genet* **7**: e1002149.
- Little, J., and Mount, D. (1982) The SOS Regulatory System of *Escherichia coli*. *Cell* **29**: 11–22.
- Little, J.W. (1984) Autodigestion of *lexA* and phage lambda repressors. *Proc Natl Acad Sci U S A* **81**: 1375–9.
- Livny, J., and Friedman, D.I. (2004) Characterizing spontaneous induction of Stx encoding phages using a selectable reporter system. *Mol Microbiol* **51**: 1691–1704.
- Locke, J.C.W., and Elowitz, M.B. (2009) Using movies to analyse gene circuit dynamics in single cells. *Nat Rev Microbiol* **7**: 383–392.
- Łoś, J.M., Łoś, M., Węgrzyn, A., Węgrzyn, G., Łoś, J.M., and Łoś, M. (2012) Altruism of Shiga toxin-producing *Escherichia coli*: Recent hypothesis versus experimental results. *Front Cell Infect Microbiol* **2**: 166.
- Lwoff, A. (1953) Lysogeny. *Bacteriol Rev* **17**: 269–332.
- Na, S., Shen, T., Jia, P., Men, D., and Chen, Q. (1991) Characterization of the natural deletion mutant of plasmid pXZ10145 in *Corynebacterium glutamicum* and construction of a recombinant plasmid. *Chin J Biotechnol* **7**: 271–7.
- Nagai, T., Ibata, K., Park, E.S., Kubota, M., Mikoshiba, K., and Miyawaki, A. (2002) A variant of yellow fluorescent protein with fast and efficient maturation for cell-biological applications. *Nat Biotechnol* **20**: 87–90.
- Nanda, A.M., Heyer, A., Krämer, C., Grünberger, A., Kohlheyer, D., and Frunzke, J. (2014) Analysis of SOS-Induced Spontaneous Prophage Induction in *Corynebacterium glutamicum* at the Single-Cell Level. *J Bacteriol* **196**: 180–188.
- Nebe-von-Caron, G., Stephens, P.J., Hewitt, C.J., Powell, J.R., and Badley, R.A. (2000) Analysis of bacterial function by multi-colour fluorescence flow cytometry and single cell sorting. *J Microbiol Methods* **42**: 97–114.
- Neumeyer, A., Hübschmann, T., Müller, S., and Frunzke, J. (2013) Monitoring of population

- dynamics of *Corynebacterium glutamicum* by multiparameter flow cytometry. *Microb Biotechnol* **6**: 157–67.
- Nikaido, H. (2010) Multidrug resistance in bacteria. *Annu Rev Biochem* **78**: 119–146.
- Nishino, K., and Yamaguchi, A. (2008) Role of xenobiotic transporters in bacterial drug resistance and virulence. *IUBMB Life* **60**: 569–74.
- Ogino, H., and Teramoto, H. (2008) DivS, a novel SOS-inducible cell-division suppressor in *Corynebacterium glutamicum*. *Mol Microbiol* **67**: 597–608.
- Oppenheim, A.B., Kobilier, O., Stavans, J., Court, D.L., and Adhya, S. (2005) Switches in bacteriophage lambda development. *Annu Rev Genet* **39**: 409–29.
- Paul, J.H. (2008) Prophages in marine bacteria: dangerous molecular time bombs or the key to survival in the seas? *ISME J* **2**: 579–589.
- Pennington, J.M., and Rosenberg, S.M. (2007) Spontaneous DNA breakage in single living *Escherichia coli* cells. *Nat Genet* **39**: 797–802.
- Pfeifer, E. (2013) Untersuchungen zur Induktion und Infektiosität des CGP3 Prophagen in *Corynebacterium glutamicum*. **Heinrich-Heine-University Düsseldorf** <http://juser.fz-juelich.de/record/141200>.
- Piddock, L., and Wise, R. (1987) Induction of the SOS response in *Escherichia coli* by 4-quinolone antimicrobial agents. *FEMS Microbiol Lett* **41**: 289–294.
- Rice, S., Tan, C., Mikkelsen, P., and Kung, V. (2008) The biofilm life-cycle and virulence of *Pseudomonas aeruginosa* are dependent on a filamentous prophage. *ISME J* **3**: 271–282.
- Rohwer, F., and Edwards, R. (2002) The Phage Proteomic Tree: a Genome-Based Taxonomy for Phage. *J Bacteriol* **184**: 4529–4535.
- Rokney, A., Kobilier, O., Amir, A., Court, D.L., Stavans, J., Adhya, S., and Oppenheim, A.B. (2008) Host responses influence on the induction of lambda prophage. *Mol Microbiol* **68**: 29–36.
- Rolfe, M.D., Rice, C.J., Lucchini, S., Pin, C., Thompson, A., Cameron, A.D.S., *et al.* (2012) Lag phase is a distinct growth phase that prepares bacteria for exponential growth and involves transient metal accumulation. *J Bacteriol* **194**: 686–701.
- Sauer, R.T., Yocum, R.R., Doolittle, R.F., Lewis, M., and Pabo, C.O. (1982) Homology among DNA-binding proteins suggests use of a conserved super-secondary structure. *Nature* **298**: 447–451.
- Serra-Moreno, R., Jofre, J., and Muniesa, M. (2008) The CI repressors of Shiga toxin-converting prophages are involved in coinfection of *Escherichia coli* strains, which causes a down regulation in the production of Shiga toxin 2. *J Bacteriol* **190**: 4722–35.
- Slilaty, S.N., Rupley, J.A., and Little, J.W. (1986) Intramolecular cleavage of LexA and phage lambda repressors: dependence of kinetics on repressor concentration, pH, temperature, and solvent. *Biochemistry* **25**: 6866–6875.

- Stackebrandt E., Rainey F.A., Ward-Rainey N.L. (1997) Proposal for a new hierarchic classification system, Actinobacteria classis nov. *Int. J. Sys. Bacteriol.* **47**: 479–491.
- Sulakvelidze, A., Alavidze, Z., and Morris, J. (2001) Bacteriophage Therapy. *Antimicrob Agents Chemother* **45**: 649–659.
- Tao, L., Wu, X., and Sun, B. (2010) Alternative sigma factor σ^H modulates prophage integration and excision in *Staphylococcus aureus*. *PLoS Pathog* **6**: e1000888.
- Tauch, A., Pühler, A., Kalinowski, J., and Thierbach, G. (2003) Plasmids in *Corynebacterium glutamicum* and their molecular classification by comparative genomics. *J Biotechnol* **104**: 27–40.
- Tauch, A., Susanne, G., Pühler, A., Kalinowski, J., and Thierbach, G. (2002) The 27.8-kb R-plasmid pTET3 from *Corynebacterium glutamicum* encodes the aminoglycoside adenylyltransferase gene cassette aadA9 and the regulated tetracycline efflux system Tet 33 flanked by active copies of the widespread insertion sequence IS 6100. *Plasmid* **48**: 117–129.
- Tomasz, M. (1995) Mitomycin C: small, fast and deadly (but very selective). *Chem Biol* **2**: 575–579.
- Twort, W. (1914) An Investigation on the Nature of Ultra-Microscopic Viruses. *Lancet* 1241–1243.
- Valbuena, N., Letek, M., Ordóñez, E., Ayala, J., Daniel, R. a., Gil, J. a., and Mateos, L.M. (2007) Characterization of HMW-PBPs from the rod-shaped actinomycete *Corynebacterium glutamicum*: peptidoglycan synthesis in cells lacking actin-like cytoskeletal structures. *Mol Microbiol* **66**: 643–657.
- Waldor, M., and Mekalanos, J. (1996) Lysogenic conversion by a filamentous phage encoding cholera toxin. *Science (80-)* **272**: 1910–4.
- Wang, Robert, L., Pelletier, J., Dang, W.L., Taddei, F., Wright, A., and Jun, S. (2010) Robust growth of *Escherichia coli*. *Curr Biol* **20**: 1099–1103.
- Wang, I., Deaton, J., and Young, R. (2003) Sizing the Holin Lesion with an Endolysin- β -Galactosidase Fusion. *J Bacteriol* **185**: 779–787.
- Wang, I.-N., Smith, D., and Young, R. (2000) HOLINS : The Protein Clocks of Bacteriophage Infections. *Annu Rev Microbiol* **54**: 799–825.
- Wang, X., Kim, Y., Ma, Q., Hong, S.H., Pokusaeva, K., Sturino, J.M., and Wood, T.K. (2010) Cryptic prophages help bacteria cope with adverse environments. *Nat Commun* **1**: 147.
- Webb, J., Thompson, L., James, S., Charlton, T., Tolker-Nielsen, T., Koch, B., *et al.* (2003) Cell death in *Pseudomonas aeruginosa* biofilm development. *J Bacteriol* **185**: 4585–4592.
- Whitman, W., Coleman, D., and Wiebe, W. (1998) Prokaryotes: The unseen majority. *Proc Natl Acad Sci U S A* **95**: 6578–6583.
- Wieschalka, S., Blombach, B., Bott, M., and Eikmanns, B.J. (2013) Bio-based production of organic acids with *Corynebacterium glutamicum*. *Microb Biotechnol* **6**: 87–102.

Wilhelm, S., and Suttle, C. (1999) Viruses and Nutrient Cycles in the Sea. *Bioscience* **49**: 781–788.

Wright, G.D. (2005) Bacterial resistance to antibiotics: enzymatic degradation and modification. *Adv Drug Deliv Rev* **57**: 1451–70.

6 Appendix

6.1 Analysis of SOS-Induced Spontaneous Prophage Induction in *Corynebacterium glutamicum* at the Single-Cell Level

All Supplemental Movie Files can be viewed online at the article's Data Supplement.

Movie S1, *C. glutamicum* P_{recA} -*eyfp* reporter strain during cultivation in PDMS-based microfluidic chip devices

<http://jb.asm.org/content/suppl/2013/12/05/JB.01018-13.DCSupplemental/zjb999092968sm1.mp4>

Movie S2, *C. glutamicum* P_{recA} -*eyfp* reporter strain during cultivation in PDMS-based microfluidic chip devices

<http://jb.asm.org/content/suppl/2013/12/05/JB.01018-13.DCSupplemental/zjb999092968sm2.mp4>

Movie S3, *C. glutamicum* P_{recA} -*eyfp* reporter strain during cultivation in PDMS-based microfluidic chip devices; in some microcolonies, cells exhibiting the classical DivS phenotype were observed

<http://jb.asm.org/content/suppl/2013/12/05/JB.01018-13.DCSupplemental/zjb999092968sm3.mp4>

**6.2 Assessing the Role of the SOS Response in the induction of prophage
CGP3 of *Corynebacterium glutamicum***

SUPPLEMENTARY TABLE 1 Differentially expressed genes in a DNA microarray-based transcriptome comparison of the *C. glutamicum* $\Delta recA$ strain and the ATCC 13032 wild type strain^{1 2}. Samples analyzed were taken before the addition of mitomycin C (t=0h) and 30 minutes after addition of 2 μ M mitomycin C (t=0.5h). Genes listed were found to be a part of either the mitomycin C stimulon, the $\Delta lexA$ regulon, or the SOS and Stress Response modulon as defined in the CRN database.*

Gene ID	Gene name	Annotation	t = 0 h	t = 0.5 h
PREVIOUSLY IDENTIFIED TO BE INDUCIBLE BY THE SOS RESPONSE *				
cg0713		hypothetical protein, conserved	0,78	0,33
cg0714		putative polymerase involved in DNA repair	0,79	0,35
cg0875		hypothetical protein, conserved	1,43	0,47
cg0938	<i>cspB</i>	cold shock protein	2,11	1,94
cg1288		putative multidrug efflux permease of the major facilitator superfamily	2,06	1,23
cg1291		putative membrane protein	2,55	3,08
cg1560	<i>uvrA</i>	excinuclease ABC subunit A	0,58	0,44
cg1602	<i>recN</i>	DNA repair protein	0,48	0,1
cg1696		putative antibiotic efflux permease of the major facilitator superfamily	2,61	1,77
cg1760	<i>sufU</i>	cysteine desulfhydrase	0,5	0,74
cg1763	<i>sufD</i>	Fe-S cluster assembly membrane protein	0,48	0,76
cg1764	<i>sufB</i>	Fe-S cluster assembly protein	0,47	0,77
cg1765	<i>sufR</i>	transcriptional regulator of suf operon	0,48	0,84
cg1891	<i>alpA</i>	putative phage DNA adapter protein CGP3 region	0,49	0,71
cg1896		putative secreted protein CGP3 region	0,47	0,56
cg1897		putative secreted protein CGP3 region	0,23	0,34
cg1975		hypothetical protein, conserved CGP3 region	0,47	0,55
cg1977		putative secreted protein CGP3 region	0,82	0,42
cg1978		hypothetical protein CGP3 region	0,76	0,44
cg1981		hypothetical protein CGP3 region	0,78	0,46
cg2008		putative membrane protein CGP3 region	0,39	0,63
cg2014		hypothetical protein CGP3 region	0,42	0,48
cg2016		hypothetical protein CGP3 region	0,45	0,76
cg2017		hypothetical protein CGP3 region	0,45	0,6
cg2018		putative membrane protein CGP3 region	0,38	0,48
cg2019		putative membrane protein CGP3 region	0,4	0,86
cg2022		putative secreted protein CGP3 region	0,29	0,41
cg2032		putative membrane protein CGP3 region	0,45	0,6
cg2062		putative protein, similar to plasmid-encoded protein PXO2.09 CGP3 region	0,39	0,68
cg2063		putative membrane protein CGP3 region	0,31	0,62
cg2064		putative DNA topoisomerase I omega-protein EC:5.99.1.2 CGP3 region	0,29	0,56
cg2112	<i>nrdR</i>	transcriptional regulator of deoxyribonucleotide biosynthesis, YbaD-family	0,87	0,32
cg2113	<i>divS</i>	transcriptional regulator, suppressor of cell division	0,72	0,2
cg2114	<i>lexA</i>	transcriptional repressor/regulator, involved in SOS/stress response, LexA-family	0,9	0,3
cg2140	<i>recX</i>	transcriptional regulator involved in DNA repair, RecX-family	0,65	0,41
cg2141	<i>recA</i>	recombinase A (EC:3.4.21.88)	0,3	0,22
cg2183	<i>oppC</i>	ABC-type peptide transport system, permease component	2,65	2,8
cg2184	<i>oppD</i>	ATPase component of peptide ABC-type transport system, contains duplicated ATPa	2,76	2,95
cg2381		hypothetical protein, conserved	2,41	0,98
cg2449		putative protein, involved in SOS and stress response, conserved	0,65	0,22
cg2636	<i>catA1 (catA)</i>	catechol 1,2-dioxygenase (EC:1.13.11.1)	0,49	0,69
cg3107	<i>adhA</i>	Zn-dependent alcohol dehydrogenase (EC:1.1.1.1)	0,47	0,65
cg3141	<i>hmp</i>	flavoheмоprotein	2,09	2,17

SUPPLEMENTARY TABLE 2 Differentially expressed genes in a DNA microarray-based transcriptome comparison of the *C. glutamicum* Δ *recA* strain and the ATCC 13032 wild type strain^{1,2}. Samples analyzed were taken before the addition of mitomycin C (t=0h) and 30 minutes after addition of 2 μ M mitomycin C (t=0.5h). Genes listed were not found to be responsive to the SOS response in previous studies (defined by not being part of either the mitomycin C stimulon, the Δ lexA regulon, or the SOS and Stress modulon as defined at the CRN database*).

Gene ID	Gene name	Annotation	t = 0 h	t = 0.5 h
SOS-RESPONSIVE GENES FOUND IN THIS STUDY				
cg0031		putative reductase, related to diketogulonate reductase	2,15	1,36
cg0043	<i>znuC2</i>	ABC-type Mn/Zn import system Znu2, ATP-binding protein	3,52	2,29
cg0053		putative iron-siderophore ABC transporter, ATP-binding protein	2,23	1,71
cg0078		putative membrane protein	2,27	1,35
cg0288		putative ABC transporter, transmembrane and ATPase subunit	3,34	0,97
cg0421	<i>wzx</i>	putative translocase involved in export of a cell surface polysaccharide, horizontally tr	0,48	0,56
cg0427	<i>tnp17b</i>	transposase fragment, putative pseudogene, horizontally transferred	2,25	1,58
cg0428	<i>tnp17c</i>	transposase fragment, putative pseudogene, horizontally transferred	2,48	2,14
cg0661		hypothetical protein, conserved	2,57	1,54
cg0666		putative membrane protein	3,92	1,59
cg0772		putative sugar efflux permease, MFS-type	1,98	2,15
cg0777		putative ABC-type iron-siderophore transporter, ATPase subunit	2,24	2,26
cg0778		putative ABC-type iron-siderophore transporter, permease subunit	1,83	2,18
cg0961		putative homoserine O-acetyltransferase	0,45	0,62
cg1149		hypothetical protein	3,92	1,76
cg1232		putative protein, conserved, LmbE-family	2,35	1,99
cg1295		putative hydrolase or acyltransferase α/β hydrolase superfamily	2,1	1,46
cg1307		putative superfamily II DNA and RNA helicase	1,34	2,01
cg1749		hypothetical protein CGP2 region	0,48	0,8
cg1808		hypothetical protein	2,06	1,63
cg1934		hypothetical protein CGP3 region	0,39	0,66
cg1936		putative secreted protein CGP3 region	0,49	0,62
cg1955		putative secreted protein CGP3 region	0,5	0,59
cg1976		hypothetical protein CGP3 region	0,4	0,62
cg1982		putative ATPase with chaperone activity, ATP-binding subunit CGP3 region	0,66	0,49
cg1995		hypothetical protein CGP3 region	0,48	0,7
cg2048		hypothetical protein CGP3 region	2,55	1,35
cg2105		hypothetical protein	2,27	1,46
cg2118	<i>fruR</i>	transcriptional regulator of sugar metabolism, DeoR-family	0,49	0,66
cg2119	<i>pfkB (fruK)</i>	1-phosphofructokinase (EC:2.7.1.56)	0,45	0,77
cg2349		putative ATPase component of ABC transporter for antibiotics with duplicated ATP	3,14	2,65
cg2633		putative restriction endonuclease	0,67	0,46
cg2637	<i>benA</i>	benzoate 1,2-dioxygenase α subunit aromatic ring hydroxylation dioxygenase A (EC:	0,37	0,52
cg2638	<i>benB</i>	benzoate dioxygenase small subunit (EC:1.14.12.10)	0,42	0,54
cg2642	<i>benK1 (benK)</i>	putative benzoate transport protein	0,49	0,51
cg2893		putative cadaverine transporter, multidrug efflux permease, MFS-type	0,26	0,25
cg2898		putative 3-ketosteroid dehydrogenase	3,87	1,82
cg2919		putative oxidoreductase	2,08	1,31
cg3080		putative secondary Na ⁺ /glutamate symporter	2,12	1,75
cg3157		putative secreted protein	1,94	2,06
cg3272		putative membrane protein	1,9	2,32
cg3329		hypothetical protein, conserved	3,83	3,62
cg3394		putative secreted protein	2,02	1,45

SUPPLEMENTARY TABLE 3 Differentially expressed genes in a DNA microarray-based transcriptome comparison of the *C. glutamicum* $\Delta recA$ strain and the ATCC 13032 wild type strain^{1 2}. Samples analyzed were taken before the addition of mitomycin C (t=0h) and 30 minutes after addition of 2 μ M mitomycin C (t=0.5h). Genes listed lie within the CGP3 genomic region (cg1981-cg2071).

Gene ID	Gene name	Annotation	t = 0 h	t = 0.5 h
ENCODED IN CGP3 GENOMIC REGION (cg1891-cg2071)				
cg1891	<i>alpA</i>	putative phage DNA adapter protein CGP3 region	0,49	0,71
cg1896		putative secreted protein CGP3 region	0,47	0,56
cg1897		putative secreted protein CGP3 region	0,23	0,34
cg1934		hypothetical protein CGP3 region	0,39	0,66
cg1936		putative secreted protein CGP3 region	0,49	0,62
cg1955		putative secreted protein CGP3 region	0,5	0,59
cg1975		hypothetical protein, conserved CGP3 region	0,47	0,55
cg1976		hypothetical protein CGP3 region	0,4	0,62
cg1977		putative secreted protein CGP3 region	0,82	0,42
cg1978		hypothetical protein CGP3 region	0,76	0,44
cg1981		hypothetical protein CGP3 region	0,78	0,46
cg1982		putative ATPase with chaperone activity, ATP-binding subunit CGP3 region	0,66	0,49
cg1995		hypothetical protein CGP3 region	0,48	0,7
cg2008		putative membrane protein CGP3 region	0,39	0,63
cg2014		hypothetical protein CGP3 region	0,42	0,48
cg2016		hypothetical protein CGP3 region	0,45	0,76
cg2017		hypothetical protein CGP3 region	0,45	0,6
cg2018		putative membrane protein CGP3 region	0,38	0,48
cg2019		putative membrane protein CGP3 region	0,4	0,86
cg2022		putative secreted protein CGP3 region	0,29	0,41
cg2032		putative membrane protein CGP3 region	0,45	0,6
cg2048		hypothetical protein CGP3 region	2,55	1,35
cg2062		putative protein, similar to plasmid-encoded protein PXO2.09 CGP3 region	0,39	0,68
cg2063		putative membrane protein CGP3 region	0,31	0,62
cg2064		putative DNA topoisomerase I omega-protein EC:5.99.1.2 CGP3 region	0,29	0,56

SUPPLEMENTARY TABLE 4 Differentially expressed genes in a DNA microarray-based transcriptome comparison of the *C. glutamicum* $\Delta recA$ strain and the ATCC 13032 wild type strain^{1,2}. Samples analyzed were taken before the addition of mitomycin C (t=0h) and 30 minutes after addition of 2 μ M mitomycin C (t=0.5h).

Gene ID	Gene name	Annotation	t = 0 h	t = 0.5 h
PUTATIVE TRANSPORT SYSTEMS AND MEMBRANE PROTEINS				
cg1288		putative multidrug efflux permease of the major facilitator superfamily	2,06	1,23
cg1291		putative membrane protein	2,55	3,08
cg1696		putative antibiotic efflux permease of the major facilitator superfamily	2,61	1,77
cg2183	<i>oppC</i>	ABC-type peptide transport system, permease component	2,65	2,8
cg2184	<i>oppD</i>	ATPase component of peptide ABC-type transport system, contains duplicated ATPa	2,76	2,95
cg0043	<i>znuC2</i>	ABC-type Mn/Zn import system Znu2, ATP-binding protein	3,52	2,29
cg0053		putative iron-siderophore ABC transporter, ATP-binding protein	2,23	1,71
cg0078		putative membrane protein	2,27	1,35
cg0288		putative ABC transporter, transmembrane and ATPase subunit	3,34	0,97
cg0421	<i>wzx</i>	putative translocase involved in export of a cell surface polysaccharide, horizontally tr	0,48	0,56
cg0666		putative membrane protein	3,92	1,59
cg0772		putative sugar efflux permease, MFS-type	1,98	2,15
cg0777		putative ABC-type iron-siderophore transporter, ATPase subunit	2,24	2,26
cg0778		putative ABC-type iron-siderophore transporter, permease subunit	1,83	2,18
cg1982		putative ATPase with chaperone activity, ATP-binding subunit CGP3 region	0,66	0,49
cg2349		putative ATPase component of ABC transporter for antibiotics with duplicated ATP	3,14	2,65
cg2642	<i>benK1 (benK)</i>	putative benzoate transport protein	0,49	0,51
cg2893		putative cadaverine transporter, multidrug efflux permease, MFS-type	0,26	0,25
cg3080		putative secondary Na ⁺ /glutamate symporter	2,12	1,75
cg3272		putative membrane protein	1,9	2,32

SUPPLEMENTARY TABLE 5 Differentially expressed genes in a DNA microarray-based transcriptome comparison of the *C. glutamicum* $\Delta recA$ strain and the ATCC 13032 wild type strain^{1,2}. Samples analyzed were taken before the addition of mitomycin C (t=0h) and 30 minutes after addition of 2 μ M mitomycin C (t=0.5h).

Gene ID	Gene name	Annotation	t = 0 h	t = 0.5 h
FURTHER DIFFERENTIALLY EXPRESSED GENES				
cg0031		putative reductase, related to diketogulonate reductase	2,15	1,36
cg0427	<i>tnp17b</i>	transposase fragment, putative pseudogene, horizontally transferred	2,25	1,58
cg0428	<i>tnp17c</i>	transposase fragment, putative pseudogene, horizontally transferred	2,48	2,14
cg0661		hypothetical protein, conserved	2,57	1,54
cg0961		putative homoserine O-acetyltransferase	0,45	0,62
cg1149		hypothetical protein	3,92	1,76
cg1232		putative protein, conserved, LmbE-family	2,35	1,99
cg1295		putative hydrolase or acyltransferase α/β hydrolase superfamily	2,1	1,46
cg1307		putative superfamily II DNA and RNA helicase	1,34	2,01
cg1749		hypothetical protein CGP2 region	0,48	0,8
cg1808		hypothetical protein	2,06	1,63
cg2105		hypothetical protein	2,27	1,46
cg2118	<i>fruR</i>	transcriptional regulator of sugar metabolism, DeoR-family	0,49	0,66
cg2119	<i>pfkB (fruK)</i>	1-phosphofructokinase (EC:2.7.1.56)	0,45	0,77
cg2633		putative restriction endonuclease	0,67	0,46
cg2637	<i>benA</i>	benzoate 1,2-dioxygenase α subunit aromatic ring hydroxylation dioxygenase A (EC:	0,37	0,52
cg2638	<i>benB</i>	benzoate dioxygenase small subunit (EC:1.14.12.10)	0,42	0,54
cg2898		putative 3-ketosteroid dehydrogenase	3,87	1,82
cg2919		putative oxidoreductase	2,08	1,31
cg3157		putative secreted protein	1,94	2,06
cg3329		hypothetical protein, conserved	3,83	3,62
cg3394		putative secreted protein	2,02	1,45
cgs02	<i>cgb_24535</i>	putative RNase P	2,06	1,1
cgtRNA_3545		Met tRNA	2,35	1,67

¹ Genes were chosen according to the criteria: log ratio of relative mRNA levels >2 or <0.5 in either condition.

² Data are mean values of three independent DNA microarrays experiments starting from independent cultures grown in CGXII minimal medium + 4% (w/v) glucose. The values represent the log ratio of mRNA in $\Delta recA$ compared to the wild type.

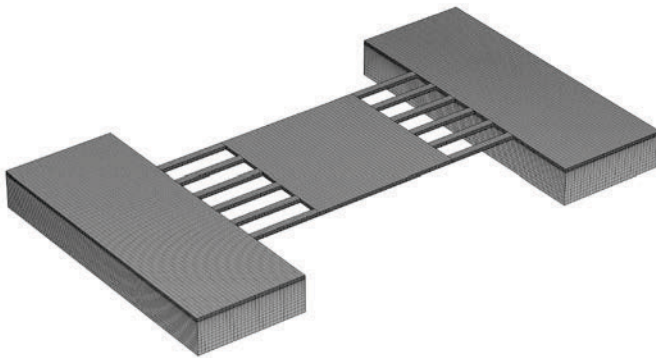
*

Gene was previously detected as part of the mitomycin C stimulon as described in the CRN database (<http://coryneregnet.mmci.uni-saarland.de/v6e/CoryneRegNet/queryElement.php?stimulon=mc01>) or gene was previously detected as part of the $\Delta lexA$ regulon as described in the CRN database (http://coryneregnet.mmci.uni-saarland.de/v6e/CoryneRegNet/queryElement.php?stimulon=delta_lex01) or gene was previously detected as part of the SOS and Stress Response modulon as described in the CRN database ([http://coryneregnet.mmci.uni-saarland.de/v6e/CoryneRegNet/queryElement.php?module=CRN-module SOS and Stress Response %28NC_006958%29](http://coryneregnet.mmci.uni-saarland.de/v6e/CoryneRegNet/queryElement.php?module=CRN-module%20SOS%20and%20Stress%20Response%20NC_006958%29))

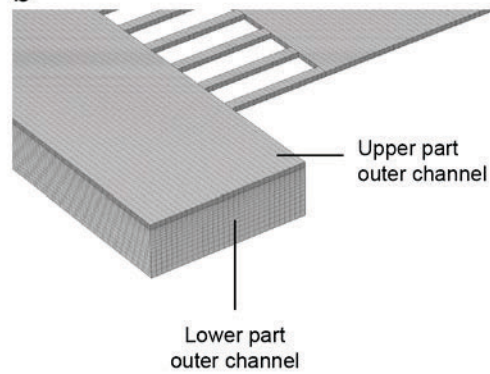
6.3 Spatiotemporal Microbial Single-Cell Analysis Using a High-Throughput Microfluidics Cultivation Platform

Supplement 1

a



b



Supplement Figure 1: (a-b) Generated mesh used for CFD simulations.

Supplement Table 1: .General overview of the mesh used for CFD simulations.

Mesh	Number of Hexahedral elements	Number of Quadrilateral elements	Number of Edge elements	Number of Vertex elements	Number of Hexahedral elements in height	Number of Hexahedral elements in depth	Number of Hexahedral elements in weight	Minimumelement quality*	Average element quality*	Mesh volume in μm^3	Average Hexahedral element volume in μm^3
Entire geometry	613120	139184	7736	120	-	-	-	0.1198	0.2482	50060	0.0816

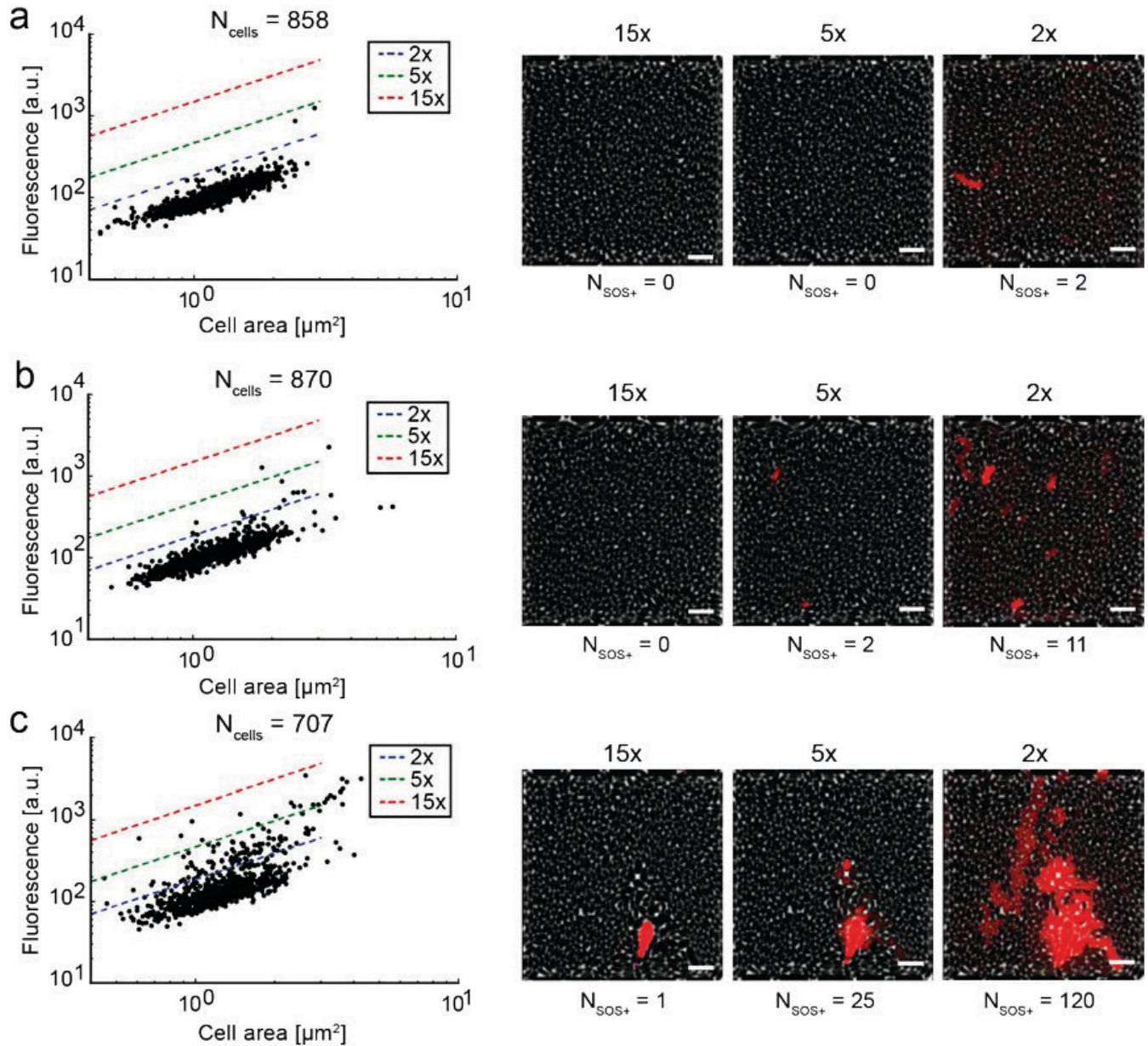
*Element quality definition of Comsol: "The absolute value of the mesh element quality is based on the ratios of the inscribed and circumscribed circles' or spheres' radii for the simplex corresponding to each corner of the element. If the simplex cannot be clearly determined (an apex of the pyramid, for example), the corresponding corner is excluded from the consideration. The absolute value is always between 0 and 1, where 0.0 represents a degenerated element and 1.0 represents the best possible element. A negative value means a contradiction to the COMSOL Multiphysics numbering convention for mesh element vertices (see Element Numbering Conventions), and the element is then referred to as an inverted element."

Table 2: Detailed overview of the mesh parameters for individual parts of the microfluidic chip geometry, used for CFD simulations.

Mesh	Number of Hexahedral elements	Number of Hexahedral elements in x-direction	Number of Hexahedral elements in y direction	Number of Hexahedral elements in z direction	Element length in x-direction in μm	Element length in y-direction in μm	Element length in z-direction in μm	Minimum element quality*	Average element quality*	Mesh volume in μm^3	Hexahedral element volume in μm^3
of the 12 ner annels	1760	22	10	8	0.86	0.2	0.125	0.1564	0.1564	38	0.021590909
amber	64000	40	200	8	1	0.2	0.125	0.1198	0.1198	1600	0.025
pper part 1 of the 2 iter annels	96000	30	400	8	1	0.2	0.125	0.1198	0.1198	2400	0.025
wer part 1 of the 2 iter annels	168000	30	400	14	1	0.2	0.214-1.07	0.1972	0.3655	21600	0.0428- 0.214

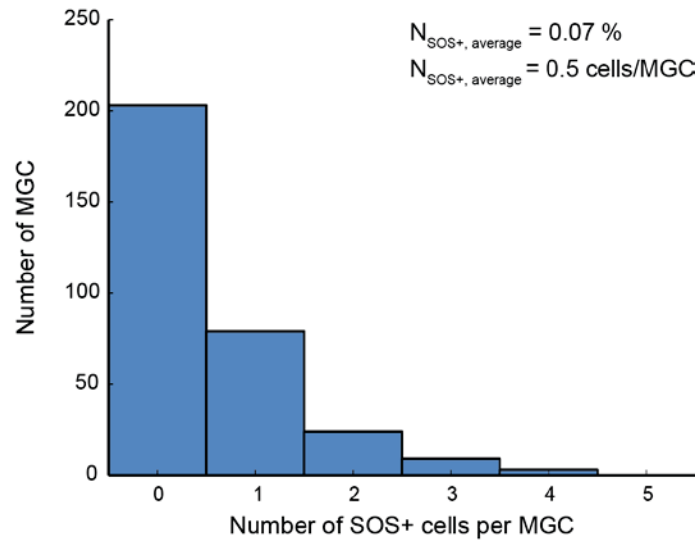
Element quality definition of Comsol: "The absolute value of the mesh element quality is based on the ratios of the inscribed and circumscribed circles' or spheres' radii for the simplex corresponding to each corner of the element. If the simplex cannot be clearly determined (an apex of the pyramid, for example), the corresponding corner is excluded from the consideration. The absolute value is always between 0 and 1, where 0.0 represents a degenerated element and 1 represents the best possible element. A negative value means a contradiction to the COMSOL Multiphysics numbering convention for mesh element vertices (see Element Numbering Conventions), and the element is then referred to as an inverted element."

Frequency of spontaneously SOS+ induced cells at MGC at various gatings



Supplement Figure 2: Occurrence of spontaneously induced cells (SOS+). Here, cells with a 2-fold (blue), 5-fold (green) and 15-fold (red) increased reporter signal were counted as SOS+ (scale bars 5 μm).

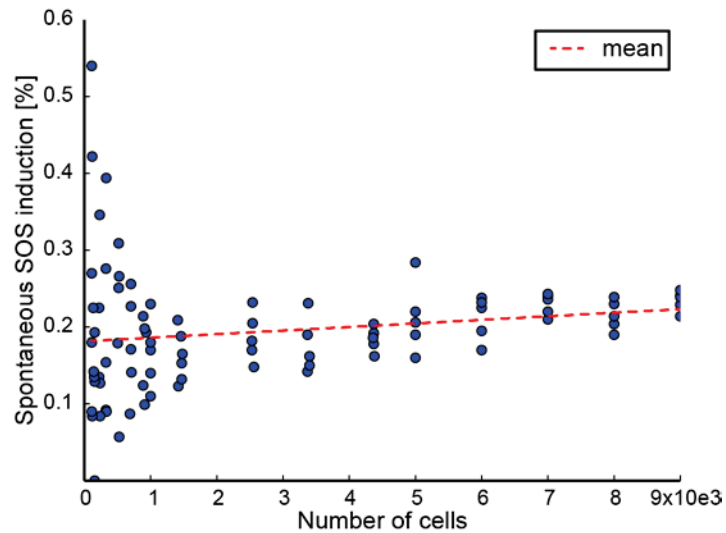
Occurrence of spontaneously induced cells



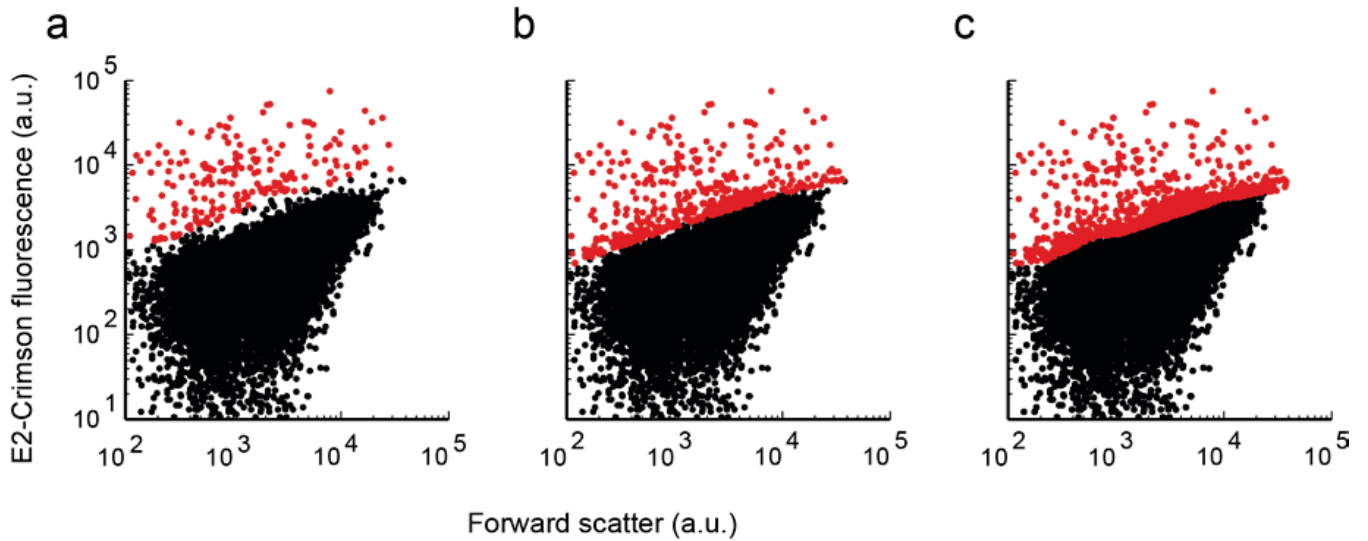
Supplement Figure 3: Frequency of spontaneous induced cells, if cells with a 15-fold increased reporter signal were considered as SOS-positive (SOS+).

Supplement 3

Occurrence of spontaneously induced cells vs. total number of analyzed cells



Supplement Figure 4: Occurrence of spontaneously induced SOS response in cells based on the number of cells analyzed by FC.

Determination of SOS positive cells for FC measurements

Supplement Figure 5: FC scatter plots of the strain *C. glutamicum/pJC1-PrecA-e2-crimson*. A total of 10^6 cells were analyzed. (a) - (c) Different gating threshold, manually selected.

Curriculum vitae

Name: Arun Nanda
Date of birth: 28.09.1983
Place of Birth: Düsseldorf

1993-2003 Humboldt Gymnasium Düsseldorf, Germany
Abitur

2005-2009 Studies of Biology at the Heinrich-Heine-
University Düsseldorf

2008-2009 Diploma thesis in the group of Prof. Dr.
Andreas Weber at the Institute for Plant
Biochemistry, Heinrich-Heine-University
Düsseldorf

Title: „C₄ photosynthesis as an adaptation to
abiotic stress“

2011-2014 PhD thesis in the group of Juniorprof. Dr. Julia
Frunzke at the Institute of Bio- and
Geosciences, IBG-1: Biotechnology,
Forschungszentrum Jülich

Title: „Characterization of the spontaneous
SOS response in *Corynebacterium
glutamicum* and its effect on the lysogenic
prophage CGP3

Danksagung

Ein ganz besonderer Dank gilt Juniorprof. Dr. Julia Frunzke für die Überlassung einer sehr spannenden und erfolgreichen Doktorarbeit, ihre schier unendliche Menge an Ideen und für die Struktur, die sie oft in meinen Laboralltag gebracht hat.

Herrn Prof. Dr. Joachim Ernst möchte ich für die freundliche Übernahme des Zweitgutachtens und für die sehr interessanten Gespräche danken.

Weiterhin möchte ich mich bei Prof. Dr. Wolfgang Wiechert, Juniorprof. Dr. Dietrich Kohlheyer und Dr. Katharina Nöh für die enge und fruchtbare Zusammenarbeit im Rahmen des gemeinsamen DFG-Schwerpunktprojekts bedanken.

Den jetzigen und ehemaligen Mitgliedern der AG Frunzke (Toni, Nurije, Andrea, Conni, Kim, Regina, Dominik, Eugen, ...) möchte ich vielmals für die schöne Arbeitsatmosphäre, für die vielen gemeinsamen Kaffeepausen und für die große Hilfsbereitschaft bedanken. Besonders möchte ich hierbei Eva für die wunderbare gemeinsame Zusammenarbeit, die kurzweiligen Autofahrten ins Forschungszentrum und für die entstandene Freundschaft bedanken.

Den Mitarbeitern des IBG-1 möchte ich für die angenehme Arbeitsatmosphäre und die große Hilfsbereitschaft danken.

Ganz besonders möchte ich meiner Familie danken; meiner Mutter für die Unterstützung aus der Ferne, Judith für die große Unterstützung aus der Nähe und ganz besonders meinem Vater für seinen Glauben an mich und für Alles.

Bei meinen Freunden innerhalb und außerhalb der Naturwissenschaften möchte ich mich ganz herzlich dafür bedanken, dass sie mich durch alle Lebenslagen begleiten. Ich freue mich auf die zukünftigen Abenteuer, die wir miteinander erleben werden.

Aus tiefstem Herzen danke ich meinem besten Freund Dan. Für deine Freundschaft und deine grenzenlose Unterstützung in allen Lebenslagen bin ich dir auf ewig dankbar.

Erklärung

Ich versichere an Eides Statt, dass die vorgelegte Dissertation von mir selbständig und ohne unzulässige fremde Hilfe unter Beachtung der „Grundsätze zur Sicherung guter wissenschaftlicher Praxis an der Heinrich-Heine-Universität Düsseldorf“ erstellt worden ist. Die Dissertation wurde in der vorgelegten oder in ähnlicher Form noch bei keiner anderen Institution eingereicht. Ich habe bisher keine erfolglosen Promotionsversuche unternommen.

Jülich, den 18.05.2016